Université d'Ottawa • University of Ottawa

THE PARTITIONING OF ^{129}I IN A SHALLOW SAND AQUIFER CHALK RIVER, ONTARIO

by

Nicolás G. Alvarado Quiroz

A thesis submitted to the School of Graduate Studies and Research

in partial fulfillment of the requirements

for the degree of M.Sc. of Earth Sciences

OTTAWA-CARLETON GEOSCIENCE CENTRE

AND

UNIVERSITY OF OTTAWA

OTTAWA, CANADA

Acknowledgements

I would like to thank my supervisor, Dr. Ian D. Clark, who accepted me for this project, introduced me to isotope hydrogeology, started my career in the environmental field and was a constant source of encouragement and information.

I would like to give many thanks to Dr. Tom Kotzer, at AECL, for his enthusiasm, words of wisdom, source of information and guidance throughout the duration of the project. I am indebted to Dr. Gwen Milton for her expertise, in the radiochemistry and isotope work involved with this project and introducing me to this field of study. Thanks to Dr. R.W.D. Killey for his assistance and insight on Waste Management Area C plumes and to Lorna Chant for her guidance and assistance.

I would like to express my gratitude to Dr. Denis Bottomley and the AECB for the selection and funding of this project.

[AECB Contract reference No. 87055-6-5043/001/SS]

A Special thanks to Dr. Owen Dixon is due, for the use of his laboratory throughout the project.

Thanks are also due to Xiaolei Zhao and Carmen Soto at Isotrace Laboratories for running my samples under recurrent time constraints, John Loop (for his understanding and patience) and Wendi Abdi at the University of Ottawa. The staff of the department of Earth Sciences at the University of Ottawa, which include Hélène DeGouffe and Sylvie Downing for their continuous assistance and support with academic administration. I would like to express my gratitude to former graduate students for their advice and expertise, Bahram Danefshar, Mark Mihalasky, Kevin Telmer and special thanks to Matt Leybourne. Thanks to fellow grad-students AJC, BS, BL, LH, L ElB, SMcC and JLB for lending me their ears (and Z-drive) along with PDFs Denis Mavrocordatos and Rob Spark. I would like to thank the late Dr. L. K. Keck for her wisdom. Finally, I would like to give thanks to BLM for her potent words of encouragement and wisdom.

Final thanks to my family who continually encouraged and supported me. I would like to give thanks to my father, Dr. Gabriel G. Alvarado Urbina, who has always assisted and guided me and to my mother Mrs. Gladys Quiroz Alvarado for endless source of advice. Finally, special thanks to my sister Constanza for her support and late night conversations and to Sebastian. Muchas gracias a mi familia!

Abstract

^{129}I is a fission product with a long half-life ($1.57x10^7$ yrs) that has important implications as a tool to monitor long-term stability and interactions in the hydrosphere, biosphere and geosphere. In the groundwaters, migration of ^{129}I, which because of its low natural concentrations is assumed to be the same as stable iodine (^{127}I), can be retarded by various reactions with geologic and biologic reservoirs. At Atomic Energy of Canada, Chalk River Laboratories, Ontario, solid, low-level radioactive wastes from industrial, academic and medical applications have been stored in trenches overlying unconsolidated sandy glacial tills and permeable very-fine to fine-grained sands overlying crystalline bedrock. The sandy aquifer system drains into a Swamp comprised of approximately 3 m of sphagnum peat. Hydrologically, most of the yearly precipitation (~340mm/a) percolates into the underlying aquifer at Area C. This has generated a contaminant plume, having chemical characteristics of a dilute, sanitary landfill leachate, containing ^{14}C (DOC, DIC), tritium (HTO) and levels of ^{129}I which are elevated above present-day precipitation levels of approximately 10^7 atoms ^{129}I/l water.

A comprehensive field and analytical program at this site has been initiated to examine the partitioning of ^{127}I and ^{129}I amongst the various reservoirs in this system and the controlling factors. This includes measurements of total iodine, ^{129}I, tritium, ^{14}C and $^{13}C/^{12}C$ ratios in groundwater and geologic and biologic materials. Groundwaters from several boreholes with multi-level piezometers transecting the flow system were sampled. Cores from sands, peats and local vegetation samples were also obtained to characterize the general hydrochemistry of the system and obtain information on the distribution of ^{127}I and ^{129}I.

The total iodine concentration [ng/ml] and ^{129}I [atoms/liter] inside the plume at the recharge site and discharge site were 6.88 ng/ml (~$6x10^{10}$ atoms/liter) and 26.00 ng/ml (~$8x10^{10}$ atoms/liter), respectively. These values are similar to fissiogenic ^{129}I concentrations previously measured in saline groundwaters from uriferous granites and high grade U-ore deposits. Positive correlations between stable iodine (and ^{129}I) and ^{14}C (0.82), tritium (0.87) and DIC (0.64) are evident. Combustion analysis of soil cores taken near the recharge (sandy soils) and discharge (peats) sites showed a total iodine concentration inside the plume of 4.8 ng/ml (C-114) and 350.0 ng/ml (CO-4) suggesting partitioning into these organic-rich peats. Cedar trees previously planted in the output area of Duke Swamp were sampled at various time intervals to distinguish between atmospheric adsorption and root uptake of ^{129}I. These samples were combusted for total iodine and did not show any correlation between iodine concentration and time of exposure (values ranged from 15-200 ng/g of vegetation). However, there was a positive correlation evident between an increase in ^{129}I concentration and exposure time. ^{129}I concentration in vegetation ranged from $3.02x10^6$ (for background) to $1.36x10^7$ (for potted) and $4.96x10^7$ (for planted).

Sommaire

L'^{129}I est un produit de fission avec une demie-vie très longue d'environ $1.57x10^7$ années. Ceci fait de lui un outil important pour suveiller les interactions et la stabilité à long-terme dans l'hydrosphere, la biosphere et la géosphere. La migration de l'^{129}I dans les eaux souterraines, peut être retardée à cause des nombreuses réactions dont cet élément fait partie. Ces réaction impliquent des réservoirs géologiques et biologiques. Dans les laboratoires de l'Agence Canadienne de l'Energie Atomique à Chalk River, Ontario, des déchets industriels solides en provenance de laboratoires de recherche universitaire et médicale de faible niveaux de radioactivité ont été entreposés dans des fossés sous-jacent un système, non consolidé, de circulation souterraine qui consiste en un mélange de sable, dépôts galaciers (tills) et des sables de taille très fine à fine. Ces formations reposent sur des bancs de roches crystallines. L'aquifère sableux verse dans une marée constituée approximativement de 3 m de tourbe de sphaine. De point de vue hydrologique, la plupart des précipitations percolent dans l'aquifère sous-jacent dans la zone C. Celà génère un panache contaminant, avec des caractèristiqeus chimiques d'un dépotoire faiblement contaminé, contenant du ^{14}C (COD, CID), tritium (HTO) et des niveaux d'^{129}I élevés par rapport à ceux enregistrés dans les précipitation modernes qui sont à peu près de 10^7 atoms/l

Un programme d'étude analytique et de terrain à ce site a été établi dans le but d'examiner le fractionnement de l'I^{127} et de l'I^{129} entre les différents réservoirs de ce système ainsi de déterminer les facteurs impliqués. Ceci inclut les mesures de l'iode total, l'I^{129}, H^3, C^{14} et le rapport C^{13}/C^{12} dans les eaux souterraines et dans les sources biologiques et géologiques environnantes. En effet, un échantionnage des eaux souterraines à partir de différents puits de niveaux piézométriques différents de part et d'autre du système d'écoulement a été effectué. Des carottes à paritr des niveaux sableux, des marrécages, et des zones de végétation locale ont été échantillonnées à fin de caractériser la chimie des eaux du système et obtenir des informations sur la distribution de l'^{127}I et de l'^{129}I.

La concentration totale de l'iode ainsi que celle de l'^{129}I à l'intérieur du panache contaminant dans les zones de recharge et de décharge est 6.88ng/ml (~6 x 10^{10} atomes/litre) et 26.00 ng/ml (~8 x 10^{10} atomes/litre), respectivement. Ces valeurs sont semblables à celles des concentrations de l'^{129}I fissiogénique mesurées au paravant dans des eaux sousterraines salines provenant de granites uranifères. Des corrélations positives entre l'Iode (^{129}I) et le ^{14}C (0.82) d'une part, et entre le tritium (0.87) et le CID (0.64) sont notées. Des tests de combustion ont été éffectués sur les échantillons des carottes de sols sableux de la zone de recharge et des marrées de la zone de recharge. Les résultats de ces tests montrent des concentrations élevées à l'intérieur du panache d'environ 4.8 ng/ml (C-114) et 350.0 ng/ml (C-4) suggérant un fractionnement dans les tourbes riches en matière organique. Des cédriers plantés auparavant à la sortie de la marée Duke ont été échantillonnés à différentes périodes à fin de différencier entre l'absorption atmosphèrique par les feuilles et pédogénique par les racines. Ces échantillons ont été combustionnés pour measurer la concentration totale de l'iode mais aucune corrélation n'a été notée entre la teneur en iode et le temps d'exposition (valeurs entre 15 et 200 ng/g de végétation). Cependant, une corrélation positive a été notée entre l'augmentation dans la teneur en ^{129}I et le temps d'exposition. La concentration de l'^{129}I dans la végétation varie entre 3.02 x 10^6 (valeur de bruit de fond), 1.36 x 10^7 (pour la végétation en provenance des pôts) et 4.96 x 10^7 (plantation).

Table of Contents

List of Figures

List of Tables

List of Equations

I. Introduction

Courtois discovered iodine in 1811 when he sublimed the element from seaweed ash and concentrated sulphuric acid. Iodine belongs in Group VII of the Periodic Table (a member of the halogens) and has an atomic number 53 and atomic weight of 126.90. It forms a large univalent anion with a radius of 0.215nm (Table 1). Besides existing as a univalent I^-, iodine occurs naturally as the complex iodate anion (IO_3^-). Figure 1 illustrates the fields of stability of various states of iodine in an aqueous system.

Table 1 Properties of selected halogens.

	Chlorine	**Bromine**	**Iodine**
Atomic Number	17	35	53
Atomic Mass	35.453	79.904	126.9045
Mass Numbers (and abundance)	35 (75.77%) 37 (24.23%)	79 (50.54%) 81 (49.46%)	127 (100%)
Electronic Configuration	$[Ne]3s^23p^5$	$[Kr]3s^23p^5$	$[Ar]3s^23p^5$
Ionization Energy ($kJ\ mol^{-1}$)	1251	1140	1008
Electron Affinity ($kJ\ mol^{-1}$)	349	325	295
Melting Point (°C)	-101.0	-7.25	113.6
Boiling Point (°C)	-34.0	59.5	185.2
X-X Distance (pm)	199	228	266
ΔH of dissociation ($kJ\ mol^{-1}$)	242.6	192.8	151.1

(Fuge and Johnson 1983; Miessler and Tarr 1991)

Iodine is widely distributed in the oceans, rocks and organisms (Fuge & Johnson, 1983). The marine environment and biota have considerably higher iodine concentrations than terrestrial plants and soils (Figure 2, Table 2). Some landmasses contain large amounts of iodine (e.g., nitrate beds in Chile) and in other areas the sources are so low in stable iodine that their inhabitants suffer from iodine deficiency (Stewart, 1990).

Figure 1 Stability field diagram for iodine in aqueous system.

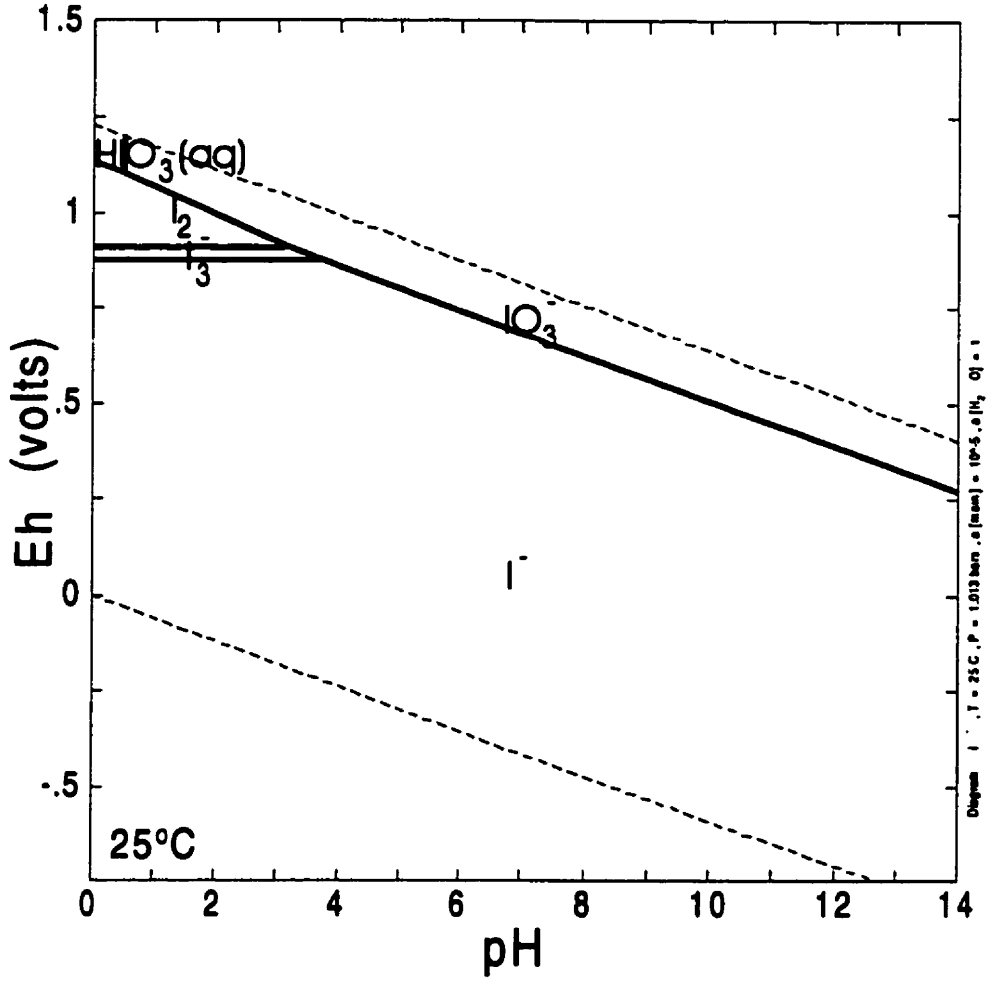

The wide variation in soil iodine content is due to the assumption that the major source of iodine in soils is from material released from the ocean surface (Goldschmidt, 1954; Myake & Tsunogai, 1963).

Iodine concentration in the atmosphere generally diminishes with increasing distance from the oceans, due to washout of marine aerosols (Goldschmidt, 1954). In the case of iodine, Fuge & Johnson (1986) reported that Zyrin & Imadi (1967) and Perel'man (1977) validates the drop from coastal to inland atmosphere in Russia. The Russian data did indicate higher iodine concentrations in the upper layers of soils than in deeper layers; however, this was due to the strong correlation of carbon content (Cohen, 1985).

Figure 2 Distribution of iodine in the environment.

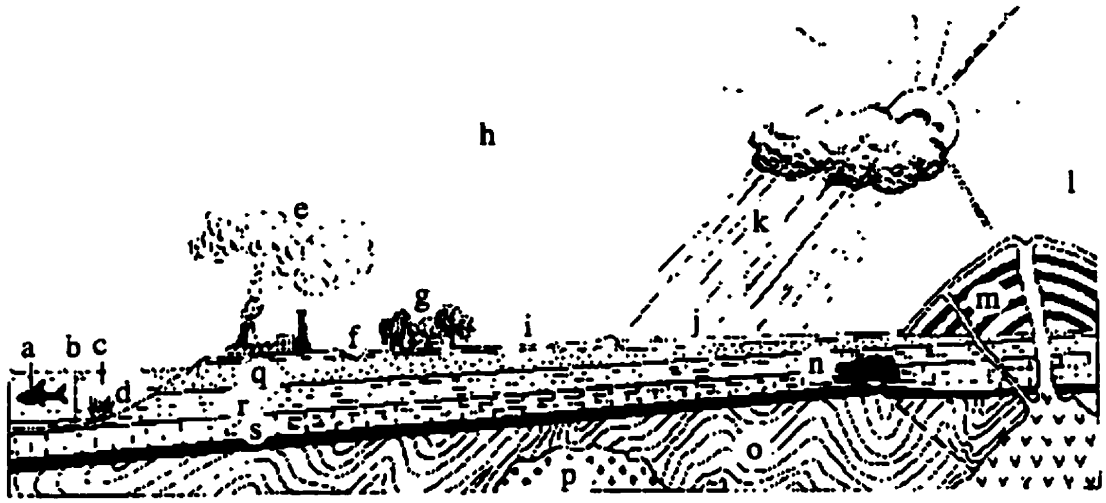

a	marine fish	1 mg/kg	l	volcanic gases	2 mg/kg (in condensates)
b	recent marine sediments	5-200 mg/kg			
c	seawater	58µg/l	m	extrusive rocks	0.24 mg/kg
d	marine plants	50 mg/kg	n	ore minerals	1.4 mg/kg
e	smoke from burning fossil fuels	1-200 mg/kg	o	metamorphic rocks	0.3 mg/kg
f	river water	1-10 µg/l	p	intrusive igneous rocks	0.24 mg/kg
g	vegetation	0.5 mg/kg	q	sandstones	0.80 mg/kg
h	atmosphere	1 µg/kg	r	shales	2.30 mg/kg
i	soil	2-15 mg/kg	s	limestones	2.70 mg/kg
k	rainwater	1-6 µg/l			

(taken from Fuge and Johnson,1983).

Whitehead (1984) reported that Duce *et al.* (1973) did not find any difference in iodine concentration from coastal to inland atmosphere of Antarctica, this may be due to the climate of that environment (low aerosol concentrations, low level of precipitation and low temperatures in Antarctica).

In contrast to this, Cohen (1985) contradicts Goldschmidt's hypothesis of iodine released from ocean surfaces and believes iodine is derived rather from the rock when it is weathered into soil. However, Fuge & Johnson, (1986) reported that Al-Ajely (1985) showed no correlation between the iodine content and the corresponding soils. Whitehead (1984) suggested that although the root uptake of iodine is important, the atmosphere is the dominant source of iodine. The reduction of iodine concentration with increasing distance

from the oceans consequently reduces the amount of iodine as well as ^{129}I transferred to inland soils as a result of washout and dry deposition (NCRP, 1983).

Table 2 Stable iodine concentrations measured in a variety of terrestial materials.

Sample type	Range of I concentrations
Fresh water	0.5 – 20 µg/l
Oceanic water	45 – 60 µg /l
Precipitation	0.5 - 5 µg/l
Soils	0.5 – 20 mg/kg
Peat	20 – 100 mg/kg
Coal	1 - 15 mg/kg
Sedimentary rock	3 – 400 mg/kg
Igneous rock	0.2 – 1.2 mg/kg
Algae	50 – 2500 mg/kg
Lichens	2 – 5 mg/kg
tree leaves, needles	0.2 – 6.9 mg/kg
Fresh water fish	0.05 – 0.2 mg/kg
Marine fish	0.5 – 6 mg/kg
Human thyroid tissue	1 – 3 mg/kg

(Milton et al., (1998) Research Contract Report to AECB, and references there in)

I.1. Natural and Anthropogenic Sources of ^{129}I

Iodine has many isotopes ranging from ^{126}I to ^{135}I. Their half-lifes range from 25 min. (^{128}I), to hours (^{126}I, ^{130}I, ^{132}I, ^{133}I, ^{134}I and ^{135}I), to days (^{126}I and ^{131}I), to 15.7 million years (^{129}I), and ^{127}I is the only stable isotope (Lederer, 1967). Of the 23 radioisotopes of iodine identified, ^{129}I is the only naturally occurring radioisotope. It is produced naturally by the interaction of high-energy particles on xenon in the upper atmosphere; neutron activated reactions: ^{128}Te (n, γ), ^{129}I and ^{130}Te (n, 2n), ^{125}I (NCRP, 1983); spontaneous fission of

thorium; fission of ^{238}U and neutron induced ^{235}U. Volcanic emissions also contain ^{129}I from fission of U isotopes in the earth's interior (Fabryka-Martin *et al.* 1989).

^{129}I is produced in nuclear fission reactions as a decay product of ^{129}Te. In 1963, J.Z. Holland tabulated the fission yields of several radioiodine isotopes from thermal neutron fission of ^{235}U. The ^{129}I mass chain is illustrated in Figure 3 with recent radioactive half-lives from Lederer (1977).

Figure 3 ^{129}I mass chain.

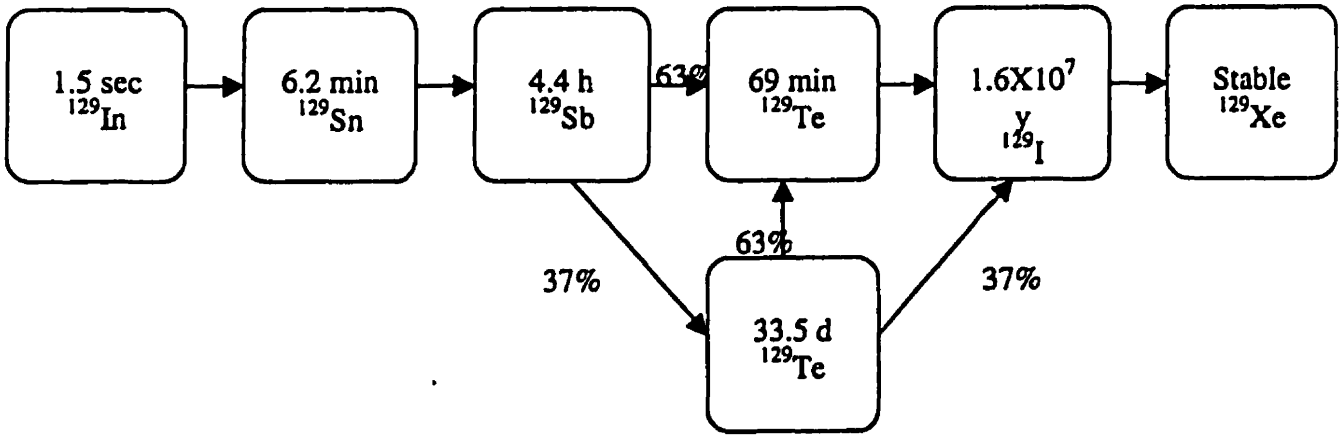

As the precursors of ^{129}I decay the quantity of ^{129}I present in a fission product mixture will increase slowly after irradiation has ceased (NCRP, 1983). Nuclear explosions of ^{235}U or ^{239}Pu also produce ^{129}I.

$^{129}I/^{127}I$ isotopic ratios from pre-1945 rainwater values were found to be 1.1×10^{-12} (2×10^{4} atoms/l) (Fabryka-Martin *et al.*, 1989). Terrestrial ratios assumed to be in secular equilibrium, from natural AgI deposits in the Great Artesian Basin in Australia, were $2.2 \times 10^{-15} \leq {}^{129}I/{}^{127}I \leq 3.3 \times 10^{-15}$ (NCRP, 1983). Since 1945, the atom ratio of ^{129}I to stable ^{127}I in the environment has been increasing due to the contribution of ^{129}I from above ground nuclear weapons testing and operation of nuclear power plants and nuclear-fuel reprocessing (NCRP, 1983; Handl, 1996).

I.2. Importance of study

Iodine-129 (^{129}I) is the longest-lived radioisotope of iodine and has a 15.7 million-year half-life. As a result of its very slow rate of decay, any ^{129}I released into the environment (from either natural or anthropogenic sources) is a long-term addition to the total inventory of global environmental iodine. In order to gain an understanding of their cycling in the short and long term behaviour, time and effort has been devoted to comparing the behaviour of radioiodine species with that of stable iodine. Because of the potential for long-term accumulation in the environment, ^{129}I is used as a tool to monitor for the presence of nuclear facilities (and as a source of radiological dose) from prolonged low-level releases, in the nuclear industry (Brauer & Strebin, 1982; NCRP, 1983; Paquette *et al.*, 1986). Waste products containing anthropogenic ^{129}I must eventually be disposed of. So regardless of whether the waste is incinerated or buried below the ground surface, there exist physico-chemical mechanisms for ^{129}I to be re-deposited on the earth's surface, or to be carried by groundwater (Milton et al., (1998) Research Contract Report to AECB). Ultimately, the final reservoir for ^{129}I is the oceans, and the resulting aquatic food chains have mankind at the top. Radioactive iodine passes rapidly through the food chain and concentrates in the thyroid gland, since the endocrine organs exhibit the highest concentrations of iodine in the human body (see Table 2, Bruner, 1963; Wood *et al.*, 1963; Colard *et al.*, 1965; Sheppard, 1996), leading to an increased risk of thyroid cancer (Fuge & Johnson, 1986).

I.3. Background ^{129}I studies

In past studies, many of the physical and biological characteristics assigned to ^{129}I were based on observations of other iodine isotopes (^{125}I, ^{127}I, ^{131}I, and ^{133}I) (Raja & Babcock, 1961; Beaujean *et al.*, 1973; Whitehead, 1974, 1978; Brauer & Ballou, 1975; Brauer &

Strebin, 1982; Bors *et al.*, 1988, 1991, 1992). The analyses of the behaviour and potential accumulation of ^{129}I released to the environment (nuclear explosions, releases of elemental vapor forms of ^{131}I in field experiments or associated with nuclear power generation (Saas & Grauby, 1973; Soldat, 1973; Kühn *et al.*, 1973; Robertson & Perkins, 1975)), were based on studies of ^{131}I as a model for short-term behaviour and stable I (^{127}I) for long term behaviour.

The occurrence and transformation of iodine involves determining the concentrations in geological, hydrological and biological settings. Studies of iodine have been conducted on natural materials (Sheppard & Thibeault, 1992; Muramatsu & Yoshida, 1995; Muramatsu *et al.*, 1995) and in the atmosphere (Uchida *et al.*, 1988, 1991; Evans *et al.*, 1988; Yoshida & Muramatsu, 1995). Equally important, is evaluating the chemical speciation of iodine (Champ *et al.*, 1984; Behrens, 1982, 1984; Muramatsu & Ohmomo, 1988; Paquette *et al.*, 1986). Determining the distribution and transformation of iodine in the environment depends on what state the iodine molecule is in (Whitehead, 1974,1984; Lang & Wolfrum, 1989).

Both reversible and irreversible fixation of iodine to matrix material occurs (Raja & Babcock, 1961; Whitehead, 1974, 1984). The behaviour and fate of radioiodine is associated with both its chemical state on the one-hand and with the chemical conditions of the system on the other (Behrens, 1982). A thorough understanding of chemical processes in the environmental systems and consequent iodine speciation is essential in order to plan studies in a given system, interpret data from experiments and predict long-term behaviour in the environment (Champ *et al.*, 1984).

From previous literature it was believed that iodide (I^-) and iodate (IO_3^-) are the dominant forms in the aquatic environment (Muramatsu & Ohmomo (1986, 1988)); whereas other studies have suggested that most of the I^- is actually taken up by and evaporated in

dissolved organics (Milton *et al.* (1992)). Fuge & Johnson (1986) and Leisser & Steinkopff (1987) indicated that iodine would exist as I^- under oxic (aerobic) conditions having a pH between 4.5 and 10. Whitehead (1974) illustrated that sorption increases with the degree of humification and I^- sorption is pH dependent (Benes, 1976). At neutral pH the I^- sorption by surface soils is largely due to organic matter and may be due to weak electrostatic bonds (primarily through physical association with the surface and entrapment in micropores) and structural cavities of intricate fabric of organic matter showing affinity to organics (Sheppard & Thibault, 1992). Several studies have correlated ^{129}I retention in organic-rich surface soils (Raja & Babcock, 1961; Brauer & Strebin, 1982; Schuttlekopff & Pimpl, 1982). Leisser & Steinkopff (1989) noted that carboniferous particles, organic substances and microorganisms, act as iodine traps taking up iodine by very slow uni-directional processes.

The chemical conversion of anionic iodine by aquatic microbes is by oxidation of I^- by extracellular enzymes to molecular iodine and then incorporation into proteins (Behrens, 1982). Previous research indicates iodine entering soils through atmospheric deposition, contaminated lake or groundwater, would be in the anionic form (I^-). Anionic exchange or incorporation into organic structure, by simple physical entrapment in water of organic matrix, could describe the retention mechanism. Soil retention of iodine has also been linked to hydrous oxides of iron and aluminum (Whitehead, 1974, 1984).

I.4. Objective of study

The objective of this study was to examine the partitioning of ^{129}I between soils, groundwater, and vegetation in a unique setting characterized by an enriched anthropogenic ^{129}I source term found in Waste Management Area C. A field and comprehensive analytical program at this site was initiated to examine the partitioning of ^{127}I and ^{129}I amongst the

various reservoirs in this system and to determine the controlling factors. This includes measurements of total iodine, ^{129}I, major elements, DIC and DOC, tritium, ^{14}C and $^{13}C/^{12}C$ ratios in groundwater and total iodine and ^{129}I in geologic and biologic materials. Groundwater from several boreholes with multi-level piezometers transecting the flow system have been sampled as well as cores from sands and peats and local vegetation to characterize the general hydrochemistry of the system and obtain information on the distribution of ^{127}I and ^{129}I.

I.4.1 Specific Objective of Study

From previous literature, iodine seemed to have an affinity for organic matter under slightly acidic pH conditions. As a result,

I) The primary objective of this study was to investigate whether iodine and radioiodine (^{129}I) was transported through the inorganic sands of the aquifer conservatively from the source area, waste management area C, to Duke Swamp, thereby determining the potential for adsorption to the organic matter in the soil of Duke Swamp.

II) The secondary objective was to quantify the extent of partitioning of ^{129}I in the study area. More precisely, to determine the amount of exchangeable iodide, oxy-hydroxide bound iodide and to the organically bound iodine. This would result in the partitioning of stable I between environmental components (aqueous, organic and mineral phases).

II. Description of Chalk River Area

II.1. Physiography

The Chalk River Laboratories of AECL (CRL) are located approximately 200 km northwest of Ottawa on the south bank of the Ottawa River (Figure 4). The laboratories are located on 37 km^2 of forested land, consisting of late Quaternary unconsolidated sediments overlying Precambrian granitic gneisses. Much of the topographic control in the area is provided by the bedrock, which is moderately to highly fractured and faulted. CRL lies within the Ottawa-Bonnechere graben, a northwest-southeast trending rift valley and subsidiary faults within the same trend to many local topographic features such as lakes and wetlands (Dolinar *et al.*, 1996).

II.2. Climate

According to Environment Canada (Environment Canada Cat. 1994), CRL is placed on the boundary between the Great Lakes/St. Lawrence climate region and the Northeaster Forest climate (Dolinar *et al.*, 1996). The average daily air temperature ranges from –12.3°C in January to 20.1°C in July. Average annual precipitation (rain equivalent) is 831 mm while annual evapotranspiration flux is estimated at 530 mm, (Noack, 1995 and references therein) leaving approximately 300 mm/year of precipitation for infiltration and runoff (Dolinar *et al.*, 1996). Where sands form upland areas (particularly in dune deposits) there is essentially no surface runoff. These upland sand aquifers are frequently very active with lateral flow velocities that range from tens to hundreds of meters per year (Killey *et al*, 1993). Prevailing winds at CRL are from west-northwest and east-southeast following the valley topography, and range between 10 to 18 km/h (Noack, 1995 and references therein).

II.3. Surficial Geology

Bouldery sandy till deposited near the end of the last glaciation (Wisconsinan) mantles the bedrock in many places. Sands deposited into Champlain Sea by glacial meltwaters, which drained through the Ottawa Valley in early post-glacial times, are the dominant unconsolidated material and cover much of the AECL property (Dolinar *et al.*, 1996). These sands were locally reworked by wind into dunes as flow in the river decreased and before vegetation cover was established (Killey *et al.*, 1993).

II.4. Description of Area C

Waste management Area C (referred to as Area C, from this point on) was established in 1963 in a sand dune on CRL property, as a facility for the storage of low-level solid waste. The site is a rectangular compound (120m X 340m) where waste has been placed in trenches between 4 to 6 meters deep. Approximately half of the low-level radioactive solid waste originated from within CRL (Dolinar *et al.*, 1996). The rest of the waste has come from hospitals, universities, industrial and research suppliers and users of radioactive materials from across Canada and from the Nuclear Power Demonstration (1963-1987) the prototype CANDU reactor. Although the wastes were inspected prior to storage, waste suppliers were asked to provide identification of radionuclide contents. Nevertheless, there are no reliable records on the total ^{129}I buried at Waste Management Area C (Milton et al., (1998) Research Contract Report to AECB).

The low-level waste consists in large part of metal, wood, plastic, paper, potentially contaminated soils and glass. A wide spectrum of laboratory and process wastes are present,

Figure 4 Geographic location of the Chalk River Laboratories (CRL), and the position of Waste Management Area "C".

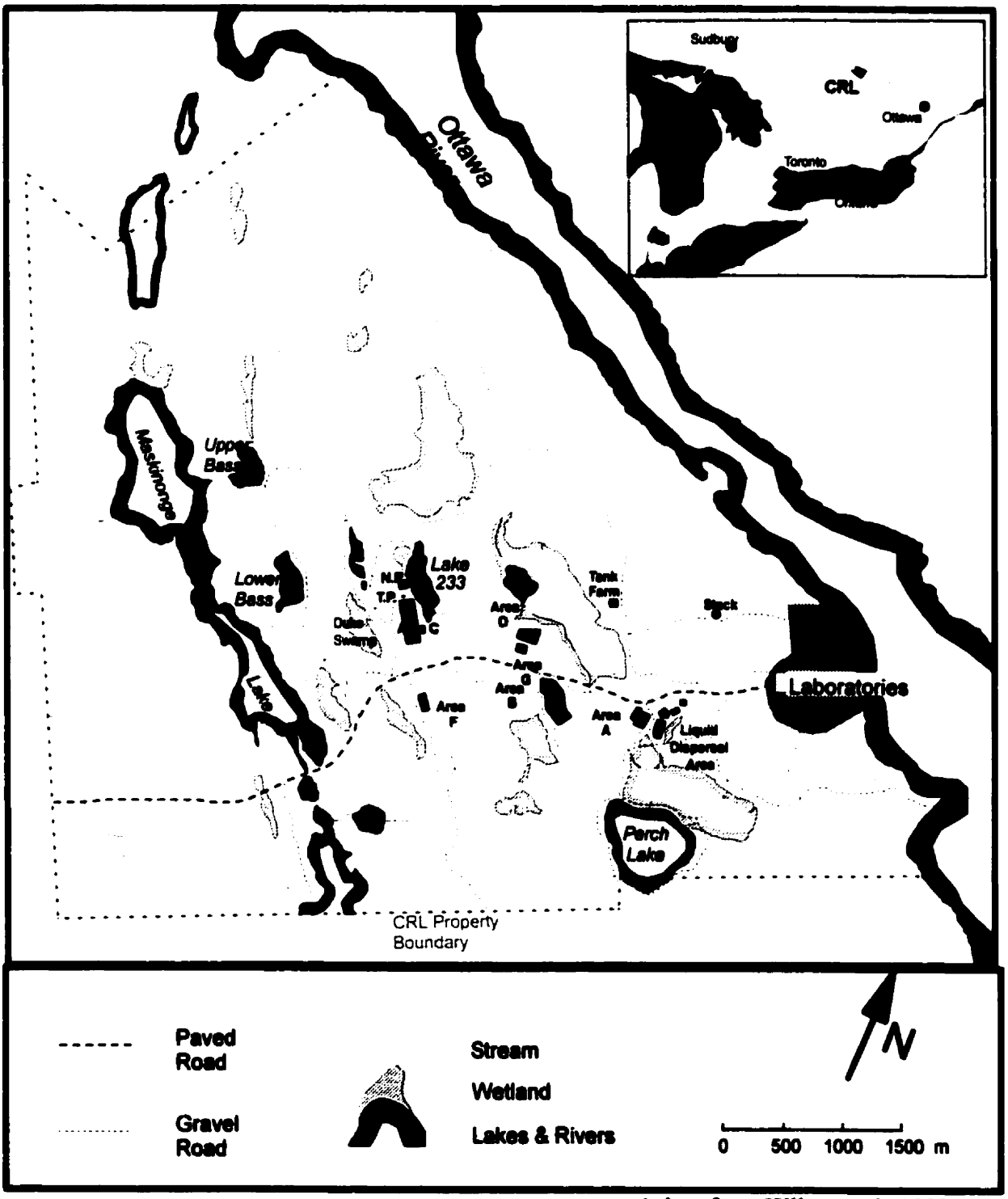

(taken from Killey *et al.*, 1993).

but in terms of major constituents Area C is considered to be similar to domestic and commercial landfill wastes without significant food-related or industrial chemical compounds (Evenden *et al.*, 1998). All wastes in Area C are located above the water table. In 1983, a polyethylene (and overlying sand) cover was placed over the trenches in the southernmost 60 m of the Area C compound, the rest of the site is only covered with sandy soils (Dolinar *et al.*, 1996).

II.5. Geology and Hydrology of Area C

Due to the site's almost flat surface and the very permeable property of the cover sands in this area, there is nearly no surface runoff. Almost all 300 mm of precipitation that is annually available for infiltration or runoff, percolates down through the waste to the underlying unconfined aquifer. Figure 5 illustrates Area C, nearby surface drainage features, locations of observation wells and contours of water table in the region's unconfined aquifer (Killey *et al*, 1993).

Figure 6, from Killey *et al.*, (1993), illustrates a stratigraphic section oriented parallel to groundwater flow. The cross section consists of bedrock, a wedge of bouldery till, unconsolidated sediments, fine and medium sands of fluvial origin below an elevation of 155m, overlain by a unit of interstratified very fine to fine sands and sandy silts. This interstratified unit is in turn overlain by fine and medium-fine sands that make up the dune ridge hosting Area C. A unit of laminated clayey silts is present in boreholes along the margin of and beneath the wetland (Duke Swamp) located about 250m southwest of Area C. Duke Swamp itself is underlain by up to 2.5m of peaty organics. At the southwest boundary of Duke Swamp and along the flow of groundwater, there is another bedrock ridge trending northwest-to-southeast (Killey *et al.* 1993, Evenden *et al.*, 1998).

Figure 5 Piezometric grid of Area C.

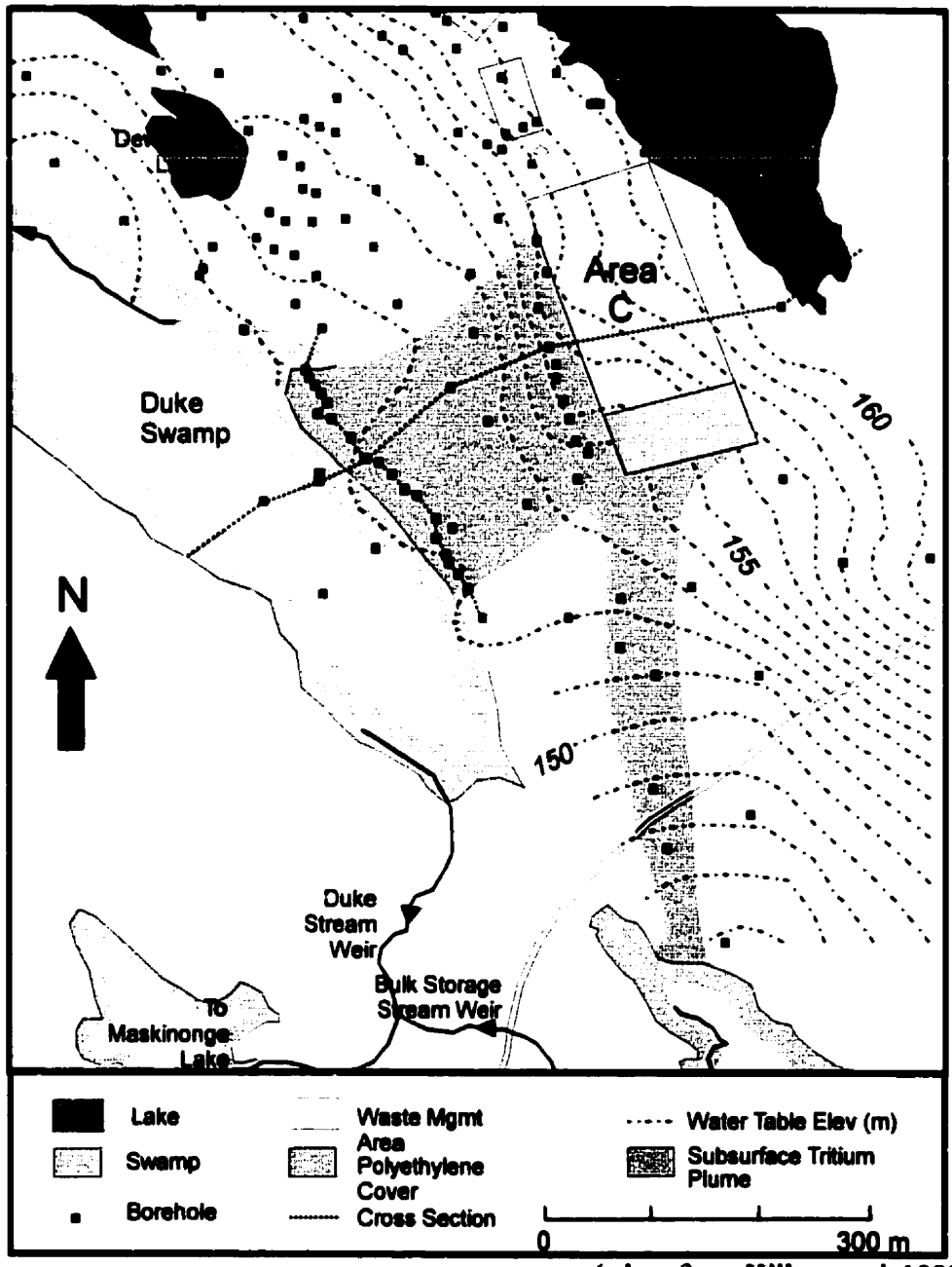

(taken from Killey *et al*, 1998)

Most of the recharge from Lake 233 passes beneath Area C flowing in a southwesterly direction through the unconsolidated sediments. Direct infiltration of precipitation (annual precipitation of 300mm) through Area C and through the downgradient sands is added to the phreatic aquifer en route. This groundwater discharges to Duke Swamp, which is drained by Duke Swamp stream and Lower Bass Creek. Tritium data from these two streams demonstrate that nearly all the Area C contaminant plume entering Duke Swamp discharges to Duke Stream. Groundwater residence times, in the aquifer system between Area C and the discharge zone are between 2 and 4 years (Killey *et al.*, 1993, Evenden *et al.*, 1998).

II.6. Site selection rationale

Waste Management Area C was chosen for this study. At this location, a source of anthropogenic ^{129}I is present in a waste disposal site situated at the summit of a sand hill. The groundwater flow system draining southwest to Duke Swamp has been well characterized by the installation of over 45 piezometers. This unique situation allows the investigation of how ^{129}I partitions in a natural setting as opposed to a laboratory setting or soil column experiments.

Figure 6 Stratigraphic section oriented parallel to the groundwater flow.

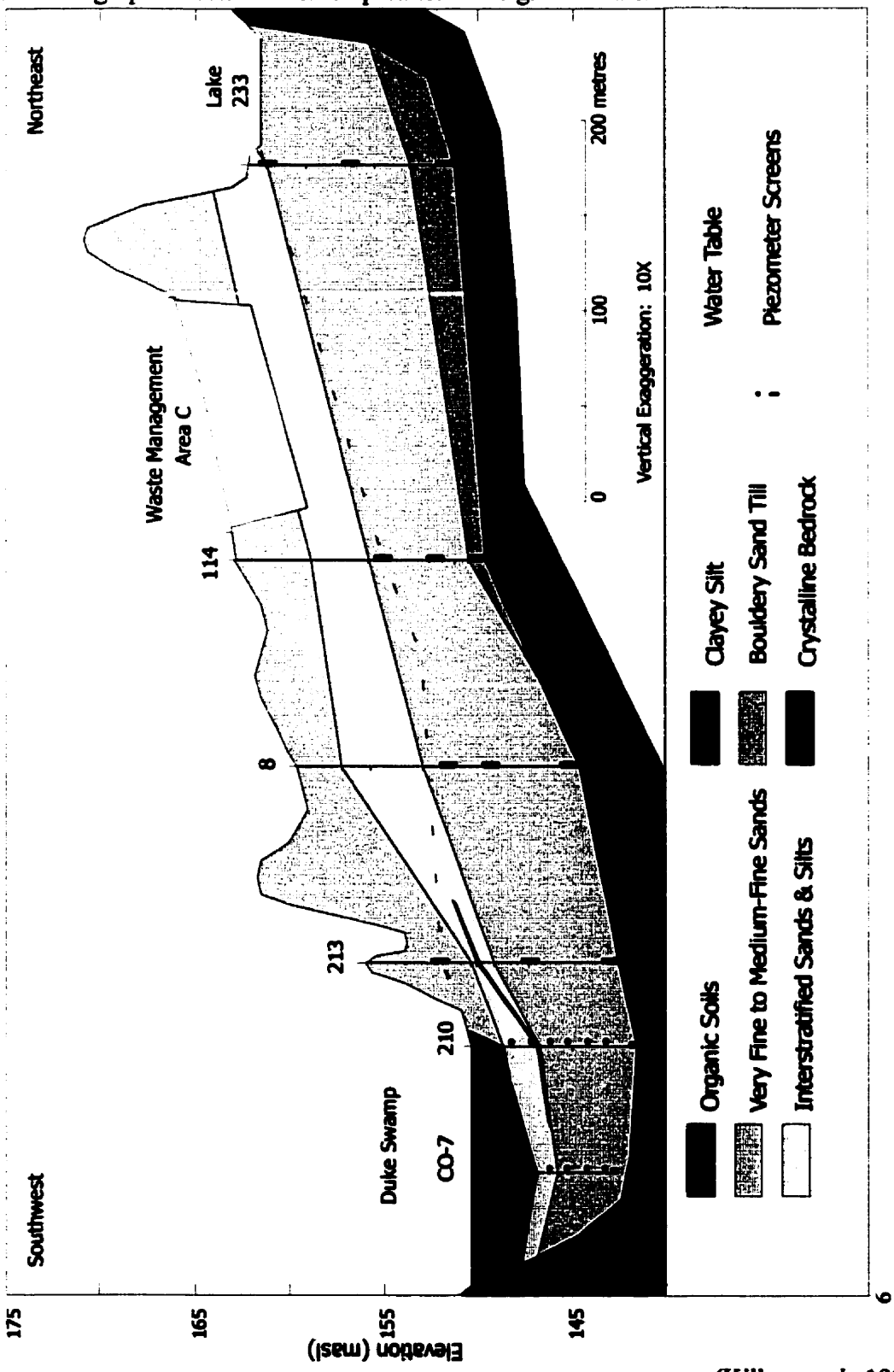

(Killey *et al.*, 1993)

III.1. Field Sampling

The objective of the field program was to collect samples from Area C that would be representative of all environmental components such as mineral, aqueous and organic phases. Samples included aquifer material (cores) for the mineral component, groundwater samples for the aqueous component and vegetation for the organic component. To these samples, various analyses and chemical treatments were performed, among which included leach experiments on soils, geochemical analysis of groundwaters and extraction (precipitation) of iodine from all mineral, aqueous and organic samples.

Figure 8 illustrates the locations of water samples that were collected from the piezometer grid in Area C (C14-7m, C14- 8.5m, C111-8m, C114-8m, C114-11m, C213-4m, C213-8m, C221-7m, C221-9m, C221-16m, CO-4, C-35, and Duke Swamp Weir (Figure 7).

Figure 7 Duke Swamp weir.

Figure 8 Sites sampled downgradient from Area C (marked in red).

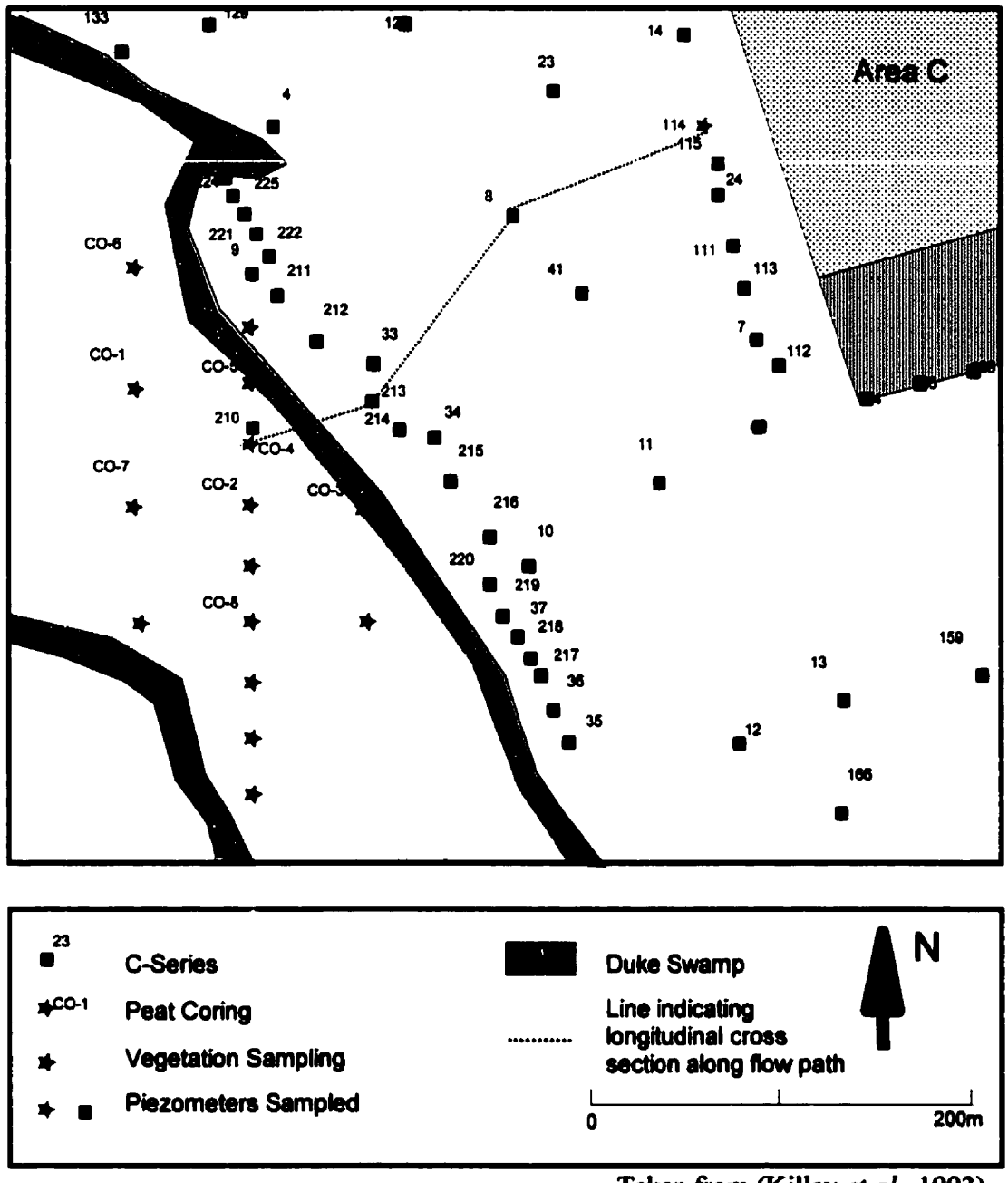

Taken from (Killey *et al.*, 1993)

III.1.1 Soil Sampling

Cores were obtained using a 9.5 cm ID hollow stem auger, driven by a CME-75 rotary rig (Figure 9), collecting continuous cores of sediment ahead of the augers using a 5 cm by 0.5-1.0 m long piston corer (Killey *et al.*, 1993). The piston sampler and core barrel, which were used in the acquisition of previous aquifer sediment samples, were used to obtain cores of the organic peat soils that have compiled in Duke Swamp. Due to restricted access into Duke Swamp, portable equipment was required. A gasoline-powered jackhammer was used to drive the core barrel into soil (Figure 10).

Drilling at C114 augured the first 15 ft. (4.57 m) to begin coring above the plume and terminating upon auger refusal. In order to avoid atmospheric or cross-contamination, the core samples were not removed from the aluminum cylinders. The samples were stored at 4°C. After the tubes were cut longitudinally and photographed, (for sediment structure such as sands, clay fractions and peat soils as seen in Figure 11), they were dried at 80°C for a period of 24 hours and subsequently ground in a puck grinder, homogenized and stored until leaching and pyrolytic experiments.

Figure 9 Drilling of core near Area C (at C114).

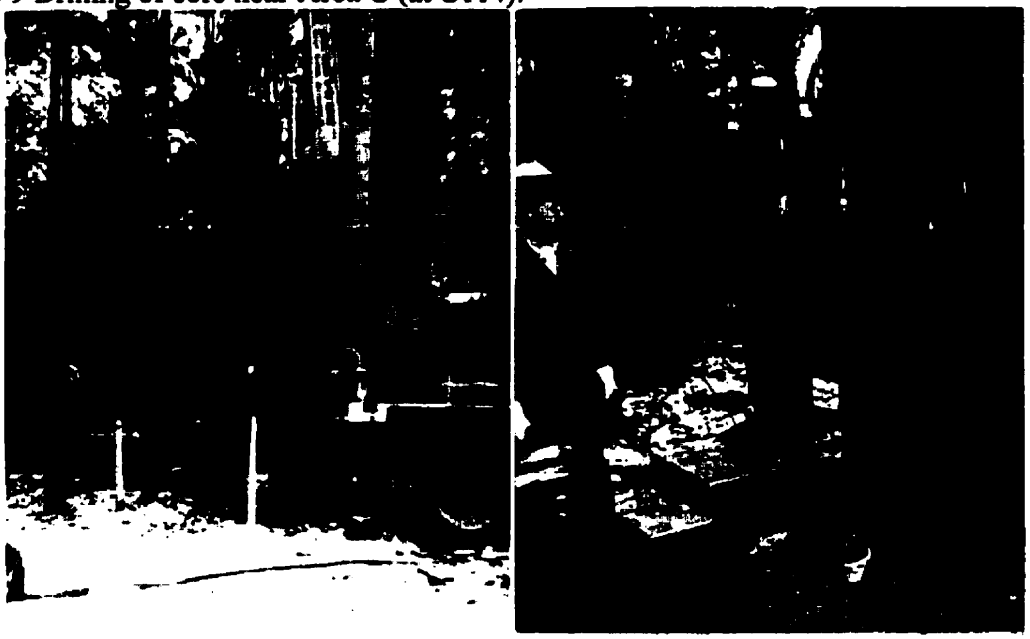

Figure 10 Core sampling in Duke Swamp (at C210).

Figure 11 Photographic logging of sediment structure.

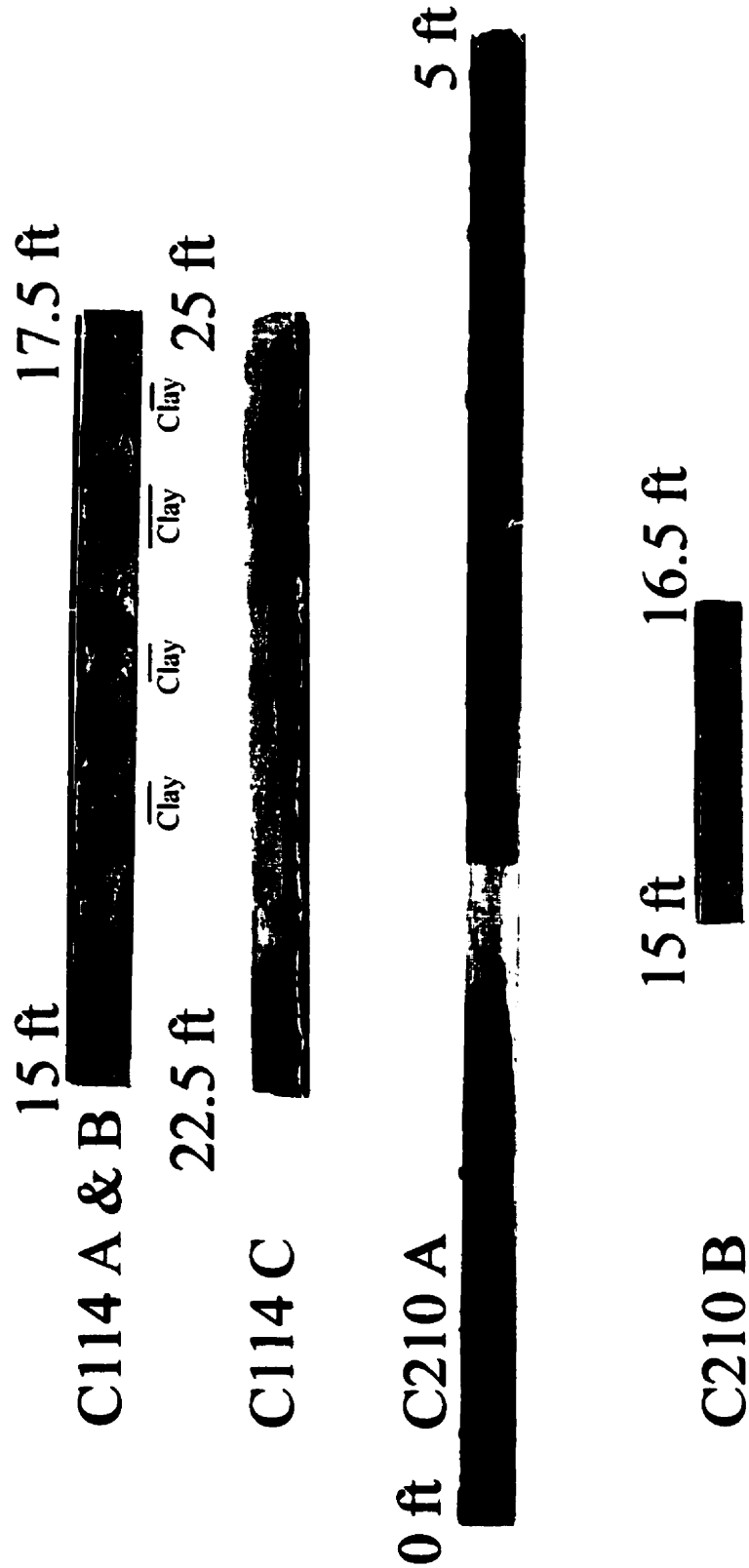

Samples from specific depths, dictated primarily by stratigraphic boundaries (Killey *et al.*, 1993), were removed and then sieved. At site C114, cores were obtained from 4.57-9.14 m (15-33ft.) depth and at C210, from 0-4.57 m (0-15ft.) depth.

The sampling procedure at C210 involved driving a 3 m long 5.0cm ID aluminum tube core barrel into the organic soil until an increase in resistance to penetration was observed (down to 2.5m). This was an indication of entry into the underlying silty sands or sands. In addition to core samples, surficial samples obtained from Twin Lakes Dunes at two intervals were taken to provide bomb fallout and background values (Figure 12).

The soil samples collected were located at C210 near the discharge area (Figure 10) in Duke Swamp, at C114 immediately downgradient from Area C (Figure 8) and from Twin Lakes sand dunes (see Figure 14 for location relative to Area C). The surficial Twin Lakes samples taken from aeolian sand dunes at various intervals (0-5cm, and –55cm below surface) were to compare the ^{129}I, in atmospheric deposition with the source ^{129}I term in Area C. Surficial sampling at Twin Lakes could also be used to determine whether ^{129}I deposited as a result of nuclear weapons testing remains in an uncontaminated sandy soil (Figure 12).

Figure 12 Surficial Dune Sampling at Twin Lakes Dune.

A) Exposing sand dune.

B) Marking depths of layers.

c) Collecting sample at specific depths.

III.1.2 Groundwater Sampling

All piezometers were either pumped using a peristaltic pump to remove at least 3 standing volumes of water or pumped dry (refusal) and subsequently allowed to recharge for sampling. This was done to remove silts and very fine sands from tube screens and the formation surrounding the screen before sampling the piezometers. In the case of 0.625cm polyethylene tubes (piezometers C221& C213), the suction line was directly attached to a piezometer tube. For piezometers and piezometer nests (piezometers C14, C111, C114, C8, C23 & C35), a 3.2 cm PVC tube was lowered into the piezometer, at which the water was withdrawn from a specific depth level in the aquifer (Figure 13).

Groundwater temperature and pH was measured in the field. Differences in the field and laboratory pH were negligible. pH was measured using the HACH pH meter with potassium chloride (KCl) electrolyte cartridges calibrated with HACH pH 4,7 and 10 buffer solutions. Alkalinity tests of all samples were conducted on site, using HACH Digital titration (Model 16900-01) and a 0.16 N H_2SO_4 cartridge provided with the kit.

Subsequently, while positioned downstream of the suction pump (and piezometer) samples were pressure filtered through 0.45 μm membrane filters. The filtration mechanism consisted of a Sartorius SM 16517E filter attached to a 60 cc syringe. A Sartorius cellulose acetate membrane filter with HACH 0.45 μm pore opening was inserted into the filter cap and the sample water was filtered accordingly. Between samples, the filter paper was discarded; the filter and syringe were raced three times with distilled deionized water, and then purged with sample water to prevent cross contamination. Latex rubber gloves were worn to prevent further cross contamination (Figure 13). The sample bottles were rinsed with sample water before being filled.

Figure 13 Sampling of piezometer nest.

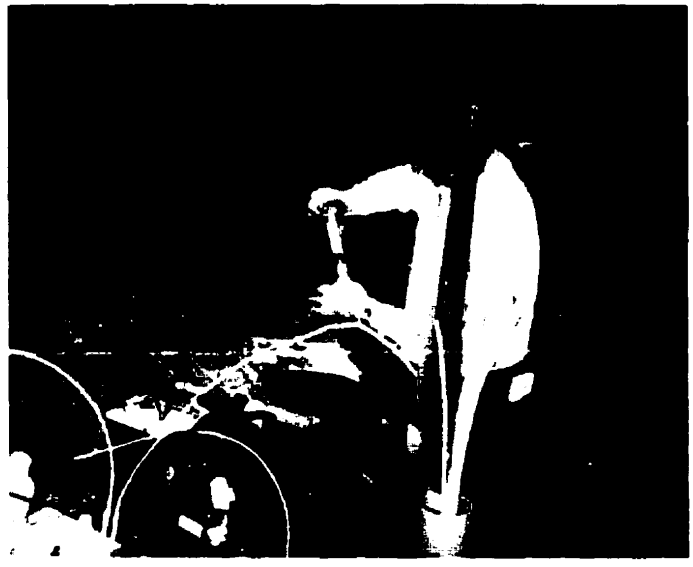

Various sized HDPE sample bottles were used in the collection of anion (50 ml), cation (50 ml), ^{13}C (100 ml), and total I analysis (1000 ml) samples stored at 4°C until analysis. 25 ml clear glass scintillation vials were used for the collection of DOC, ^{14}C and ^{3}H. Samples for DOC and geochemical cation analysis had 10% (v/v) HCl acid solution added to them.

III.1.3 Vegetation sampling

Vegetation samples were used to establish the relative ^{129}I contributions from atmospheric and groundwater sources. Samples (White Cedar) were collected in Duke Swamp over a period of 8 weeks, during which an experiment on photosynthetic ^{14}C and ^{3}H was conducted (Milton *et al.*, 1998). One set of plants were potted to observe any contribution from atmosphere and the other set was planted into the Duke Swamp peat soil in order to observe root uptake contribution of ^{129}I. Needles were collected once a week and stored in HDPE 250 ml wide mouth bottles. A background plant was sampled to obtain a

background ^{129}I value and an old cedar tree that has been growing in Duke Swamp was also sampled to obtain an estimate of an equilibrium value resulting from long-term exposure.

III.1.4 Air sampling

Air samples were collected by bubbling air through NaOH solutions at approximately 0.5L per minute, in one case for 8 hours, and another for 3 days, attempting to establish an atmospheric background ^{129}I concentration at the discharge site (Duke Swamp). To provide further information on the equilibrium air concentrations, lichen samples (also provided by AECL) had been collected from nearby trees (at approximately the same height from the ground as the cedar sampling was done). In addition, samples of fresh growth from a large cedar tree growing down at Duke Swamp were also sampled during this study.

Figure 14 Location of soil sampling relative to Area C, Duke Swamp and Twin Lake Dunes.

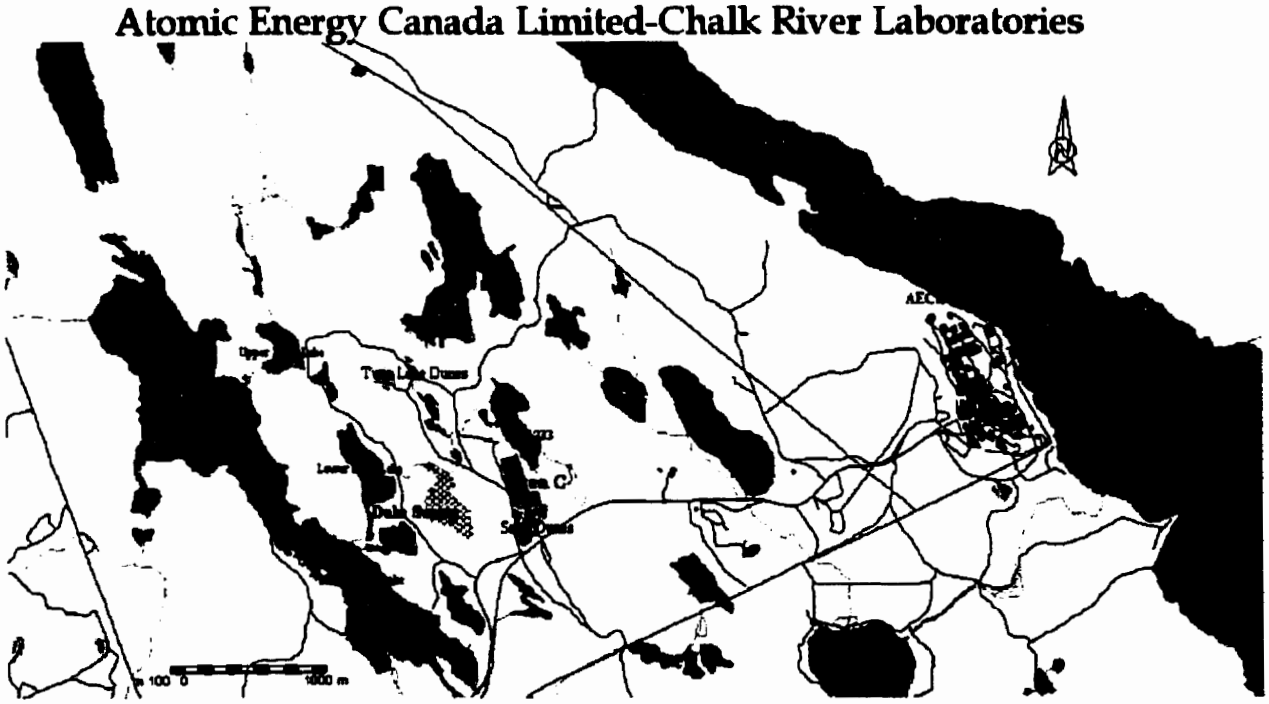

III.1.5 ^{3}H and ^{14}C (LSC)

^{3}H and ^{14}C analyses were conducted at AECL by personnel in the Environmental Research Branch-CRL. ^{3}H and ^{14}C concentrations in groundwaters were determined by Liquid Scintillation counting. Mechanical pipettes (Eppendorf and Oxford) were calibrated gravimetrically before being used to transfer 3.00 ml of water to a 22 ml polyethylene scintillation vial. A calibrated dispenser (Brinkmann Dispensette) was used to add 15.00 ml of Canberra-Packard Ultima Gold scintillation cocktail. The samples were capped, shaken vigorously, and loaded into a Canberra-Packard Model 1500 Liquid Scintillation Counter (LSC). Samples were counted for 30 or 45 minutes in 15-minute cycles. The conventional energy window for tritium (0.5 to 12 keV) was selected; for ^{14}C, blanks spiked separately with ^{3}H and ^{14}C used an energy window of 18 to 156 keV. Using these settings, detection limits for ^{3}H analysis is 10 Bq/l and for ^{14}C analysis 20 Bq/l. Analysis yielded ±10% error.

III.1.6 Geochemical Analysis (ICP-AE, HPLC)

Groundwater samples were analyzed for standard chemistry parameters including major cations and anions. Analyses were performed at the University of Ottawa's Geochemistry Laboratory. Groundwaters were collected for the analysis of major cations including, calcium (Ca^{2+}), magnesium (Mg^{2+}), potassium (K^{+}) and sodium (Na^{+}), minor elements including aluminum (Al^{3+}), iron ($Fe_{Tot.}$) boron (B^{3+}), barium (Ba^{2+}), manganese ($Mn_{Tot.}$), silicon (Si^{4+}) and strontium (Sr^{2+}). Detection limit for Ba^{2+} $Mn_{Tot.}$ and Sr^{2+} is 0.002 mg/l (ppm). Detection limits for Ca^{2+}, $Mg_{Tot.}$, Na^{+}, Al^{3+}, $Fe_{Tot.}$, B^{3+} and Si^{4+} are 0.01 mg/l (ppm). Detection limit for K^{+} is 0.10 mg/l (ppm). Analysis yielded ±10% error.

Groundwaters were collected for the analysis of major anions including fluoride (F^{-}), bromide (Br^{-}), chloride (Cl^{-}), nitrate (NO_3^{-}), sulfate (SO_4^{2-}), nitrite (NO_2^{-}) and hypophosphate

(HPO_4^{2-}). The analysis of major anions were performed by high-pressure liquid chromatography (HPLC) using a Dionex DX-100 ion chromatography system accompanied by a Dionex AS40 automated sampler, and a 2.7 mM $NaCO_3$/0.3 mM $NaHCO_3$ eluent solution (Dionex, 1992). Detection limit for F^- is 0.01 mg/l (ppm). Detection limit for Cl^-, Br^-, NO_3^- and NO_2^- is 0.05 mg/l (ppm). Detection limit for HPO_4^{2-} is 0.50 mg/l (ppm). Detection limit for SO_4^{2-} is 0.1 mg/l (ppm). Analysis yielded ±10% error.

Groundwater samples were collected for the analysis of dissolved organic carbon. Approximately 20 ml of sample water was filtered into a 25 ml clear glass bottle. The sample was then acidified with a few drops of 10 % hydrochloric acid to prevent loss of DOC. DOC analysis was performed with the Astro 2001 total organic carbon autoanalyzer. Analysis yielded ±10% error.

III.1.7 DIC-Carbon-13 Analysis (IR-MS)

Groundwater samples were collected for ^{13}C in dissolved inorganic carbon as a geochemical tracer as well. The sampling technique involved filtering 30 ml of sample water. The extraction procedure for ^{13}C involves the reaction of 85% phosphoric acid with sample water to generate CO_2. The carbon dioxide is then cryogenically purified and frozen to a break seal. Carbon-13 in the CO_2 was measured on an automated triple collector VG SIRA 12 gas source mass spectrometer in the G.G. Hatch Isotope Laboratories. Isotopic results are expressed in standard δ-‰ fashion against VPDB, according to:

$$\delta^{13}C_{sample} = \left(\frac{R_{sample}}{R_{VPDB}} - 1\right) \cdot 10^3 \text{ ‰ VPDB} \qquad \text{where } R = \frac{^{13}C}{^{12}C}$$

Analysis yields a precision of ±0.10‰ for analysis.

III.2. Iodine Geochemistry

III.2.1 Iodine Precipitation Procedure

The method used for precipitation of iodine from solutions was outlined in Chant *et al.* (1996). Sample bottles were weighed prior to and following the addition of samples being decanted (in case of groundwaters) or collection water for combustion reactions. To each sample, approximately 6 ml of conc. HNO_3 was added to reach a pH of 1. 10 mg of I^- was added in the form of KI (500µl of 2.42 g/100ml solution). A sufficient quantity of 10% $AgNO_3$ solution was added to precipitate all Cl^- and I^- as AgI and AgCl. Samples were allowed to settle overnight at 4°C in the dark. Samples were then decanted, the precipitate transferred to 50 ml centrifuge tubes and washed with dd H_2O (distilled deionized water). Concentrated ammonium Hydroxide was added to the samples until they became basic in order to dissolve all AgCl (slowly in an ice-bath). The remaining AgI precipitate was then washed with dd H_2O (X3) and ethanol (X2) and transferred into a vial, dried and ready for ^{129}I analysis by accelerator mass spectrometry (AMS).

III.2.2 Isolation of Iodide in High Salinity Solutions for ^{129}I Isotope Analysis

Because of problems of precipitation of I^- with Cl^-, subsequent partial loss of I during separation of AgCl from AgI, a column separation method was used. The method of separation was originally developed by Ross and Gascoyne (1995) for the isolation of I^- from saline groundwaters, which was subsequently analyzed for ^{127}I. In our case, we are isolating the I^- (for ^{129}I isotope analysis) from leach extraction solutions containing elevated $MgCl_2$ levels. The Chant *et al.*, (1996) method did not work in precipitating out AgI in the

magnesium chloride solutions, so a method of isolation was required. 10 mg of I^- was added in the form of KI (500µl of 20 of I^- mg/ml) prior to running the sample through the column. The glass column was loaded with 4-5 ml of Dowex Anion Exchange Resin AG1-X8, 100-200 mesh (Bio-Rad Laboratories cat. No.140-1441) in the form of a water based slurry, to form a bed 5 cm long (Figure 15a). Forty ml of 1.0 M sodium bisulphate ($NaHSO_4$) solution was introduced at a flow rate of 1.5 ml/minute, allowing it to flow through the column (this converts the ion exchange resin to the bisulphate form). 40 ml of the magnesium chloride ($MgCl_2$) leach sample was flushed through the column, followed by 10 ml of sodium hypochlorite, commercial bleach (Javex) and 20 ml of dd H_2O (Figure 15b). The solution was transferred to a 250 ml separatory funnel where it was acidified by slowly adding 5 ml of conc. HNO_3. The solution was shaken at intervals to allow the release of pressure due to the formation of Cl_2 gas. Ten ml of $NH_2OH{\cdot}HCl$ solution was added to the separatory funnel and shaken well. This converts iodide (I^-) to iodine (I_2) and is visible as a brown color appearing in the aqueous phase. Five ml of carbon tetrachloride (CCl_4) were added and shaken to extract the iodine into the organic (CCl_4) phase. Subsequent to the shaking of the solution, the organic phase containing the iodine settled out as a purple-colored eluant and was collected (Figure 16a). Further extractions with 5 ml of CCl_4 were carried out on the remaining solution until it was colorless indicating no more iodine existed in the aqueous phase (Figure 16b). 5 ml of $NH_2OH{\cdot}HCl$ solution were subsequently added to the funnel and CCl_4 extractions were repeated again, until the CCl_4 layer was colorless. Five ml of conc. HNO_3 and 2.5 ml of 1.0M sodium nitrite ($NaNO_2$) were added, shaken and subsequently extracted with CCl_4 until no more I_2 remains. All of the collected CCl_4 fractions were then placed in a clean separatory funnel where, 20 ml of deionized water and 0.5 ml of sodium

bisulphite ($NaHSO_3$) were added to it and shaken until the CCl_4 phase turned colorless. The CCl_4 was discarded and the aqueous phase was transferred to a centrifuge tube, where it was heated to evaporate any residual CCl_4. After the solution was allowed to cool, 4 ml of 0.1M silver nitrate ($AgNO_3$) solution was added and stirred. AgI precipitate is quickly formed along with AgCl. The solution was centrifuged and a subsequent aliquot of $AgNO_3$ was added to confirm the completion of the precipitation. The supernate was decanted and the precipitate was washed with 30 ml of conc. ammonium hydroxide (NH_4OH) to dissolve any AgCl. The tube was again centrifuged and the supernate was decanted. At this point the precipitate is AgI, and was washed with dd H_2O (X3) and ethanol (X2) and transferred into a vial, dried and ready for ^{129}I analysis by AMS.

Figure 15 A) Glass column loaded with Dowex Anion Exchange Resin.
B) Flushing the column with sodium hypochlorite (Javex).

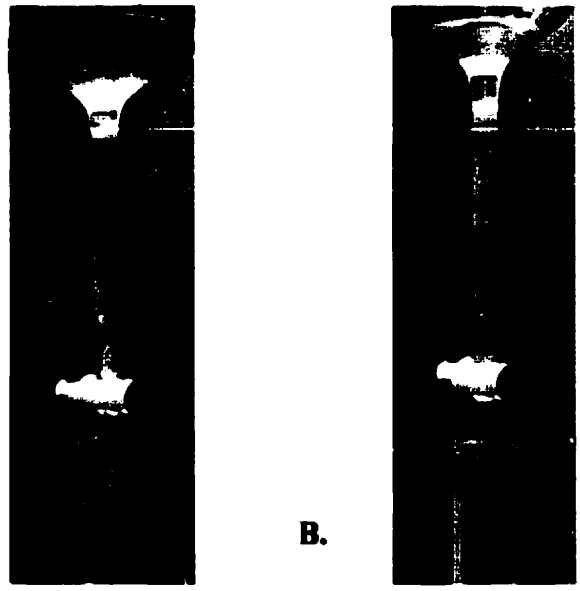

A. B.

Figure 16 A) Separatory funnel showing the aqueous phase (brownish-yellow color) and the organic phase (purple color).
B) Separatory funnel showing subsequent extractions carried out until the organic (CCl_4) layer was colorless indicating no iodine in the aqueous phase.

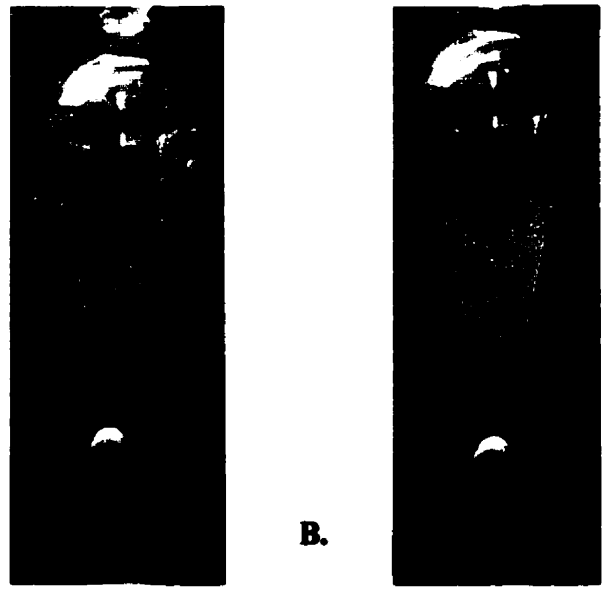

A. B.

III.2.3 Sequential Iodine Extraction Procedure

Core samples were leached with a modified method based on Tessier *et al.* (1979) to extract iodine from silty sand, sand sediments and peaty organic soil fractions. Chemical treatments were performed on soil samples from C114, C210 and Twin Lakes Dune samples.

i) Leaching Exchangeable Iodine.

25.0 g of selected fractions from each sediment was extracted at room temperature for 1 hour using 200 ml magnesium chloride (1 M $MgCl_2$, pH 7.0) and continuous agitation. The samples were subsequently centrifuged and the leachate was analyzed for stable I. I was subsequently precipitated out as AgI and ^{129}I using the method outlined in Section III.2.2.

ii) Leaching Iodine Bound to Fe-Mn Oxides.

200 ml of 0.04 M $NH_4OH{\cdot}HCl$ in 25%(v/v) HOAc was added to the sample remaining from the previous step. This was performed at ~96° ± 3°C, with occasional agitation for complete dissolution of the free iron oxides to occur. The samples were subsequently centrifuged and the leachate was decanted, analyzed for stable I and subsequently precipitated out as AgI using the method outlined in Section III.2.1. This AgI was then analyzed for ^{129}I.

iii) Leaching Iodine bound to Organic Matter.

The residue from step (*ii*) above was treated with a solution containing 100 ml of 0.02 M HNO_3 and 100 ml of 30% H_2O_2 at a pH of 2. The mixture was heated to 85 ± 2°C for 3 hours with occasional agitation. A second 20 ml aliquot of 30% H_2O_2 (pH 2 with HNO_3) was then added and the sample was heated again to 85 ± 2°C for 3 hours with frequent agitation. After cooling, 100 ml of 3.2 M NH_4OAc in 20% (v/v) HNO_3 was added and the

sample was diluted to 100 ml and agitated continuously for 1 hour. The addition of ammonium acetate prevents absorption of the extracted iodine onto the oxidized sediment.

The eluent from step iii) (above) could not be analyzed for stable I as the precipitate did not produce a voltage signal during AMS analysis. Therefore, another method was used to obtain I for isotopic ratio analysis on the organic fraction. Fresh soils samples were weighed (20 g of C210A (peat) and 40 g for C210B, C114A-C (sands)) and allowed to soak in 1M KOH (at 25°C) for 24 hours. This alternative treatment degrades organic molecules to determine fraction of stable I and ^{129}I. Fifty ml of 1M KOH was added to the 40 g samples and 30 ml of 1M KOH to the 20 g of peat sample. It was not possible to determine the stable iodide concentrations in the eluant by ICP-MS because of matrix problems. Furthermore, because of the dark brown colors produced in the solutions, analysis by colorimetric methods was not possible. However ^{129}I analysis by AMS could be conducted on the precipitates. Yields for KOH extractions using ^{125}I was performed and ranged between 49-51% $K^{129}I$ recovery.

Distilled deionized water used, in preparing the stock solutions and in each step of the leaching procedure, was obtained from a MILLIPORE system. All glassware used was previously soaked in 14% HNO_3 (v/v) and rinsed with deionized water. All reagents used were analytical grade or better.

III.2.4 Pyrolytic Extraction of Iodine from Sediment Core and Vegetation Samples

Pyrolytic extraction of iodine was conducted on sand, peat organic soil samples (C-114, C210 and Twin Lake Dune samples) and vegetation samples from Duke Swamp (at various time intervals). To do this, sand samples were crushed to powder using a tungsten

carbide grinder. Sample sizes were 0.5 g for vegetation and 1.0 g for sand and organic peat soil. Soil samples were mixed with a V_2O_5 (0.03mg) accelerator to facilitate combustion. Each sample was placed in a pre-combusted nickel boat. The boat was then placed in a quartz tube furnace and heated to 1000°C. Iodine, along with other volatiles, was removed from the combustion tube by a wet oxygen stream flowing over the sample at 1.6 l/min (Chant *et al.*, 1996). Vegetation samples were completely combusted to ash fully in the furnace without V_2O_5.

Gases were initially collected in 50 ml centrifuge tubes, containing 40 ml of 0.1M NaOH. However, the NaOH precipitated from the solutions blocked the nebulizer on the ICP-MS, which precluded sample aspiration, and hence analyzing these NaOH solutions for stable I by ICP-MS. To rectify this, the combustions were repeated and gases were subsequently collected in 50 ml centrifuge tubes containing 40 ml of dd H_2O, cooled in an ice bath. A known amount of ^{125}I tracer was added to the samples to be combusted to determine the efficiency of collection using water instead of NaOH. The combustion gases were collected over a 15 minute period. Blanks, consisting of 5 minutes of wet oxygen stream flowing without a sample in quartz tube, were inserted between samples to observe if there was any I being carried over between combustions of the samples. The blanks indicated that an average of less than 1.7% was being carried over (Table 3). Stable I measurements were conducted on all samples combusted via ICP-MS and iodine was precipitated using the method outlined in Section III.2.1 for AMS analysis.

Table 3 Combustion yields of vegetation samples.

Samples Spiked with ^{125}I Radio tracer	^{125}I Recovery (%)
Blanks between combustions	<1.7
Vegetation samples combusted at 800°C	24.8 - 41.6
Vegetation samples combusted at 1000°C	51.3 - 63.6
Vegetation combusted at 1000°C, 24h after spiking with tracer	42.8 - 47.4
Vegetation combusted at 1000°C, immediately after spiking with tracer	60.9 - 63.6
Sediments combusted at 1000°C	90.7 - 96.7

Radiotracer ^{125}I was analyzed using a Canberra Packard Minaxi Auto Gamma 5000

III.3. Stable Iodine Analysis (ICP-MS)

Inductively Coupled Plasma-Mass Spectrometry (ICP-MS) was chosen for stable iodine determination. It showed good linearity in the analysis of samples with highly variable iodine concentrations (refer to Table 2 for various ranges of iodine concentration that exist in environmental samples). Samples were run using the ICP-MS facility in the General Chemistry Branch of AECL at Chalk River. Groundwaters, vegetation and soil experiments were analyzed for stable I. For the $MgCl_2$ and KOH leachates, difficulties were encountered during the analysis of combustion solutions (0.01M NaOH) and as a result, distilled deionized water was used instead of sodium hydroxide. Detection limit for the instrument is 0.2 µg/l and analysis yielded ±10% error.

III.4. ^{129}I Accelerator Mass Spectrometry Analysis (AMS)

Accelerator Mass Spectrometry was chosen as the method for determination of ^{129}I because it has a low detection limit as it counts atoms of the ^{129}I nuclide in the sample. In comparison to counting techniques (i.e. Liquid Scintillation Counting, LSC), the latter use only a small fraction of the atoms that decay during the measurement experiment thus increasing error. In cases where the half-lifes of the nuclides are less than 1000 years,

resulting in high decay rates, β^- counting determinations (LSC) are preferred. However, for longer-lived nuclides, as in our case where ^{129}I, has a half-life of 15.7 million years, accelerator mass spectrometry is the method of choice. Sample preparation for AMS is simpler than other methods such as Neutron Activation Analysis (NAA), which requires pre- and post-irradiation chemistry (Burns & Ryan, 1995; Muramatsu & Yoshida, 1995). $^{129}I/^{127}I$ ratio and ^{129}I detection limits with AMS are generally lower [10^{-13}, 10^7 ^{129}I atoms (Elmore *et al.*, 1980; Fabryka-Martin *et al.*, 1985)] compared to NAA [10^{-8}, 10^7 ^{129}I atoms (Dickin, 1997)], respectively.

"The principal attributes of the tandem accelerator used in AMS are the charge-exchange process, which removes molecular interferences and the very high ion energies achieved which allow energy-loss detectors to resolve atomic isobars. The initial acceleration of negative ions by a positive potential in the megavolt range, followed by charge exchange of the ion beam, after which positive ions are accelerated back to zero potential is the essence of the tandem accelerator. During the charge-stripping process, isobars of the different elements often behave in a different ways, allowing their subsequent separation, while molecular isobaric interferences are destroyed. Charge stripping may be accomplished by passing an ion beam through an electron-stripping gas (e.g. argon) through a thin graphite film, or (in very high energy accelerators) a thin metal foil" (Dickin, 1997).

^{129}I analysis by AMS has only one isobaric interference, ^{129}Xe, which does not form stable negative ions (Kilius *et al.*, 1990). The principal interference is ^{127}I, which at isotope ratios above 10^{12} forms a peak tail that must be removed by a time-of-flight analysis in addition to magnetic and electrostatic analyzers. Analysis was conducted at IsoTrace Laboratory at the University of Toronto. The minimum $^{129}I/^{127}I$ ratio detectable using the

AMS at IsoTrace laboratory is 10^{-14} (Dickin, 1997). Total errors, including errors introduced by stable iodide measurement, are considered to be on the order of ±20 % for ^{129}I measurements.

IV.1. Plume Definition

In order to fully understand the dynamics of the ^{129}I plume and systematics of iodine in the study area, the groundwaters were also analyzed for ^{3}H and ^{14}C. Groundwater flows from Lake 233, beneath Waste Management Area C, and 200m southwest towards Duke Swamp. As groundwater flows beneath Area C, there is a potential to acquire contaminants that have percolated downwards through the sands from the storage site. The levels of tritium in the contaminant plume guided the selection of piezometers sampled because tritium concentrations of >10 Bq/ml have previously been used to define the boundaries of the contaminant plume originating from Area C (Figure 17).

IV.1.1 ^{3}H Plume

Evapotranspiration plays a substantial role in the atmospheric tritium systematics in Duke Swamp (Killey *et al.*, 1993). With the water table within a meter of the wetland's surface throughout the year, Killey *et al.*, (1993) suggested that it was reasonable to assume that vegetation in the discharge area will transpire at the maximum (or potential) rate. This results in the release of tritium to the atmosphere as water vapor (as HTO). Based on an annual average potential evapotranspiration of 630 mm/a and the surface area of the contaminated portion of Duke Swamp (60,000 m2), Killey *et al.*, (1993) calculated that evapotranspiration accounts for an average loss of 37,800 m^3/a of water from the wetland. Within the swamp, tritium concentrations vary geographically. However, Killey *et al.*, (1993) assumed that evapotranspiration affects all regions equally and that average tritium

concentrations in Duke Swamp also represent the average concentrations in evapotranspiration losses.

A second feature to note in Figure 18, is the confinement of most of the tritium to the aquifer beneath the clayey silt stratum that lies within the interstitial sand and silt stratigraphic unit. This distribution supports the inference (Killey *et al.*, (1993)) that the low-permeability clayey silt unit, which has limited lateral extent towards Area C, does not present an impediment to the downward movement of groundwater along much of the aquifer flow path (between the source and the transect). The sinking of the contaminant plume along the flow path should be considered a response to the addition of water to the aquifer by infiltration between Area C and Duke swamp, the slight density contrast between the dilute leachate plume and uncontaminated groundwater may also play a minor role.

A third feature of the tritium plume is its pronounced lateral and vertical heterogeneity, with concentrations at C-221 that are almost an order of magnitude higher than concentrations encountered in samples from any other borehole along the transect. This pattern is a reflection of two processes, the heterogeneity in the sedimentary strata and the heterogeneous nature of ^{3}H released from the multiple trenches in waste management Area C. The very large differences in concentration over short vertical and horizontal distances also helps to illustrate the fact that the Area C plume is better envisioned as a collection of overlapping small plumes rather than a single source feature (Killey *et al.*, (1993).

Figure 17 Cross section of Area C along flow path illustrating ^{3}H plume.

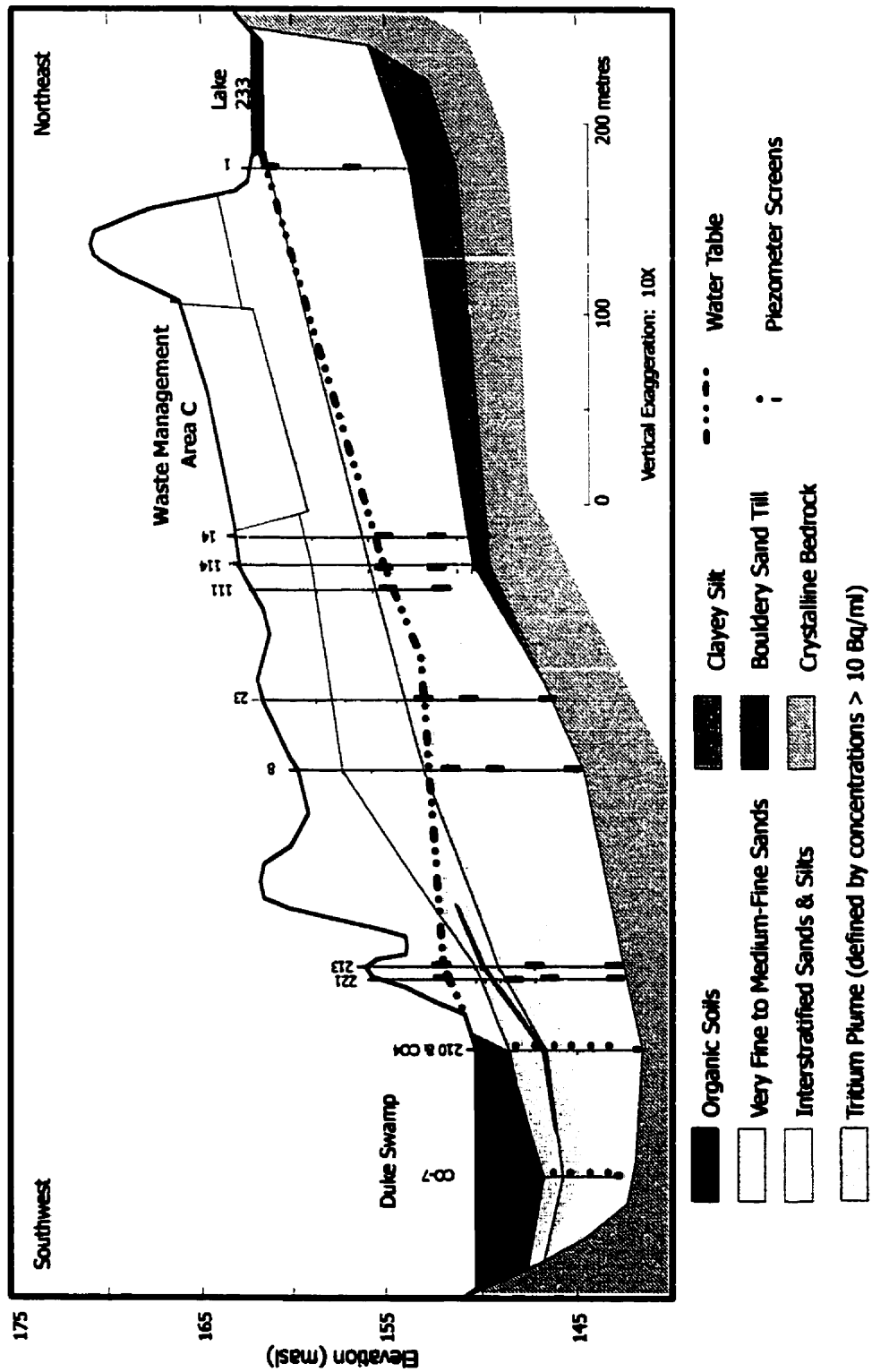

(Taken from Killey *et al.*, 1993)

Figure 18 Cross section perpendicular to groundwater flow of ^{3}H plume near discharge site.

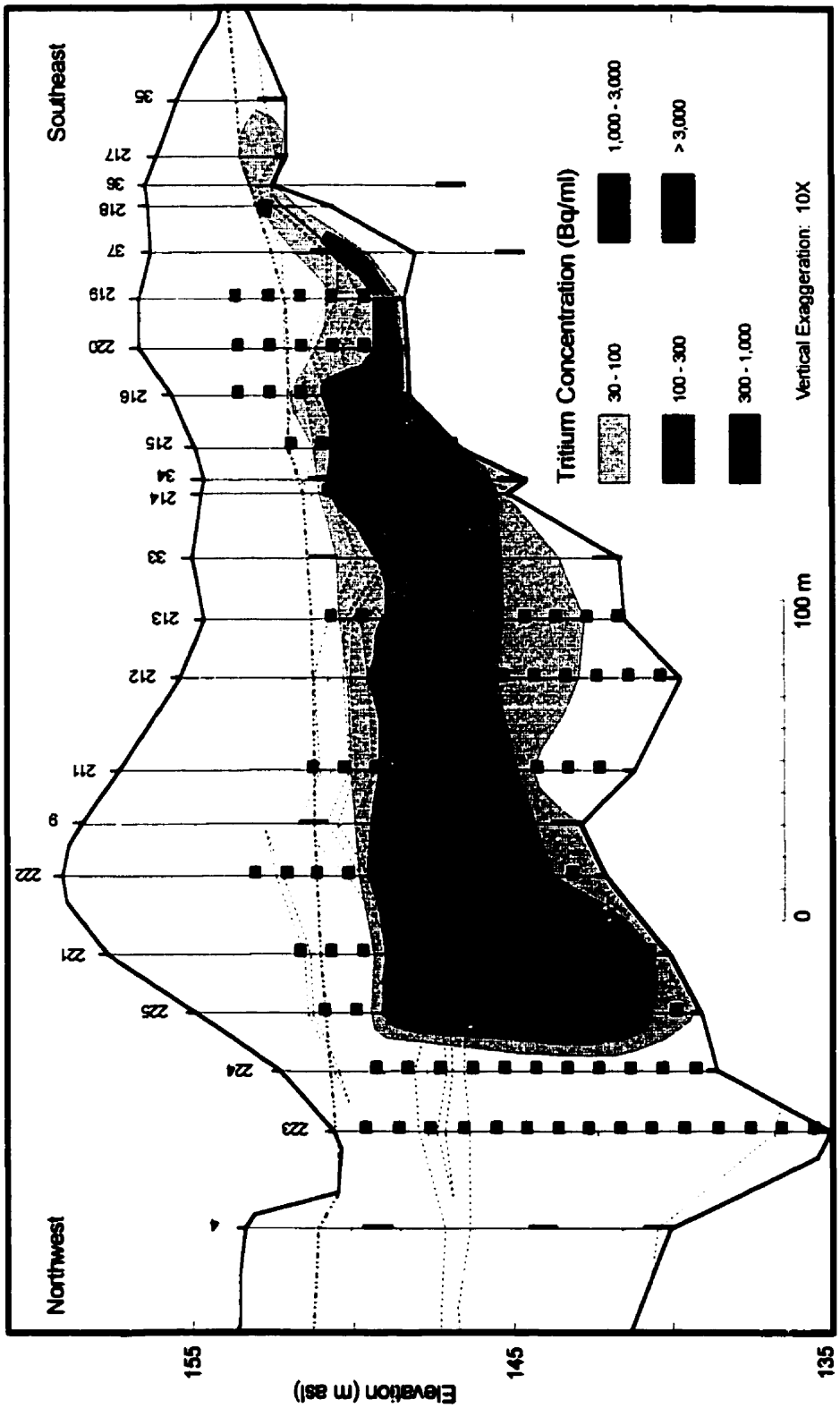

(Killey *et al.*, 1993)

Figure 19 Spatial distribution of ^{3}H.

(A., B. and C. represent above, in and below plume, respectively)

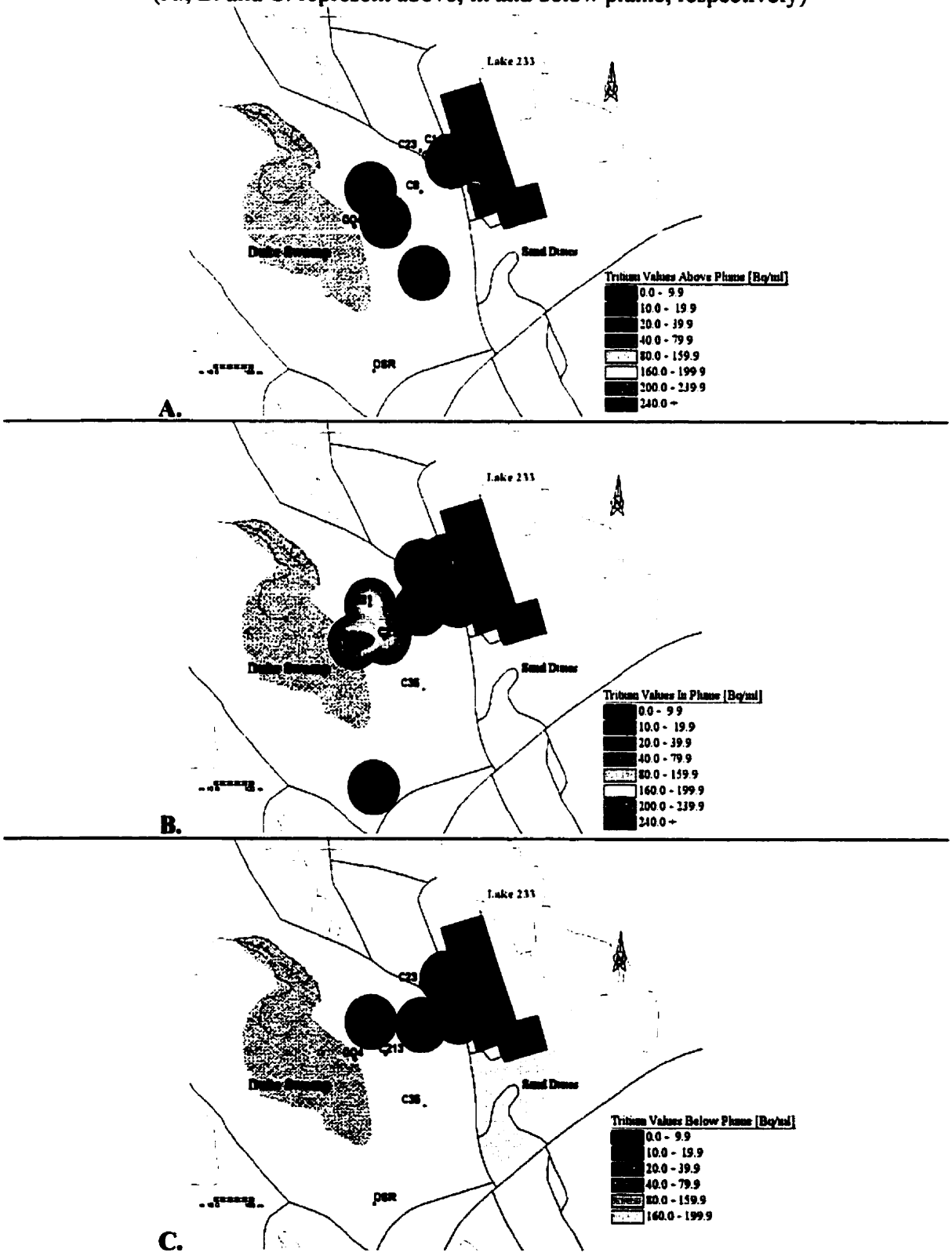

IV.1.2 ^{14}C Plume

The distribution of radiocarbon in the plume is presumably very similar to the distribution of tritium (Killey et *al.*, 1993). However, the analytical detection limit of 20 Bq/l, as a result of the method of direct counting used in groundwater samples, effectively limits the interpretation as the ^{14}C contours are defined for a substantially smaller portion of the aquifer (Killey *et al.*, 1993). As with the tritium, most of the radiocarbon occurs in the contamination plume below the clayey silt stratum that lies at elevations between 148 and 151 masl, with concentrations decreasing towards the bedrock (Figure 20). There are two areas of maximum ^{14}C concentration evident in the transect and the spatial distribution maps (Figures 20 and 21); both lying southeast of the subsurface plumes having the highest tritium concentrations (Figure 18) (Killey *et al.*, 1993). The displacement of ^{3}H relative to ^{14}C in the groundwaters is assumed to be a reflection of the variable geographical distribution of contaminants within the buried wastes at Area C (Killey *et al.*, 1993).

Figure 20 Cross section perpendicular to groundwater flow of ^{14}C plume near discharge site.

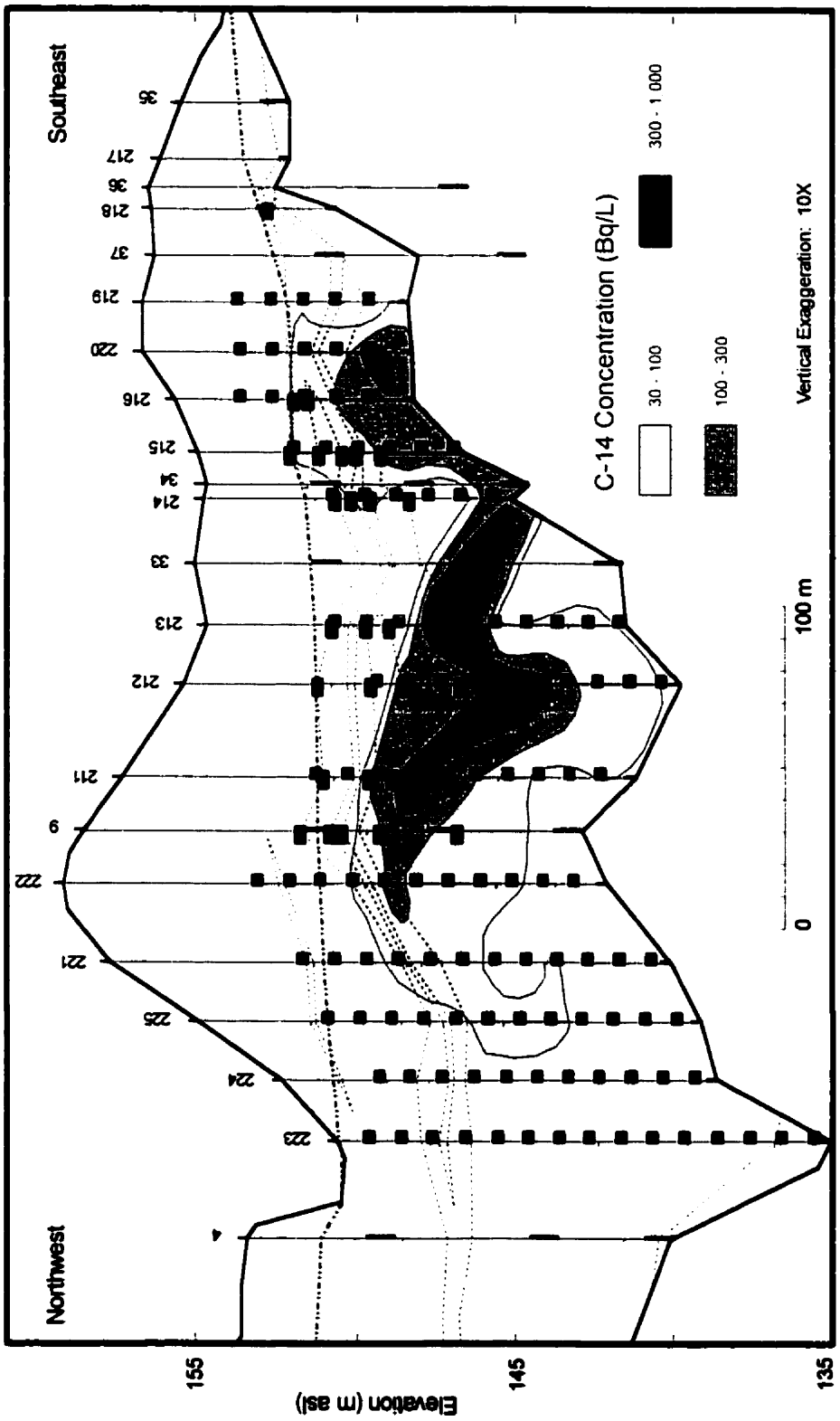

(Killey *et al.*, 1993)

Figure 21 Spatial distribution of ^{14}C.

(A., B. and C. represent above, in and below plume, respectively)

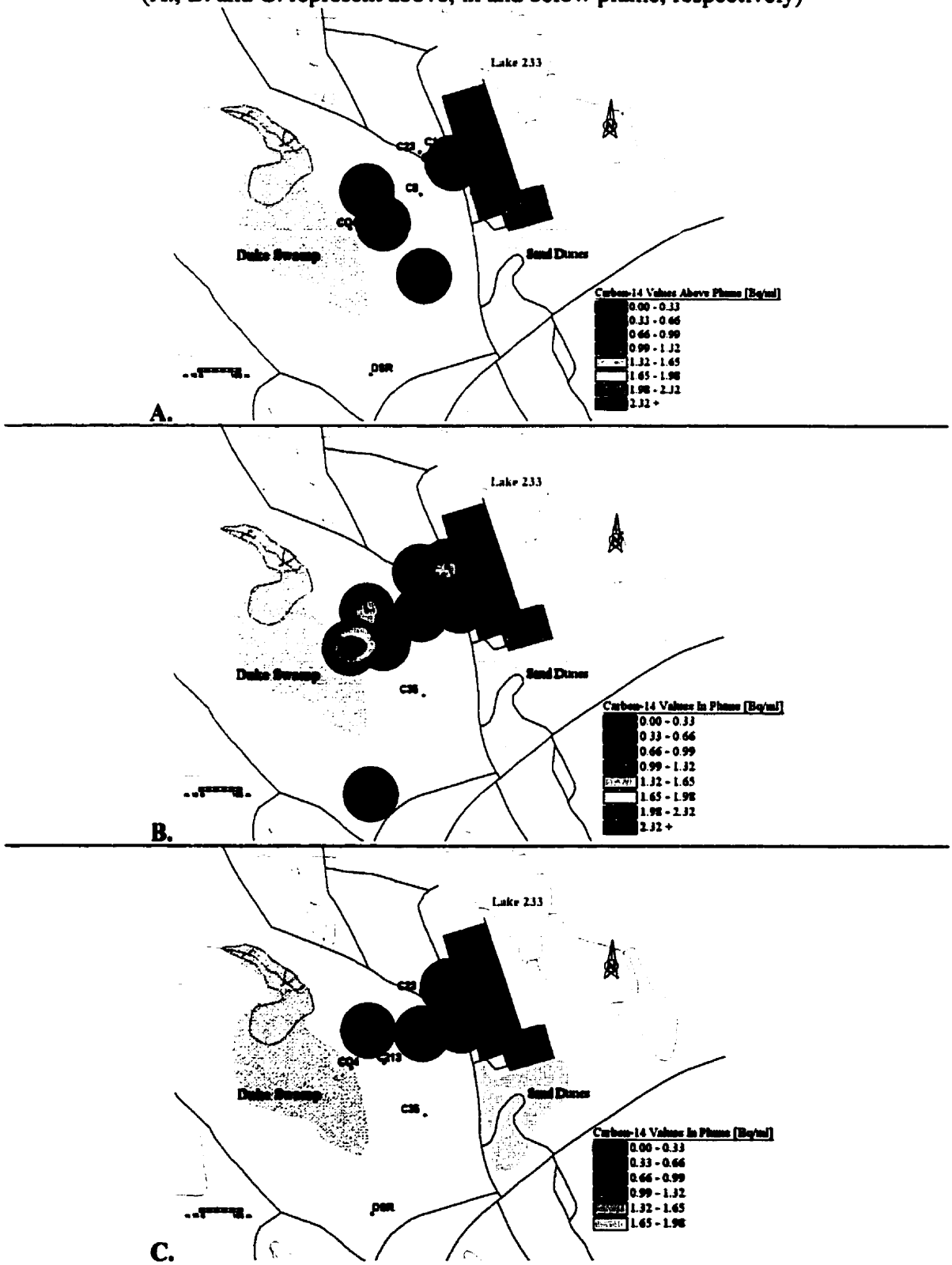

IV.2. Aqueous Geochemistry

Geochemical analyses on all groundwater samples are given in Table 5 and Table 6. Cross-correlation results between ^{3}H, ^{14}C, stable I and ^{129}I and all major geochemical species are given in Table 4. The flow system throughout is characterized by the Na-Ca/Cl-HCO_3 geochemical facies illustrated by the piper diagram in Figure 22. There is no geochemical distinction evident between groundwaters in the C14, C111 and C114 (recharge area) and C213, C221, C35 and DSR (the discharge area along Duke swamp). However, the higher Na-Cl component in the samples from C14 is an apparent exception (Table 5).

Figure 22 Piper diagram of geochemical results for groundwaters.

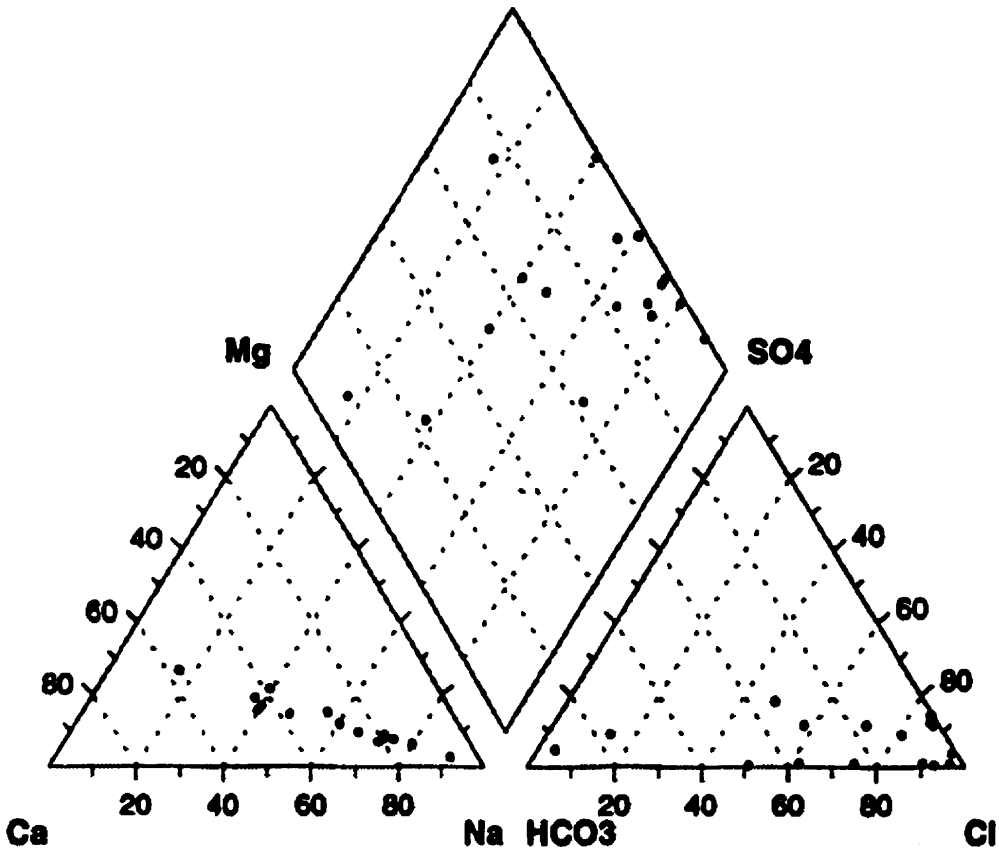

IV.2.1 Cations and Anions

An obvious geochemical aspect of the interpretation of the piper diagram plots for these groundwaters is the strong Cl^- component. This is fully supported in some groundwaters by Na^+, indicating a NaCl source, possibly from road salt. The groundwaters in the recharge area have a concentration between 55 and 90 mg/l Cl^- with up to 672 mg/l (C14-7). Dust suppressant agents ($CaCl_2$) are the most likely indication as to why there is an excess of Cl^- relative to Na^+ (Figure 22). Only two samples have strong Na^+ excess, indicating additional sources of Na^+. These results fall above the expected range of results for Na^+ and Cl^- in comparison to the values found in the Preliminary Safety Analysis Report (PSAR) for the Intrusion Resistant Underground Structure (IRUS) (Dolinar *et al.*, 1996). Normal background chloride concentrations in local groundwaters are between 0.6 and 1.5 mg/l. However, much of the chloride observed is related to the salt contamination of Lake 233, which has part of its water input from a ditch that drains a section of the CRL plant highway into the south end of the lake. The application of de-icing salt is the source of the increased concentrations of chloride in all the sampling wells immediately downgradient of Lake 233 (Dolinar *et al.*, 1996). The residence time in the aquifer system between Area C and the discharge zone is between 2-4 years (Killey *et al.*, 1993, Evenden *et al.*, 1998). It is evident that the Na^+ and Cl^- concentrations would increase year after year and accumulate in Lake 233 more readily than the groundwater influx can pick up this salt contamination. In addition there seems to be a local contribution to the Na^+ and Cl^- concentration in Area C from salting the access road which leads to the entrance of the compound (Figures 23 to 25). The entrance is located adjacent to piezometer C14, and at this point there is a large open area that allows salt trucks access to turn around and go back to salting main or other access

roads. Figures 23, 24 and 25 illustrate the elevated concentrations of Na^+ and Cl^- in the environment.

There is no statistical indication that any major geochemical species evolved from the waste compound. This is validated by the cross-correlation analysis of ^3H with geochemical species illustrated in Table 4. The water quality of the contaminant plume from Area C has been described as a dilute landfill leachate (Killey *et al.*, 1993). Groundwater from piezometer C35 contains very low to no measurable tritium. In a comparison with this and other piezometers sampled indicates that there does not appear to be any distinction amongst the major and minor trace elements in groundwaters with little to no measurable tritium relative to groundwaters having high tritium.

The concentration of Ca^{2+} in the groundwaters ranged from 6.6 to 43.4 mg/l and upon initial inspection of these data, it was thought to reflect the low reactivity of the quartz sand aquifer. This included minor contribution of Ca^{2+} may come from weathering of feldspar grains within the aquifer, or release from clay minerals through cation exchange for Na^+. In spite of that, when the spatial distribution Ca^{2+} data were drawn (Figure 25) a more reasonable explanation came to light with respect to the Na^+, Cl^- and Ca^{2+} concentrations. The spatial diagrams of Na^+, Cl^- and Ca^{2+} all illustrate the local contribution of road salt to the infiltrating groundwaters in Area C. Road salt is predominantly composed of NaCl, however; it is treated with Ca^{2+} in the 'Pre-wetting' process, prior to salting roads (Dunn, personal communication). This is further supported by the cross-correlation analysis of Na^+, Cl^- and Ca^{2+} with geochemical species illustrated in Table 4.

WAT4 thermodynamic computer software program (Ball, 1991) was used on the geochemical data and yielded results that indicates the waters are undersaturated with respect

to calcite (log $SI_{cal.}$ = –3.3 to –3.5; where log SI = log [ion activity product/mineral solubility constant]) (Table 5)). Similarly, silicate alteration products, including kaolinite and illite, are highly undersaturated. However, these waters are close to saturation with respect to amorphous silica.

Figure 23 Spatial distribution of Na^+.

(A., B. and C. represent above, in and below plume, respectively)

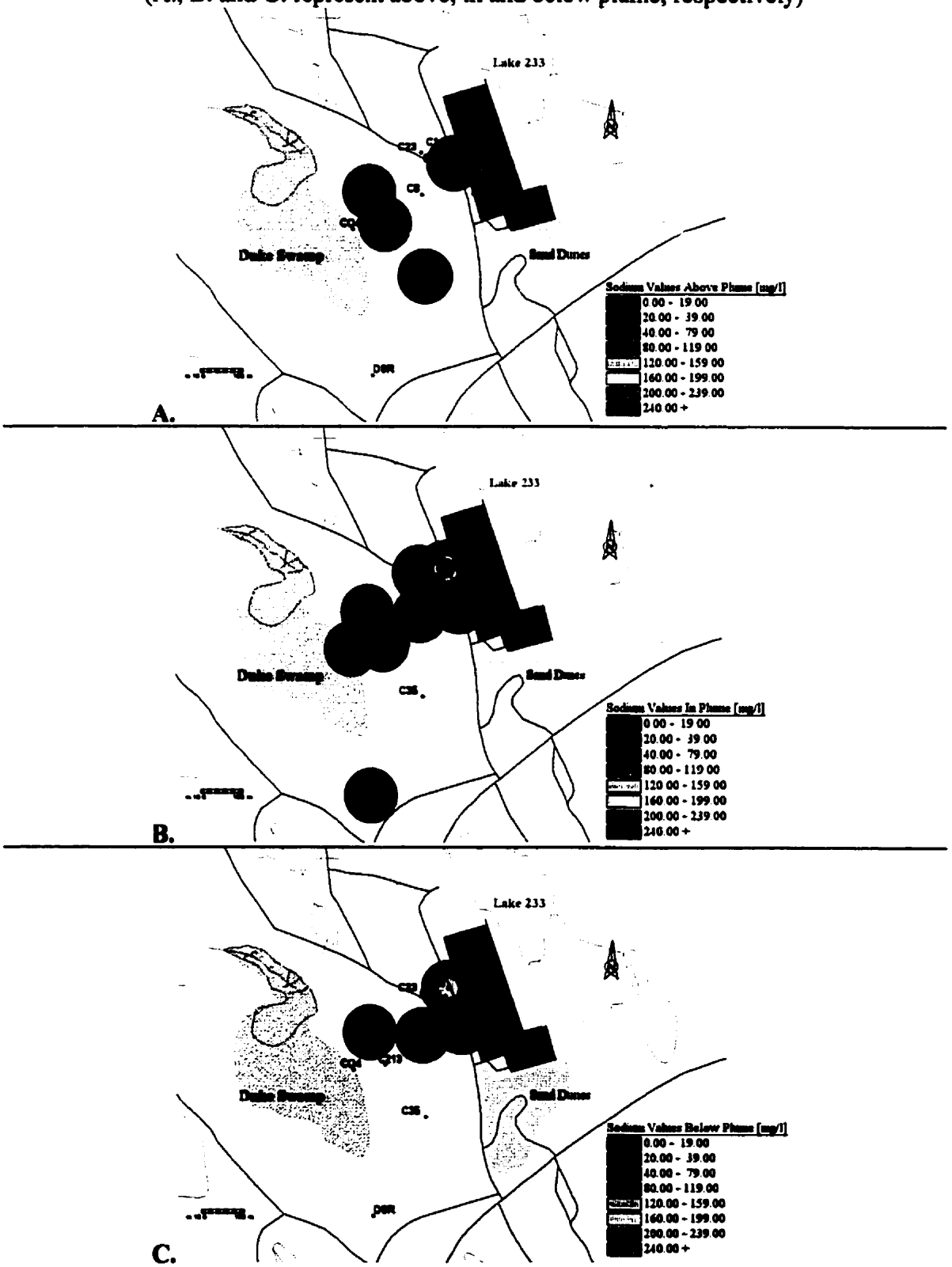

Figure 24 Spatial distribution of Cl^-.

(A., B. and C. represent above, in and below plume, respectively)

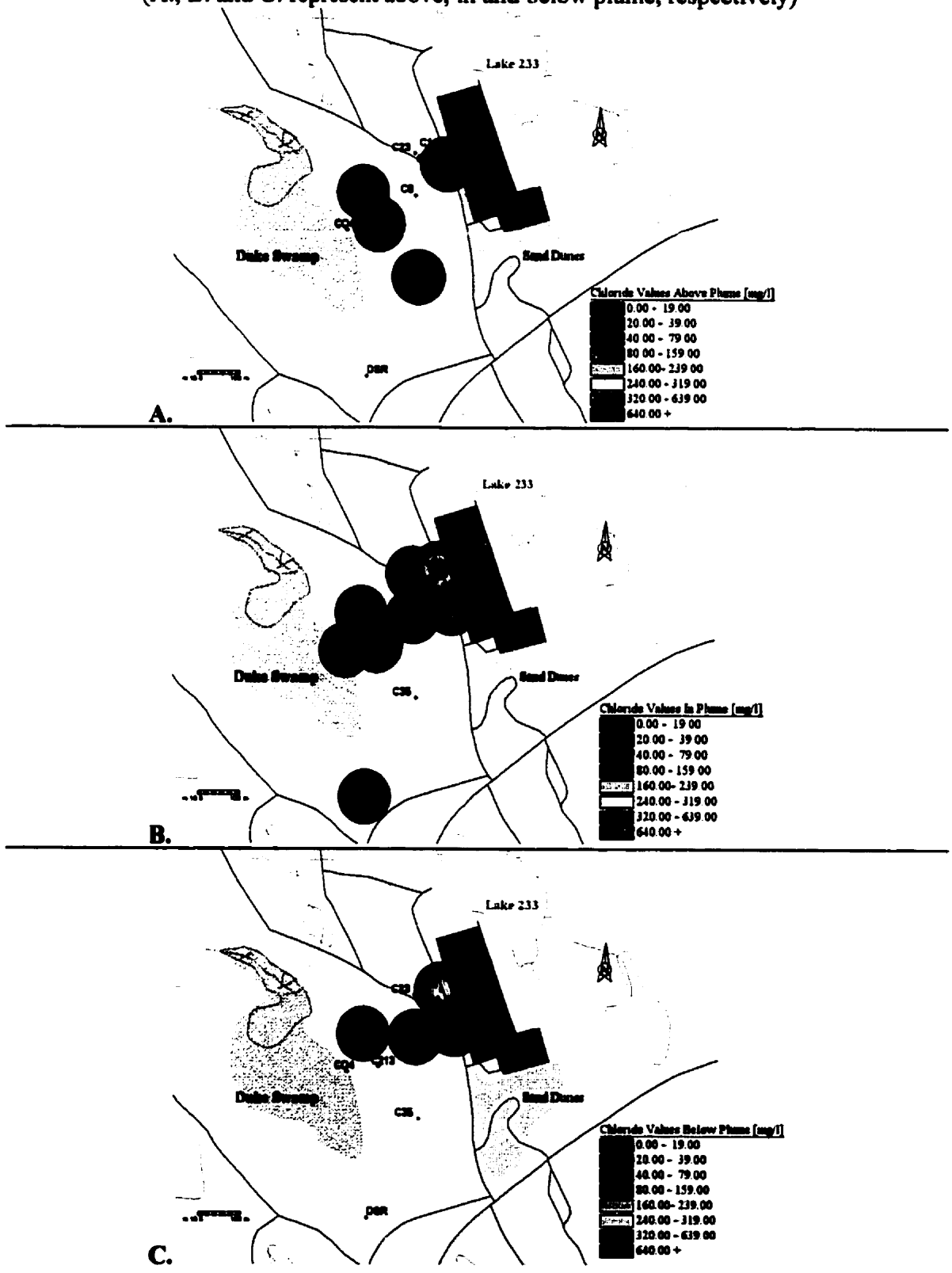

Figure 25 Spatial distribution of Ca^{2+}.

(A., B. and C. represent above, in and below plume, respectively)

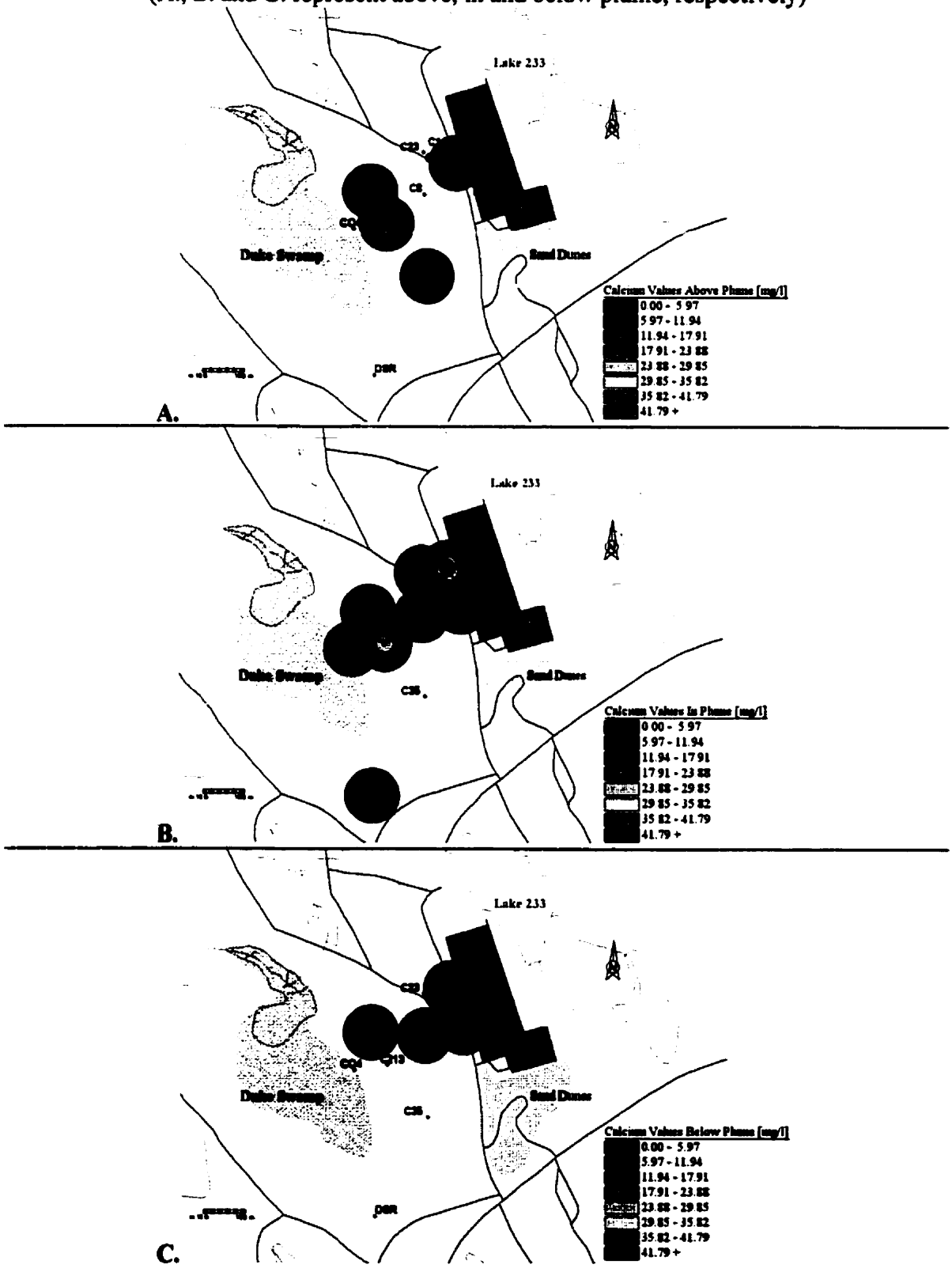

Table 4 Table showing geochemical analysis and statistical cross-correlations with geochemical species

Correlations Between	Alk.	^{3}H	^{14}C	^{13}C	DOC	DIC	Stable I	^{129}I	Na	Ca	Mg	Cl	SO_4^{2-}	Al	B	Ba	Fe	K	Mn	Si	Sr	NO_3^-
Stable I	0.46	0.87	0.82	0.20	0.28	0.64	1.00	-0.01	-0.29	0.18	0.22	-0.33	-0.30	0.09	0.39	-0.25	0.15	-0.25	0.01	0.60	-0.16	0.21
In plume	0.84	0.84	0.79	0.55	0.47	0.66	1.00	-0.23	-0.48	-0.03	0.03	-0.47	-0.31	-0.11	0.85	-0.43	0.11	-0.40	-0.16	0.71	-0.19	0.00
Out of Plume	0.01	0.84	0.70	0.34	0.09	0.19	1.00	0.49	-0.13	0.32	0.01	-0.30	-0.34	0.32	-0.30	-0.33	0.57	0.10	0.38	-0.15	-0.31	0.40
$^{129}I/^{127}I$	-0.25	0.17	0.08	-0.29	0.05	-0.17	0.04	0.69	0.00	-0.01	-0.06	-0.05	-0.06	0.63	-0.04	0.00	-0.28	-0.18	0.13	-0.13	-0.05	-0.68
^{129}I	-0.21	0.00	-0.04	-0.18	0.18	-0.08	-0.01	1.00	-0.08	-0.11	-0.13	-0.09	-0.20	0.48	-0.06	-0.05	-0.14	-0.23	-0.16	0.08	-0.20	-0.29
In plume	-0.35	-0.22	-0.24	-0.29	0.27	-0.19	-0.23	1.00	-0.17	-0.31	-0.35	-0.16	-0.24	0.46	-0.18	-0.15	-0.19	-0.31	-0.39	-0.19	-0.29	0.00
Out of Plume	0.26	0.24	0.24	-0.18	0.15	-0.28	0.49	1.00	0.08	0.59	0.06	-0.18	-0.32	0.37	0.14	-0.25	-0.13	0.01	0.91	-0.09	0.18	-0.36
^{3}H	0.30	1.00	0.95	0.09	0.23	0.64	0.87	0.00	0.05	0.47	0.53	0.05	-0.02	0.07	0.37	0.14	0.21	-0.01	0.02	0.58	0.16	0.25
In plume	0.61	1.00	0.95	0.39	0.49	0.63	0.84	-0.22	-0.06	0.37	0.43	-0.03	0.10	-0.12	0.72	0.03	0.35	-0.07	0.05	0.67	0.20	0.00
Out of Plume	-0.27	1.00	0.89	0.24	-0.28	0.37	0.84	0.24	0.19	0.13	-0.18	0.04	0.13	0.25	-0.27	-0.02	0.47	0.44	0.09	0.29	0.07	0.40
^{14}C	0.20	0.95	1.00	0.12	0.23	0.72	0.82	-0.04	0.09	0.42	0.48	0.11	-0.01	-0.13	0.29	0.16	0.39	0.10	0.09	0.70	0.13	-0.11
In plume	0.59	0.95	1.00	0.47	0.63	0.78	0.79	-0.24	0.01	0.33	0.42	0.03	0.05	-0.35	0.74	0.06	0.54	0.02	0.19	0.83	0.19	0.00
Out of Plume	-0.49	0.89	1.00	0.12	0.47	0.08	0.70	0.24	0.18	0.10	-0.20	0.11	0.15	0.38	-0.44	-0.02	0.53	0.52	0.10	-0.06	-0.13	-0.08
Na	-0.30	0.05	0.09	-0.28	-0.30	-0.05	-0.29	-0.08	1.00	0.70	0.67	0.97	0.73	-0.26	-0.13	0.94	0.17	0.64	0.28	-0.32	0.79	0.63
In plume	-0.30	-0.06	-0.01	-0.29	-0.30	-0.12	-0.48	-0.17	1.00	0.85	0.83	1.00	0.86	-0.24	-0.32	0.99	0.44	0.92	0.51	-0.28	0.93	0.00
Out of Plume	-0.33	0.19	0.18	-0.34	-0.35	-0.06	-0.13	0.08	1.00	0.06	0.01	0.92	0.84	-0.59	0.04	0.90	-0.12	0.27	0.13	-0.66	0.45	0.94
Ca	0.14	0.47	0.42	-0.06	-0.05	0.11	0.18	-0.11	0.70	1.00	0.98	0.73	0.26	-0.07	0.09	0.83	0.22	0.48	0.24	0.05	0.80	-0.26
In plume	0.09	0.37	0.33	-0.02	-0.21	0.02	-0.03	-0.31	0.85	1.00	0.98	0.85	0.82	-0.19	-0.02	0.88	0.38	0.74	0.40	-0.08	0.96	0.00
Out of Plume	0.55	0.13	0.10	0.07	0.40	-0.10	0.32	0.59	0.06	1.00	0.79	-0.27	-0.37	-0.43	0.36	0.00	0.20	0.23	0.50	0.26	0.47	-0.24
Cl	-0.35	0.05	0.11	-0.24	-0.27	-0.04	-0.33	-0.09	0.97	0.73	0.72	1.00	0.66	-0.25	-0.21	0.97	0.24	0.63	0.25	-0.24	0.75	0.50
In plume	-0.31	-0.03	0.03	-0.24	-0.23	-0.06	-0.47	-0.16	1.00	0.85	0.83	1.00	0.83	-0.28	-0.31	0.99	0.49	0.91	0.54	-0.22	0.91	0.00
Out of Plume	-0.57	0.04	0.11	-0.37	-0.48	-0.14	-0.30	-0.18	0.92	-0.27	-0.17	1.00	0.90	-0.39	-0.18	0.91	-0.07	0.15	-0.02	-0.62	0.20	0.53

Table 5 Results of geochemical analysis on groundwaters

Site	Depth m	Water m b.g.s.	pH	T °C	Alk. $CaCO_3$	DOC mg-C/l	Cl^- mg/l	SO_4^{2-} mg/l	NO_3^- mg/l	Ca^{2+} mg/l	Mg^{2+} mg/l	Na^+ mg/l	K^+ mg/l	$Fe_{tot.}$ mg/l	Si mg/l	P_{CO_2} (Log)	LogSI Cal.	LogSI Am.Si.
Recharge																		
C14-1(7)	7	6.5	5.64	12.2	13.42	11.09	672.00	37.60	<0.05	43.39	12.42	292.59	8.33	33.11	5.59	-1.60	-3.26	-1.19
C14-2(8.5)	8.5	6.5	5.84	12.0	3.28	9.49	290.00	63.00	<0.05	11.43	2.98	180.56	4.89	7.33	4.29	-2.41	-4.26	-1.30
C111-8	8	8	5.90	12.1	14.55	12.31	84.60	1.40	<0.05	10.45	3.04	46.11	3.81	18.15	5.12	-1.80	-3.48	-1.23
C111-11	11	8	5.50	12.2	2.44	9.33	86.90	15.80	38.29	9.55	2.52	41.94	4.74	<0.01	5.14	-2.18	-4.71	-1.23
C114-8 (10/97)	8	7	6.00	13.0	57.95	15.35	56.20	1.30	<0.05	15.45	3.12	59.63	3.76	0.01	5.57	-1.30	-2.61	-1.20
C114-11 (10/97)	11	7	5.70	12.4	4.37	16.49	79.40	1.10	<0.05	9.46	2.32	40.46	2.36	6.47	5.38	-2.12	-4.23	-1.21
Intermediate																		
C8-III	11.5	7.5	5.60	11.0	30.50	7.88	25.00	13.10	1.17	12.95	3.14	13.89	7.74	0.12	7.46	-1.19	-3.37	-1.05
C8-II	14m	7.5	5.78	11.0	28.06	8.28	71.80	15.90	7.03	14.91	3.62	45.93	4.68	0.10	6.48	-1.41	-3.20	-1.12
C23-II	10	8.5	5.59	11.0	16.80	11.79	81.40	12.40	<0.05	9.55	2.59	47.31	3.11	4.02	5.47	-1.44	-3.79	-1.19
Discharge																		
C213-4	4	4	5.93	15.5	33.50	17.07	36.90	10.30	2.20	13.21	3.16	19.17	3.49	56.58	5.87	-1.45	-2.93	-1.21
C213-8	8	4	5.92	11.0	92.72	11.44	10.14	8.90	<0.05	23.93	6.44	23.80	2.32	0.25	5.52	-1.03	-2.32	-1.19
C221-7	7	6	5.20	9.5	0.92	11.18	93.20	21.60	2.32	6.62	1.45	6.81	1.56	0.18	5.69	-2.31	-5.61	-1.16
C221-9	9	6	5.49	9.5	3.34	13.34	98.00	19.20	<0.05	20.27	5.44	51.20	2.70	0.22	6.00	-2.05	-4.31	-1.13
C221-16	16	6	6.15	10.0	11.91	13.58	93.00	0.80	<0.05	12.95	4.20	29.07	3.31	38.72	7.07	-2.15	-3.26	-1.07
CO4	Art.		6.22	13.0	84.78	24.49	51.30	0.60	<0.05	16.25	5.58	19.07	3.09	42.90	11.20	-1.36	-2.22	-0.90
C35	9	3.1	5.04	9.50	117.80	25.61	3.00	5.00	<0.05	13.08	3.71	4.26	1.16	0.27	5.70	-0.04	-3.36	-1.16
DSR	0		6.15	17.0	24.89	14.90	44.00	0.80	<0.05	15.36	5.19	17.41	1.55	2.04	8.22	-1.79	-2.74	-1.08

IV.2.2 Carbonate System (pH, DIC, DOC)

The carbonate system, throughout the flow path, is characterized by low pH values that are accompanied by high CO_2 partial pressures. The pH values are all less than neutral, averaging 5.7 along the flow path from recharge (Area C) to the discharge zone (Duke Swamp) and show little variation. This acidity can be attributed to dissolution of soil CO_2, with perhaps a minor contribution from humic and fulvic acids with no subsequent consumption by carbonate or silica weathering. This is in agreement with the $\delta^{13}C$ values measured for dissolved inorganic carbon ($\delta^{13}C_{DIC}$) which averages –20.6‰ for the up-gradient piezometers and –19.8‰ for the down-gradient sites (Table 6). These values are close to the $\delta^{13}C$ value of –23‰ on soil CO_2 in an open system typical of temperate regimes. Piezometer C213-4 has a ^{13}C-enriched value of –9.9‰, which is very close to that of the atmosphere (–7‰). This is likely due to the location of a pond immediately upgradient of this well, which is contributing ^{13}C-enriched water to the shallower piezometer water. The more enriched ^{13}C pondwater has a higher atmospheric CO_2 component, as a consequence of atmospheric exchange. Piezometer C213-8, which is four meters below C213-4, has a more depleted $\delta^{13}C$ value signifying the piezometer contains only deeper groundwater (value of –18.6‰).

In the recharge area (Area C) the log P_{CO_2} varies between –1.29 and –2.38 with a geometric mean of –1.7 (typically soil P_{CO_2} values vary between –1.5 and –2.5). In the discharge area (Duke Swamp), the log P_{CO_2} varies between –0.02 and –2.29 with a geometric mean of –0.8, while the intermediate area (C8 and C23) has a geometric mean for log P_{CO_2} of –1.3. The increased P_{CO_2} of the down-gradient samples is an indication of a subsurface

source of CO_2, as the waters dissolve carbonates under closed system conditions in the saturated zone of the aquifer. One possible source of CO_2 is the aerobic and anaerobic microbial oxidation of high concentrations of dissolved organic carbon (DOC, Table 5) found in groundwaters. These findings are consistent with the ^{13}C content measured on dissolved inorganic carbon ($\delta^{13}C_{DIC}$). The average value of $\delta^{13}C$ is –20.6‰ for the up-gradient piezometers and –19.8‰ for the down-gradient sites (Table 6). Typical soil CO_2 $\delta^{13}C_{DIC}$ values are –23‰ (Clark & Fritz, 1997). Duke swamp runoff has geochemical characteristics similar to those of groundwaters in the discharge area. However, the slightly elevated pH, lower DIC and decreased P_{CO_2}, are attributed to the influence and equilibration of atmospheric P_{CO_2}.

DOC values in groundwaters vary between 8 mg-C/l and 26 mg-C/l. The source of the DOC is not known although it may be a result of a mixture of organic waste from Area C with modern ^{14}C-enriched organic materials (Figure 26). These organic materials are leached from soils in the vicinity of Area C, and older ^{14}C-depleted organic material within the late Quaternary sand sediments (Milton *et al.*, 1998). Ten percent of the ^{14}C-activity in the contaminant plume is carried by DOC (Killey *et al.*, 1993). Much of the carbon in the groundwaters must be derived from recharge through and bordering Area C, given the high ^{14}C- activity of the dissolved carbon (DIC plus DOC), varying between 10 and 50 Bq/g.

The source of the carbonate alkalinity in the contaminant plume groundwaters is varied (Figure 27). DIC may have originated from soils in the recharge area, during incorporation of soil CO_2, in addition to the contribution of dissolved organic constituents which have oxidized originating from the Area C wastes (Milton *et al.*, 1998; Milton et al., (1998) Research Contract Report to AECB and references therein).

Figure 26 Spatial distribution of DOC.

(A., B. and C. represent above, in and below plume, respectively)

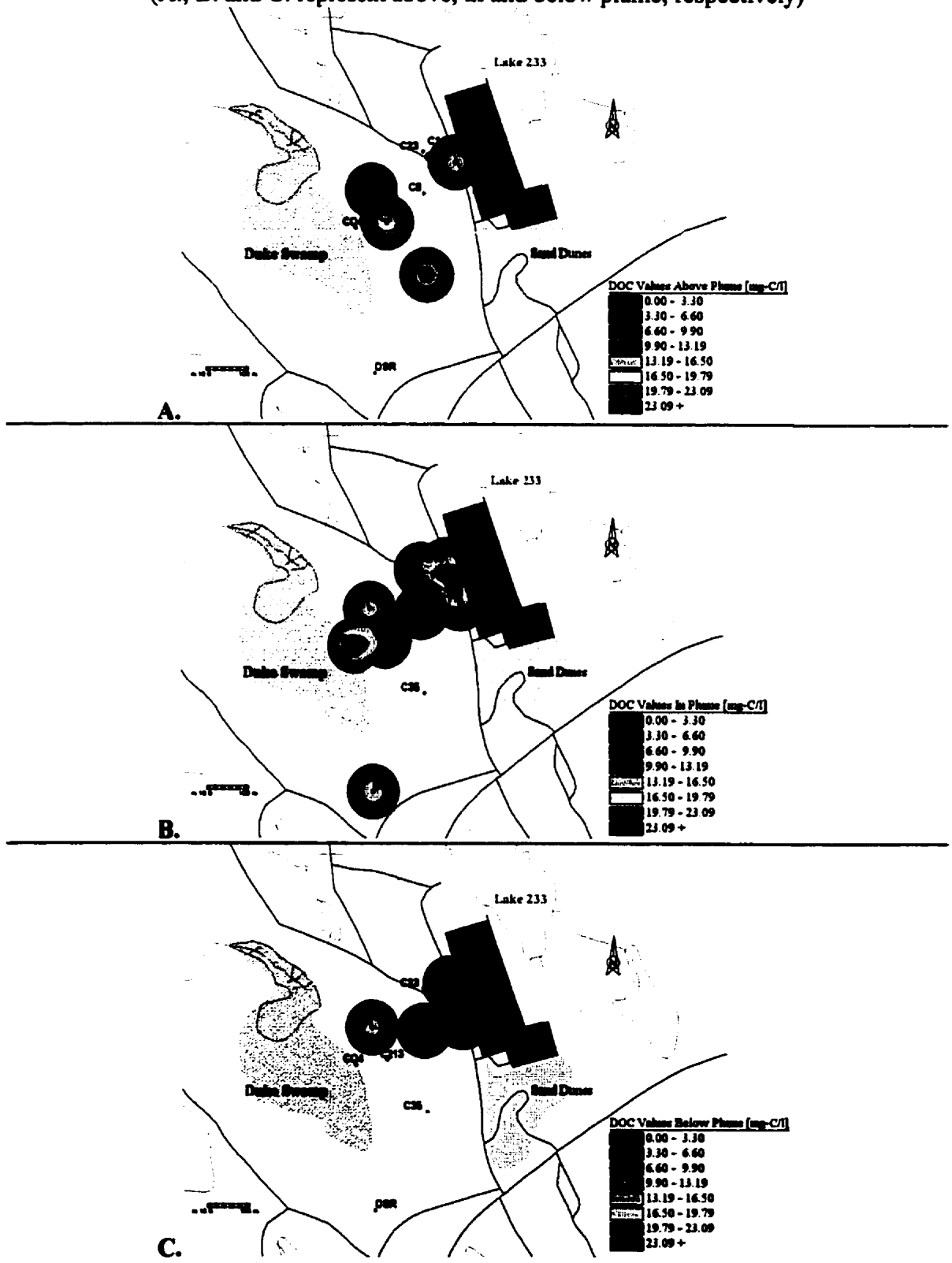

Killey *et al.*, (1998) observed a better ^{14}C correlation between DIC than DOC. Similar behaviour is apparent between bicarbonate alkalinity (Figure 29) and stable iodine within the plume (0.84) relative to out of plume (0.01) and to a lesser degree between DIC and stable iodine in-plume (0.66) and out-of-plume (0.19; Figure 28). A poor to non-existent correlation exists between DOC and stable iodine (0.47 in-plume and 0.09 out-of-plume), but this is based on a limited data set (Table 5).

Table 6 Analysis of carbon, tritium and radiocarbon isotopes and selected ion ratios of groundwaters.

	Alk. $CaCO_3^-$	DIC mg-C/l	Na/Ca (meq)	Na/Cl (meq)	TDS mg/l	$\delta^{13}C$ DIC	^3H Bq/ml	^{14}C Bq/ml
Recharge								
C14-7	13.4	20.1	5.9	0.67	912	-20.0	104.0	1.2
C14-8.5	3.3	3.3	13.7	0.96	516	-20.2	31.0	0.62
C111-8	14.6	13.3	3.8	0.84	158	-21.4	0.3	0.33
C111-11	2.4	4.9	3.8	0.74	185	-19.9	54.0	0.68
C114-8	58.0	44.3	3.4	1.64	225	-21.6	33.0	0.63
C114-11	4.4	5.8	3.7	0.79	130	-20.3	0.4	0.33
Intermediate								
C8-2	28.1	31.9	2.7	0.99	192	-19.5	76.0	0.93
C8-3	30.5	49.5	0.9	0.86	114	-21.0	28.0	0.67
C23-11	16.8	27.8	4.3	0.90	166	-19.6	8.3	0.4
Discharge								
C213-4	33.5	28.9	1.3	0.80	121	-9.9	65.0	1.08
C213-8	92.7	81.5	0.9	3.62	194	-18.6	159.0	1.13
C221-7	0.9	3.5	0.9	0.11	74	-18.6	5.9	0.42
C221-9	3.3	6.8	2.2	0.81	187	-20.8	200.0	1.5
C221-16	11.9	7.1	2.0	0.48	129	-21.1	0.6	0.37
C35	117.8	632.7	0.3	2.19	140?	-12.9	0.95	0.17
CO4	84.8	45.7	1.0	0.57	175	-17.4	257.0	2.57
DSR	24.9	14.9	1.0	0.61	105	-15.5	99.0	1.13

Figure 27 Spatial distribution of DIC.

(A., B. and C. represent above, in and below plume, respectively)

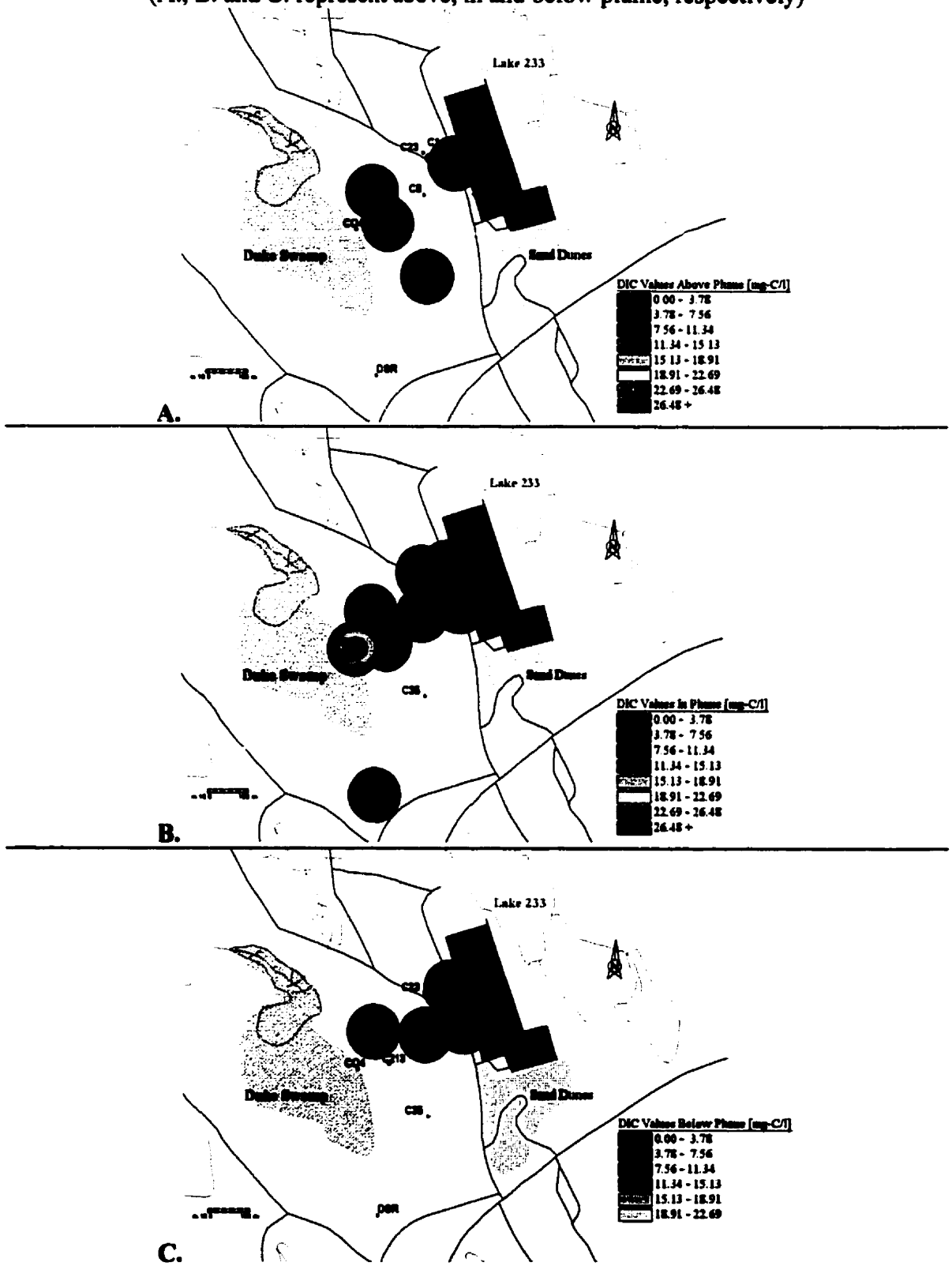

Figure 28 Alkalinity relationship with total stable iodine in and out of plume.

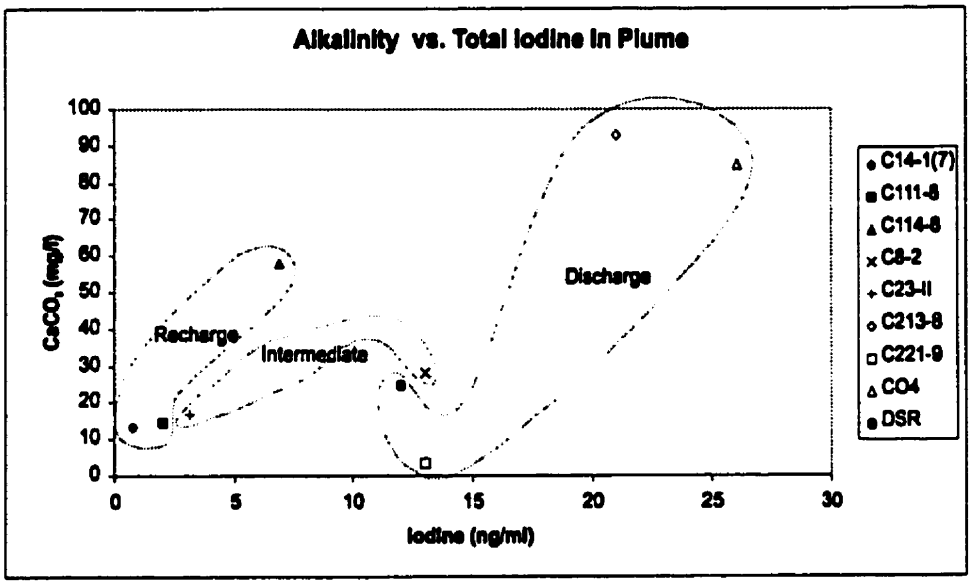

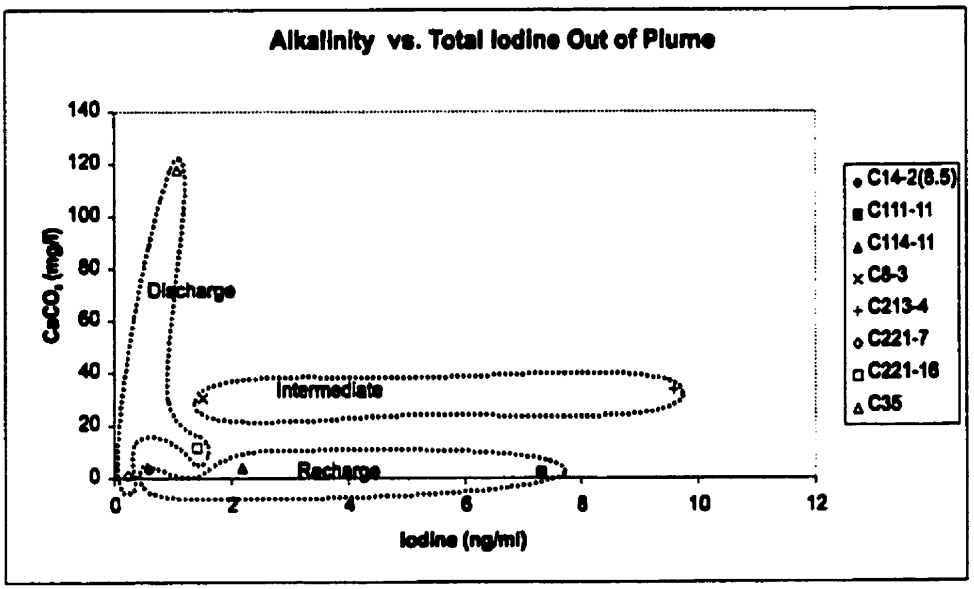

Figure 29 Spatial distribution of alkalinity.

(A., B. and C. represent above, in and below plume, respectively)

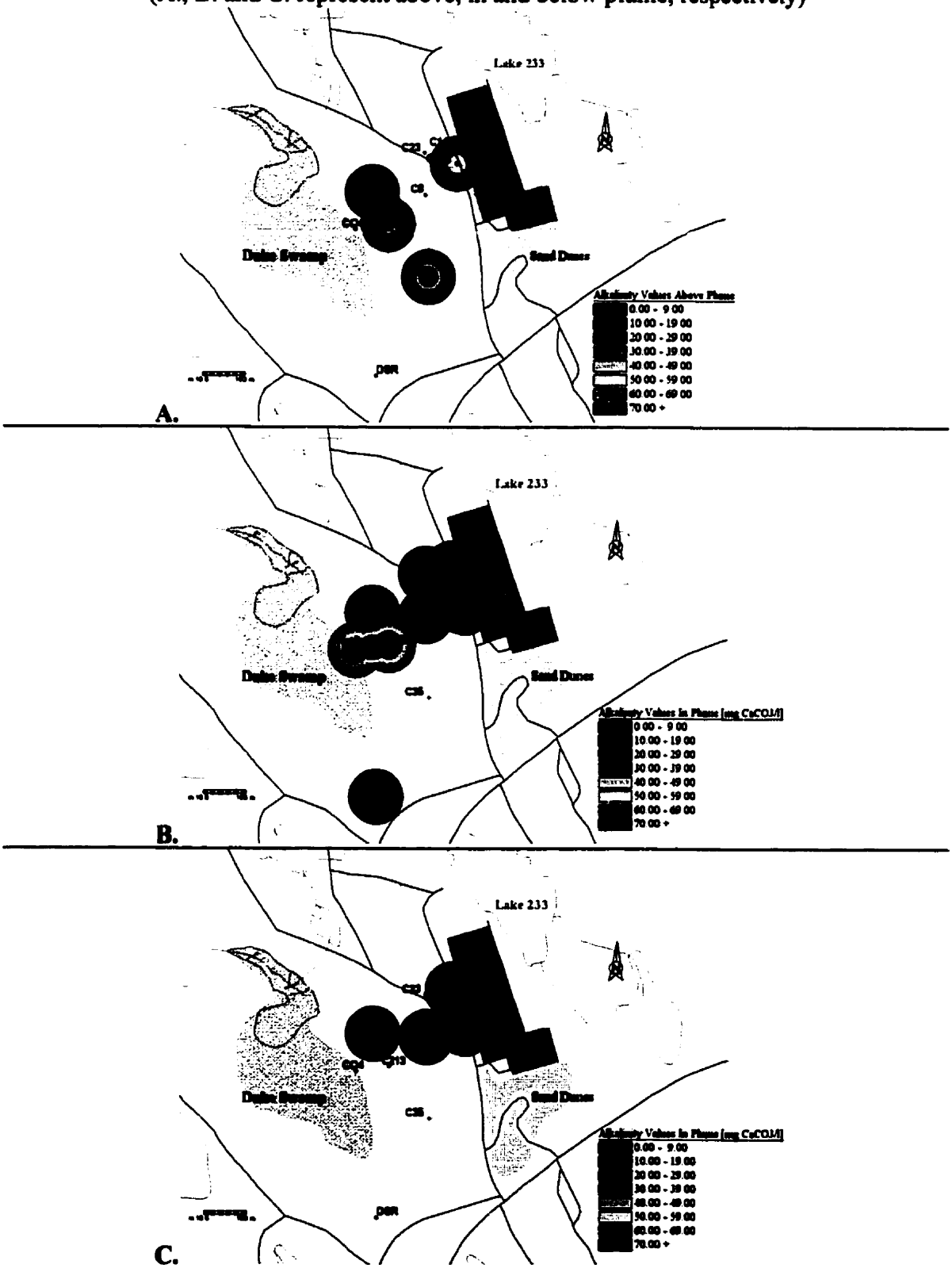

IV.2.3 Redox Conditions

Groundwater Eh was not measured directly, but dissolved iron ($Fe_{Tot.}$), nitrate (NO_3^-) and sulphate (SO_4^{2-}) provide a relative indication of aquifer redox conditions. Samples with elevated iron concentration represent low redox potential (Figure 30). Inverse correlation with electron acceptors including NO_3^- and SO_4^{2-} corroborates this observation more evidently for nitrate than sulphate. Dissolved iron concentrations range from less than 1 mg/l to over 50 mg/l. Dissolved iron concentrations greater than 1 mg/l for the pH range in these groundwaters is attributed to the reduced Fe^{2+}. With the exception of C213-4, which is affected by surface water infiltration (from a pond located upgradient from piezometer), an inverse correlation is apparent in groundwaters. $Fe_{Tot.}$ concentrations greater than 1 mg/l have no detectable nitrate, while those with low $Fe_{Tot.}$ have measurable NO_3^- (up to 38 mg/l). A similar correlation for SO_4^{2-} is also apparent in the system.

At first glance it seems that there is no consistent pattern for the distribution of $Fe_{Tot.}$. Elevated $Fe_{Tot.}$ concentrations are observed in samples from the recharge area and from the discharge area near Duke swamp, yet both regions also display low $Fe_{Tot.}$ concentrations (oxidizing conditions). Moreover, there is no indication that high $Fe_{Tot.}$ concentrations (reducing conditions) correlate with increased depth or DOC. A possible interpretation is that oxidizing (low $Fe_{Tot.}$) conditions occur in areas that have greater permeability where dissolved O_2 transport from recharge is greater (Dolinar *et al.*, 1996). In further investigating the in-plume versus out-of-plume scenarios, we see that (with the exception of CO4 (in plume)) Figure 31 (in-plume) illustrates that as $Fe_{Tot.}$ decreases, stable iodine increases (correlation of 0.57 in-plume, 0.11 out-of-plume). The same relationship cannot be said for

the $Fe_{Tot.}$ relationship with ^{129}I (correlation of –0.19 in-plume, –0.13 out-of-plume) (Figure 32).

A possible interpretation to the low redox indicated, by high dissolved iron ($Fe_{Tot.}$), high bicarbonate (low NO_3^- and SO_4^{2-}) observed in water recharged from Lake 233, can be ascribed to biological activity in the organic mat that covers the bed of the lake. As water percolates downward through the organics, oxygen is consumed and CO_2 is produced during microbial degradation of the organic litter on the lake bed. The loss of O_2 lowers the redox potential in the water and increases the solubility of iron oxides that are abundant in the sediments. The CO_2 respired by the microbes increases the bicarbonate concentrations (Dolinar *et al.*, 1996). The stable iodine concentration of CO4 can be attributed to the environment in which the groundwater is found. The artesian water sample was obtained from a zone of high organic peat content, with which iodine has an affinity. It may be possible that the organic matter with $Fe_{Tot.}$ increases the ^{129}I affinity to organic matter and hence ^{129}I concentration. This may potentially explain the high iodine concentration in CO4 sample. Unfortunately, the geochemistry of water sampled from the deeper piezometer in sand (hence lower iodine content) was not possible to provide further evidence.

Table 7 Selected parameters for Eh analogy with $Fe_{Tot.}$, NO_3^- and ^{129}I.

	Total Iodine (ng/ml)	^{129}I (atoms/l)	$Fe_{Tot.}$ mg/l	NO_3^- mg/l	SO_4^{2-} mg/l
Recharge					
C14-7	0.72	1.66E+09	33.11	<0.05	37.60
C14-8.5	0.59	1.37E+09	7.33	<0.05	63.00
C111-8	2.00	1.18E+09	18.15	<0.05	1.40
C111-11	7.30	9.83E+08	<0.01	38.29	15.80
C114-8	6.88	6.03E+10	0.01	<0.05	1.30
C114-11	2.17	8.93E+08	6.47	<0.05	1.10
Intermediate					
C8-2	13.00	2.08E+10	0.10	7.03	15.90
C8-3	1.50	2.89E+09	0.12	1.17	13.10
C23-11	3.10	4.75E+10	4.02	<0.05	12.40
Discharge					
C213-4	9.60	1.28E+10	56.58	2.20	10.30
C213-8	21.00	3.40E+10	0.25	<0.05	8.90
C221-7	0.23	1.02E+08	0.18	2.32	21.60
C221-9	13.00	2.99E+11	0.22	<0.05	19.20
C221-16	1.40	7.30E+08	38.72	<0.05	0.80
C35	26.00	8.40E+10	42.90	<0.05	0.60
CO4	1.08	6.45E+08	0.27	<0.05	5.00
DSR	12.00	1.82E+10	2.04	<0.05	0.80

Figure 30 Spatial distribution of $Fe_{Tot.}$.

(A., B. and C. represent above, in and below plume, respectively)

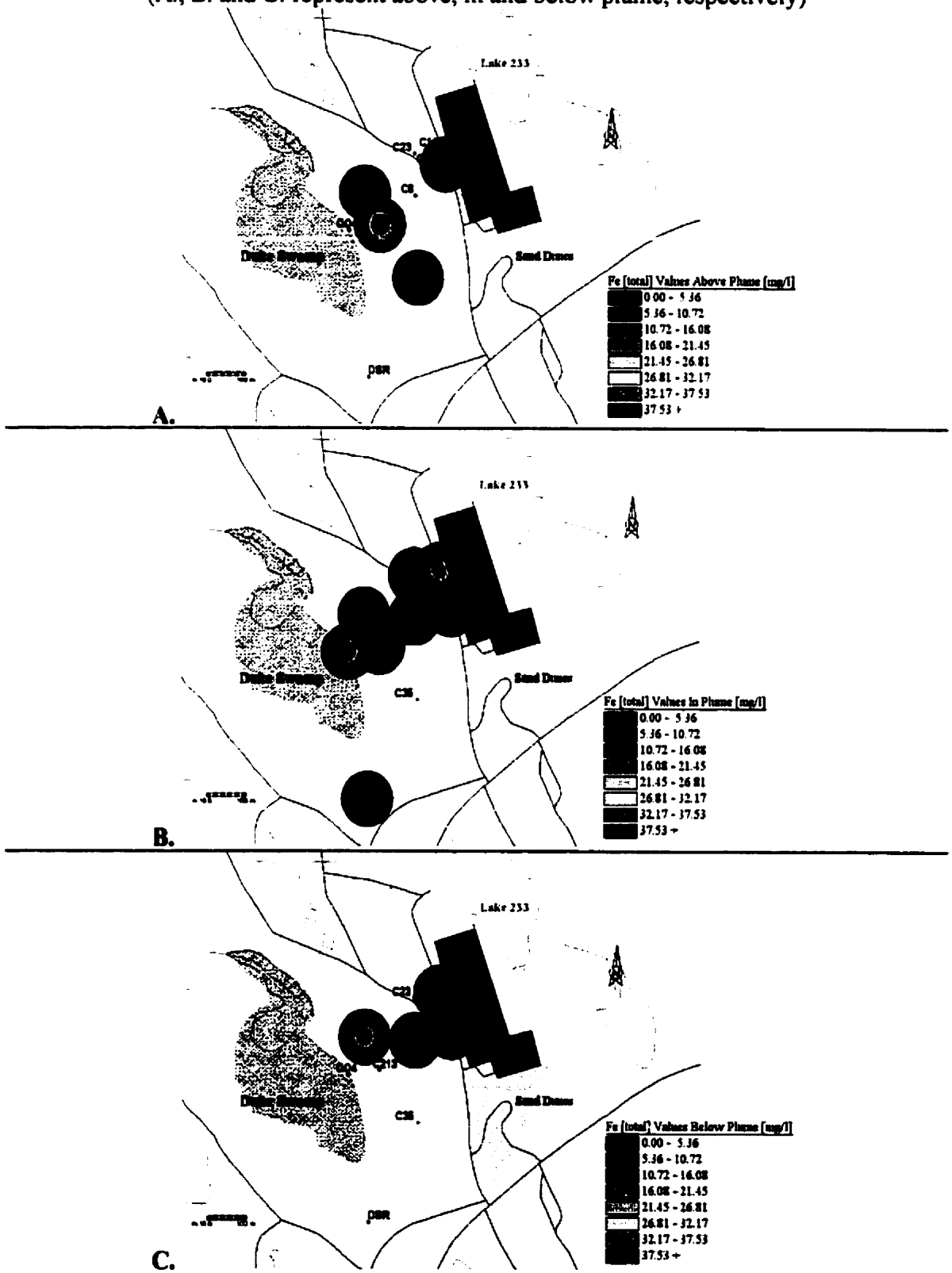

Figure 31 $Fe_{Tot.}$-I concentrations from groundwaters supplied within and out of plume.

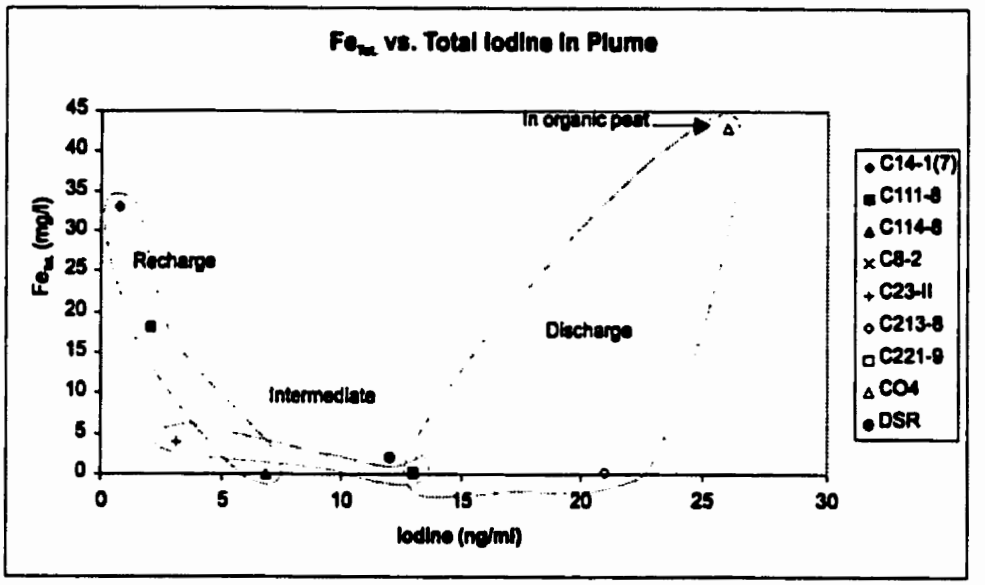

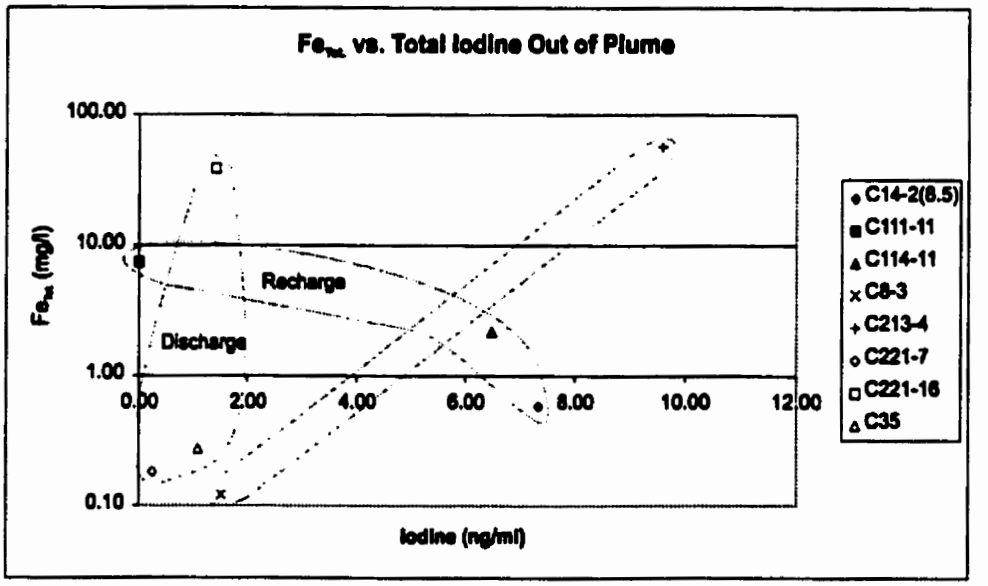

Figure 32 $Fe_{Tot.}$ - ^{129}I concentrations from groundwaters supplied within and out of plume.

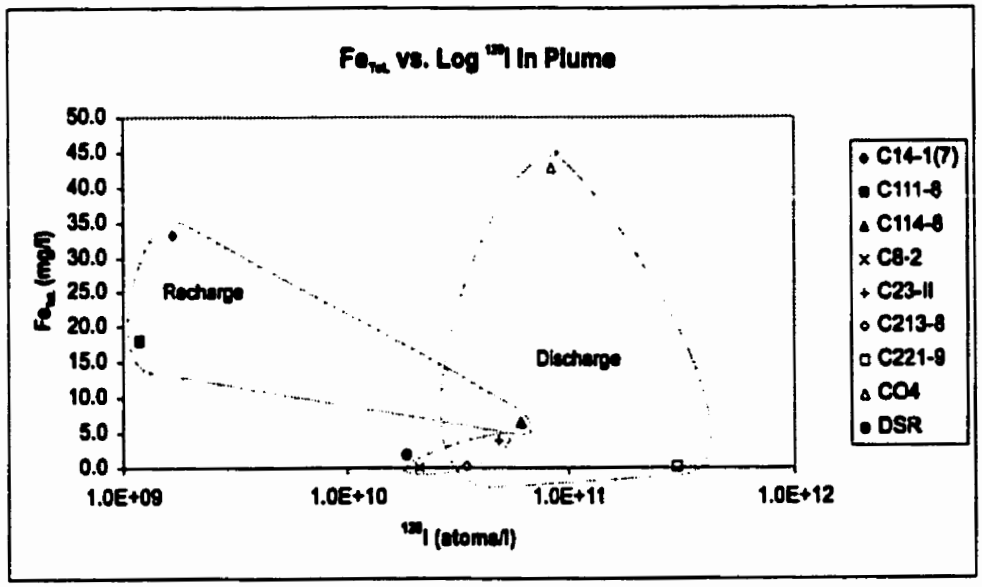

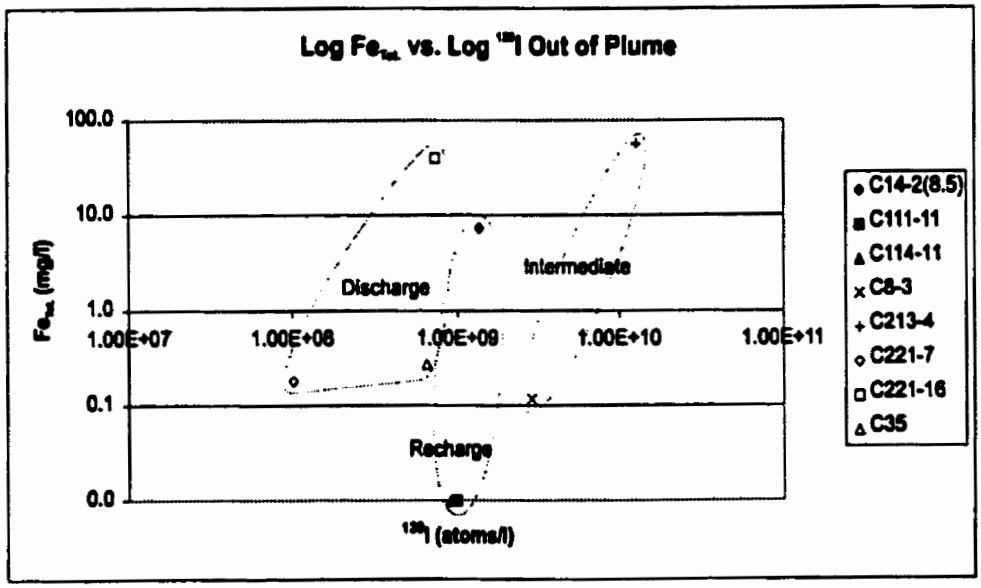

IV.3. Iodine Systematics

The concentrations of total iodine and ^{129}I in samples within the contaminant leachate plume are given in Table 8 and in Table 9 for groundwaters outside of the contaminant plume. Analytical results for selective leaches from soil samples, soils, vegetation, and air samples are given in Tables 10, 11 and 14.

IV.3.1 Total Aqueous Iodine & ^{129}I

Groundwaters collected along the hydrologic flow path from multi-level piezometers were analyzed for their hydrogeochemistry and stable- and radio-iodine systematics. Piezometer locations (Figure 8) and sampling depths were selected based on:

(1) location within the flow system so as to have 3 regions of study (input, intermediate and output) and

(2) location with respect to the contaminant plume originating from Area C as previously discussed in section IV.1. This plume is largely delineated by elevated concentrations of tritium and ^{14}C in the groundwaters (Killey *et al.*, 1998).

^{129}I concentrations were calculated using a sample calculation illustrated below (Equation 1). $^{129}I/^{127}I$ ratio measured in the sample was subtracted from the "background" $^{129}I/^{127}I$ ratio, then the new sample ratio was corrected for the dilution resulting from the addition of stable iodide carrier (10 mg). From this ratio, atoms ^{129}I per litre or gram of sample were then calculated. In cases where there were very low concentrations of natural ^{129}I in the sample, the dilution exceeded 10,000. Here, it was not possible to determine the original ratio of the sample without a large degree of error. Here only the atoms per litre

could only be calculated by assuming the total stable iodide present was dominantly the stable iodide carrier added at precipitation.

Equation 1 Calculation required to obtain corrected isotopic ratios and ^{129}I data (atoms/liter).

Sample	mass of sample (g)	Total Iodine (ng/ml)	stable I in Sample mg	I added (10mg)	Dilution	129 I/127I	129I/127I Bkgd Corr.	129/127I - Bkgd	129/127 Dilution. Corr. Ratio	Total I in Sample g/l	mol/l	129I (atoms/l) Corrected
CO4	100.00	26.00	0.0026000	10.00260	3847	1.772E-10	1.36E-13	1.77E-10	6.81E-07	2.60E-05	2.05E-07	8.40E+10

$$\text{Dilution} = \frac{\text{mass of I carrier added + natural iodide in sample}}{\text{mass of I in sample}}$$

$$\text{Dilution} = \frac{10.0026\ \text{mg}}{0.002600\ \text{mg}}$$

$$= 3847.15384615$$

$$\equiv 3847$$

$$\text{Dilution corrected Ratio} = \text{Dilution}\,[1] \times \left({}^{129}I/_{127}I \text{ measured} - {}^{129}I/_{127}I \text{ background} \right)$$

$$= 3847 \times 1.77E-10$$

$$= 6.81E-7\ [2]$$

$$\text{Moles of I} = \frac{\text{mass of I in sample}}{\text{molecular mass of } {}^{127}I}$$

$$= 2.05E-7\ {}^{\text{moles}}/_{\text{liter}}\ [3]$$

$$\text{Moles of } {}^{129}\text{I} = \text{Moles of I}\,[3] \times \text{Dilution corrected Ratio}\,[2]$$

$$= 2.05E-7 \times 6.81E-7$$

$$= 1.39E-13\ {}^{\text{moles}}/_{\text{liter}}\ [4]$$

$$\text{Atoms of } {}^{129}\text{I per liter} = \text{Avogadros number } ({}^{\text{atoms}}/_{\text{mole}}) \times \text{Moles of } {}^{129}\text{I } ({}^{\text{moles}}/_{\text{liter}})\ [4]$$

$$= 6.022E23 \times 1.39E-13$$

$$= 8.40E10$$

Groundwaters from all the piezometers sampled have stable I, $^{129}I/^{127}I$ ratios and ^{129}I concentrations which vary from 0.23 to 67 ppb, 2.14×10^{-13} to 2.61×10^{-9} and 1.02×10^{8} to 8.28×10^{11} a ^{129}I /l, respectively (Table 8 and 9). As a result of the low stable I in the groundwaters, the addition of a stable I carrier to the samples was deemed necessary in order to precipitate sufficient quantities of AgI for AMS measurements (minimum of 2 mg of AgI

Table 8 Total stable, radio-iodine, tritium and radiocarbon in plume groundwater.

Samples	Total Iodine (ng/ml)	Dilution	$^{129}I/^{127}I$ Ratio -background	^{129}I (atoms/l)	^{3}H (Bq/ml)	^{14}C (Bq/ml)
R echarge						
C14-7	0.72	1.39E+05	3.50E–12	1.66E+09	104.0	1.20
C111-8	2.00	5.00E+04	2.48E–12	1.18E+09	0.3	0.33
†C114-8 05/97	67.00	‡1.49E+02	4.80E–09	2.30E+11		
C114-8 10/97	6.88	1.45E+04	1.27E–10	6.03E+10	33.0	0.63
†C114-8 06/98	49.00	‡1.36E+03	2.61E–09	8.28E+11	342.0	
Intermediate						
C8-2	13.00	‡ 7.72E+03	4.37E–11	2.08E+10	76.0	0.93
C23-II	3.10	3.24E+04	9.97E–11	4.75E+10	8.3	0.40
Discharge						
C213-8	21.00	‡ 4.78E+03	7.13E–11	3.40E+10	159.0	1.13
C221-9	13.00	‡ 7.73E+03	6.28E–10	2.99E+11	200.0	1.50
†CO4 05/97	32.4	‡3.08E+02	1.12E–09	5.40E+10		
CO4 10/97	26.00	‡ 3.85E+03	1.77E–10	8.40E+10	257.0	2.57
DSR	12.00	‡ 8.33E+03	3.85E–11	1.82E+10	99.0	1.13

† Sample shown only to illustrate seasonal variation from within Area C.
‡ Where Dilutions were >10,000 values for atoms/l have been calculated on the assumption that the total stable iodine in the sample was equal to the carrier iodine added (10 mg). Only values marked with ‡ have been dilution corrected.

Table 9 Total stable, radio-iodine, tritium and radiocarbon in non-plume groundwater.

Samples	Total Iodine (ng/ml)	Dilution	$^{129}I/^{127}I$ Ratio -background	^{129}I (atoms/l)	^{3}H (Bq/ml)	^{14}C (Bq/ml)
Recharge						
C14-8.5	0.59	1.69E+05	2.89E–12	1.37E+09	31.0	0.62
C111-11	7.30	1.37E+04	2.07E–12	9.83E+08	54.0	0.68
C114-11 10/97	2.17	4.63E+04	1.87E–12	8.93E+08	0.4	0.33
†C114-11 06/98	2.50	2.67E+04	5.92E–12	1.88E+09		
Intermediate						
C8-3	1.50	6.71E+04	6.06E–12	2.89E+09	28.0	0.67
Discharge						
C213-4	9.60	‡ 1.04E+04	2.70E–11	1.28E+10	65.0	1.08
C221-7	0.23	4.38E+05	2.14E–13	1.02E+08	5.9	0.42
C221-16	1.40	7.17E+04	1.53E–12	7.30E+08	0.6	0.37
C35*	1.08	9.30E+04	1.35E–12	6.45E+08	0.95	0.17

*Groundwater taken outside of plume as representation of 'background' value.

for analysis). As a result, the dilution factors for ^{129}I are variable and quite large (Table 8 and 9).

Recharge area groundwaters from piezometers C14, C111 and C114 (near Area C) have stable I and ^{129}I concentrations of between 0.59 to 67 ng/ml (ppb) and $9.83x10^{8}$ to $8.28x10^{11}$ atoms/l, respectively (Figure 33 and 34 illustrate measurements taken in 10/97). Discharge area groundwaters (in or near Duke Swamp) from piezometers CO4, C-213 and C-221 have stable I and ^{129}I concentrations ranging from 0.23 to 32.4 ppb and $1.02x10^{8}$ to $8.4x10^{10}$ atoms $^{129}I/l$, respectively, which are slightly higher than the average for recharge-area groundwaters from borehole C-114 for 10/97 values. By averaging all three sampling dates for C114 measurements, a stable I concentration of 40.1 ppb and $5.5x10^{11}$ atoms/l was obtained. In retrospect, the discharge area groundwater values now become slightly lower than the average for recharge-area groundwaters.

Contaminant plume groundwaters had higher tritium, ^{14}C, stable I and ^{129}I levels relative to nearby, out-of-plume groundwaters (Table 8 and 9), similar to the recharge area. Groundwaters from the intermediate area (piezometers C8 and C23) have stable I and ^{129}I concentrations ranging from 1.5 and 13.0 ppb and $2.89x10^{9}$ to $4.75x10^{10}$ atoms/l, respectively. These recharge values compared to values at (or near) discharge zones are similar.

The spatial distributions of stable I (Figure 33) and ^{129}I (Figure 34) in the groundwaters suggest that there is a limited amount of change in their concentrations, in the direction of groundwater flow. If we consider groundwaters from piezometers C114 - C8 - C213 - CO4 to represent a single, continuous plume (of elevated ^{129}I) in the direction of groundwater flow, there is a measurable increase in stable I and ^{129}I by a factor of 3.8 and 1.4,

between recharge and discharge zones (Table 8). This increase in stable I and ^{129}I can be attributed to the flow system. However, if we consider the seasonal average C114 groundwater value- C8 - C213 - CO4 to represent a single, continuous plume (of elevated ^{129}I) in the direction of groundwater flow, there is a measurable decrease in stable I and ^{129}I by a factor of 1.5 and 8, between recharge and discharge zones. It is not clear whether the observed decrease in stable I and ^{129}I can be attributed to loss in the flow system. Part of the observed decrease can be accounted for in the observed degree in natural variation in ^{129}I concentrations lateral to flow path. This suggests either a heterogeneous input function or that the internal stratigraphy of the sand aquifer has control over the distribution of the radionuclides within the aquifer. This hypothesis may be valid in suggesting a similar behaviour in relation to the iodine plume with respect to ^{3}H and ^{14}C plume (Killey *et al.*, 1993). The laterally and horizontally confined distribution of tritium (Figure 18 and 19) and ^{14}C (Figure 20 and 21) within the aquifer near the discharge points; show the highest ^{14}C concentrations centered near piezometers C212 - C213 and highest tritium levels slightly more northwest (near C221- C222; Killey *et al.*, 1998). ^{14}C concentrations at piezometer C35 (above natural background levels), situated near the extreme edge of the contaminant plume, indicate longitudinal and transverse dispersion processes are influencing it, resulting in a concentration gradient away from the center of the plume, similar to that observed for ^{14}C (Killey *et al.*, 1998).

Comparisons of stable I and ^{129}I concentrations (Table 8 and 9) along the length of the flow system, indicate that there is more stable I (ranging from a factor of 0.3to 56) and ^{129}I (ranging from a factor of 1.2 to 2931) in the contaminant plume groundwaters relative to out of plume waters. Tritium and ^{14}C show similar variations, indicating that the stable I in the

aquifer is associated with the groundwaters having higher ^{3}H and ^{14}C and that ^{129}I is intrinsically associated with groundwaters elevated in ^{3}H and ^{14}C.

Stable iodine and ^{129}I systematics have been compared with the ^{3}H and ^{14}C concentrations in the groundwaters in an effort to constrain the physico-chemical nature of the controls on stable iodine and radioiodine in the subsurface. Taking into account all the groundwaters, tritium, stable I and ^{129}I concentrations on all groundwaters, are relatively well constrained, with correlation co-efficients of 0.87 for ^{3}H versus stable I and 0.82 for ^{14}C versus stable I (Table 4, Figure 35, 36, 37 and 38). The relationship between stable I, ^{129}I and dissolved organic carbon on all groundwaters is diminished with correlation co-efficients of 0.47 (in-plume) to 0.09 (out-of-plume) (Figure 39 and 40). However the relationship between stable I, ^{129}I and total alkalinity on all groundwaters is rather interesting with correlation co-efficients of 0.84 (in-plume) to 0.01 (out-of-plume). For waters sampled within the contaminant plume only, there is still a strong correlation between stable iodine and tritium (0.84) and, again, slightly less for ^{14}C (0.79).

Recalling the various features of the tritium plume, evapotranspiration is a factor involved in the interpretation of ^{3}H systematics. The confinement of the ^{3}H (and ^{14}C) plume beneath the clayey silt stratum that lies within the interstitial sand and silt stratigraphic unit plays a role in the tritium (and ^{14}C) behaviour. In addition, the non-uniformity of the ^{3}H plume indicates either a heterogeneous nature of the ^{3}H released from multiple trenches in Area C or heterogeneous nature of the aquifer matrix itself. These parameters that affect the tritium and carbon-14 plume may also be applied to the stable I (and ^{129}I) plume, specifically that of the heterogeneous aquifer matrix and variable input of ^{3}H and ^{14}C through time. The

resulting heterogeneous nature of the plume indicates various elevated regions of ^{129}I downgradient of Area C.

Overall, there appears to be a strong association between stable iodine and tritium in the groundwaters. As HTO is largely considered to be conservative in a groundwater system with respect to water/rock interactions, this association may suggest that, for the sands in the Area C flow system, stable iodine is also behaving conservatively.

Figure 33 Spatial distribution of stable iodine.

(A., B. and C. represent above, in and below plume, respectively)

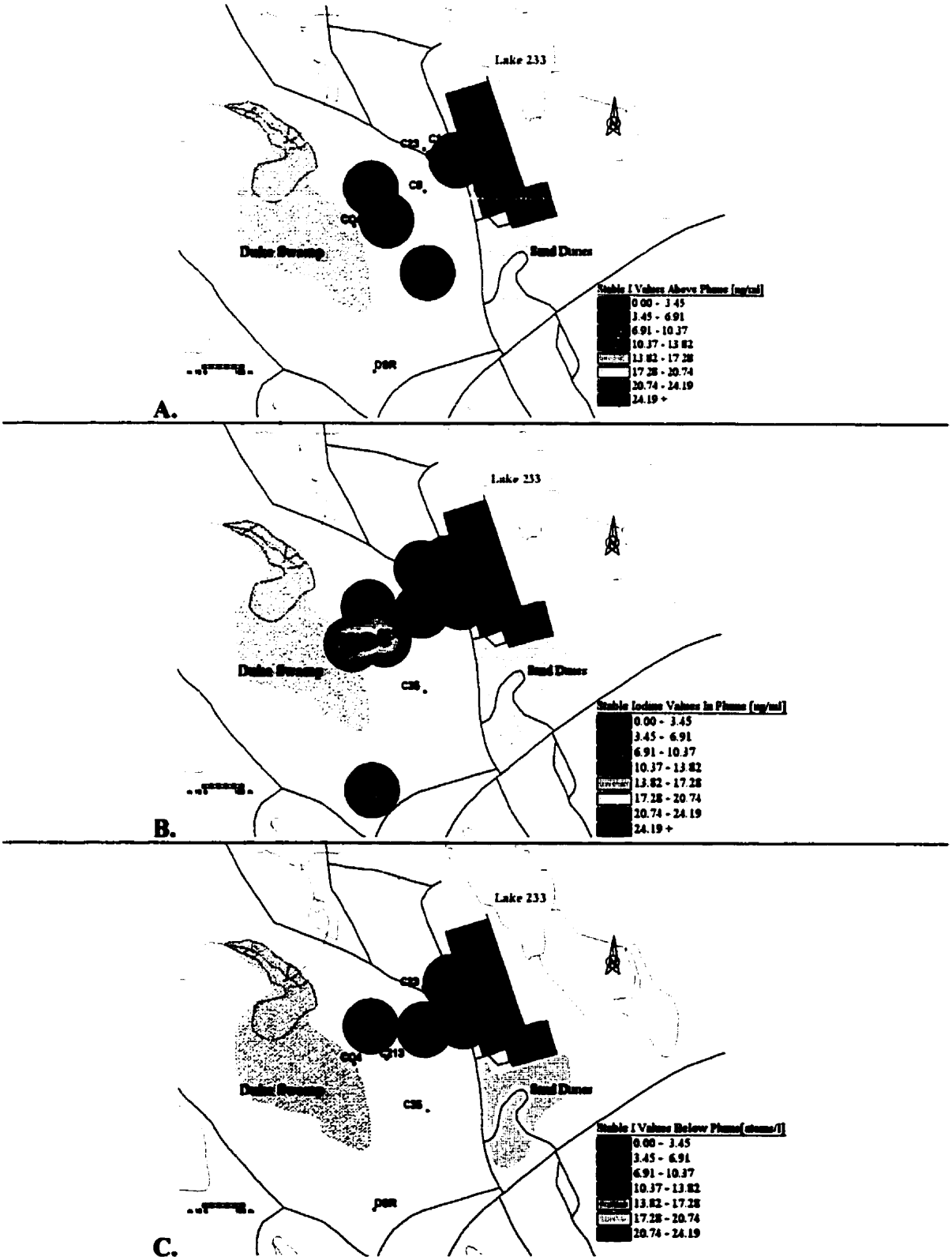

Figure 34 Spatial distribution of ^{129}I.

(A., B. and C. represent above, in and below plume, respectively)

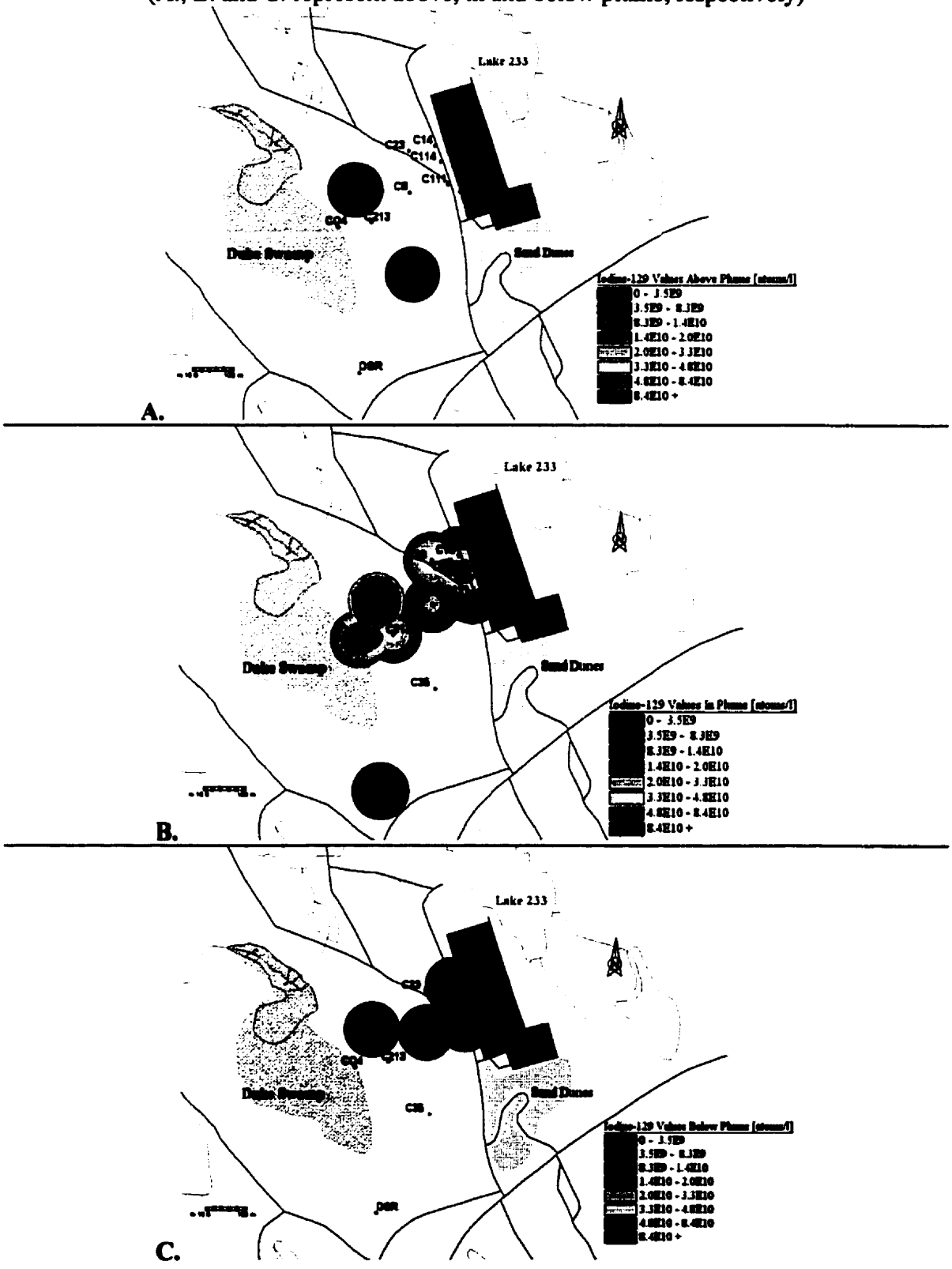

Figure 35 Tritium and stable iodine in and out of plume.

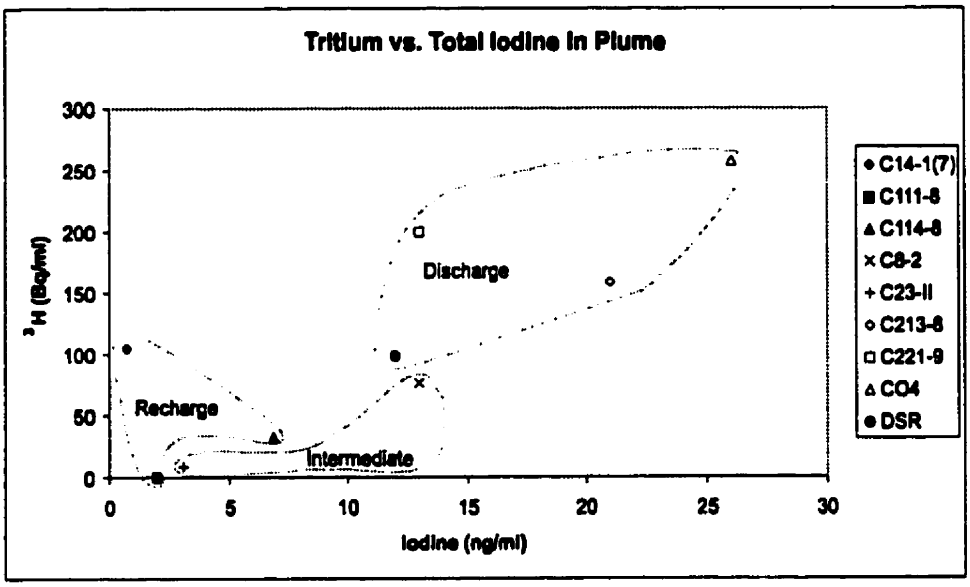

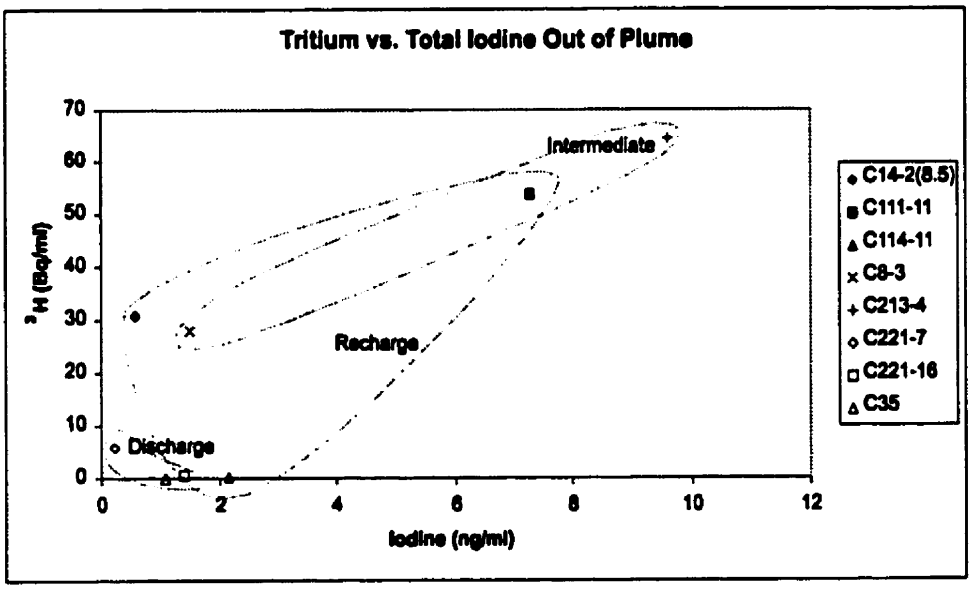

Figure 36 Tritium and ^{129}I in and out of plume.

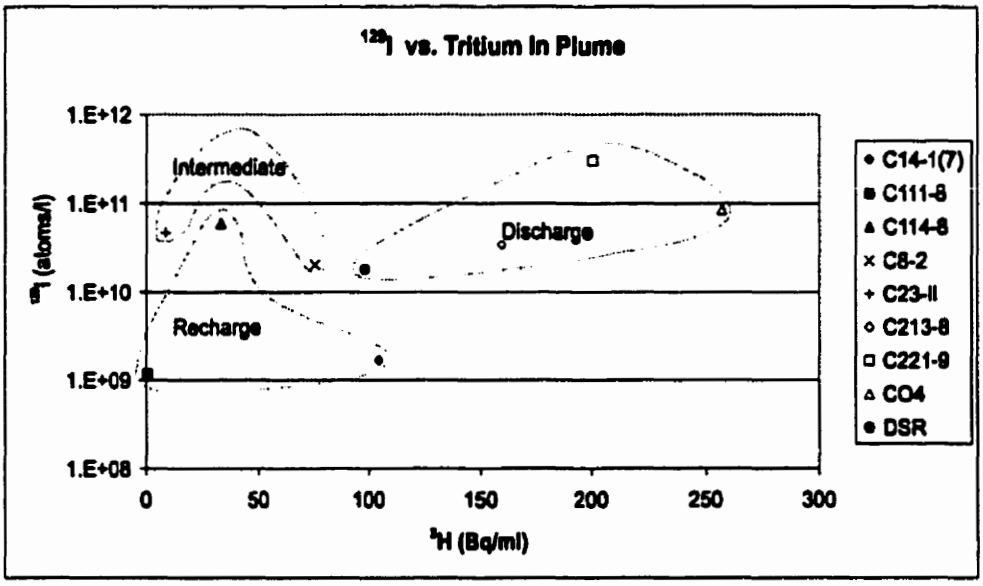

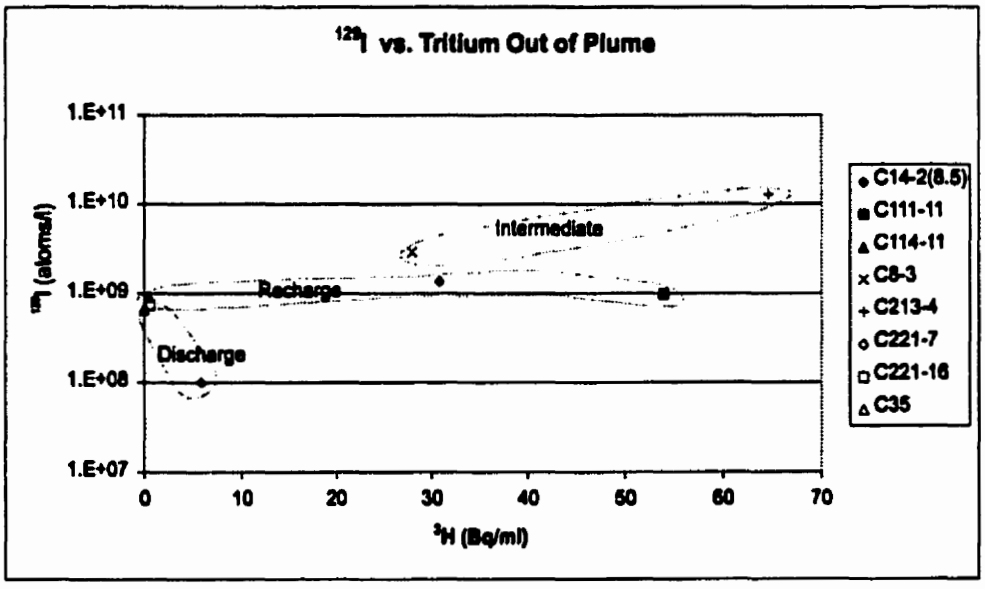

Figure 37 Carbon-14 and stable iodine in and out of plume.

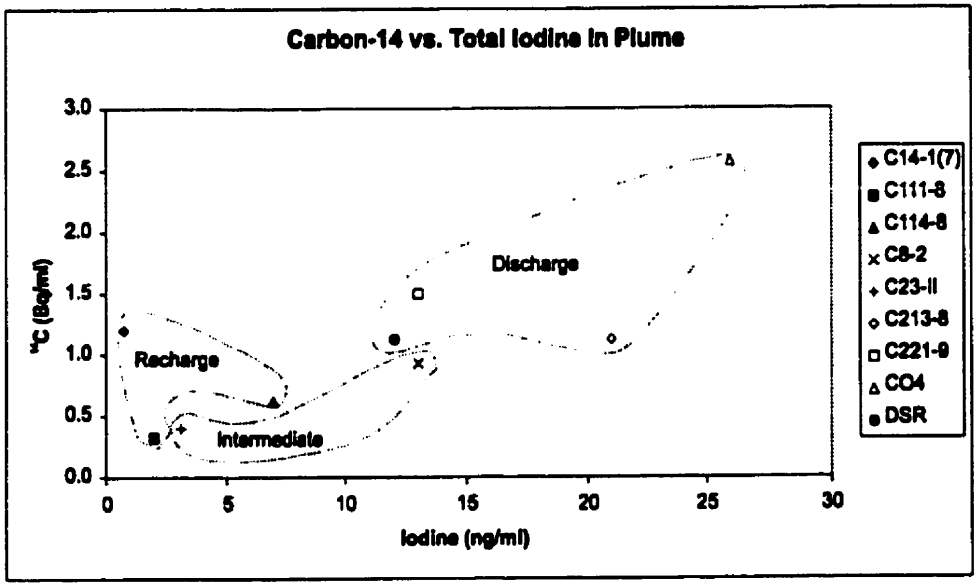

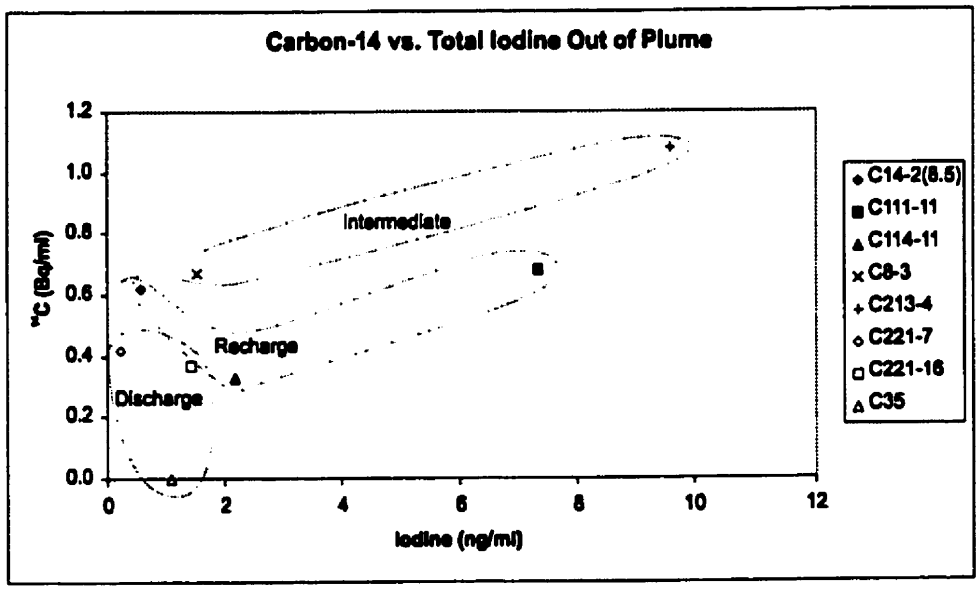

Figure 38 Carbon-14 and ^{129}I in and out of plume.

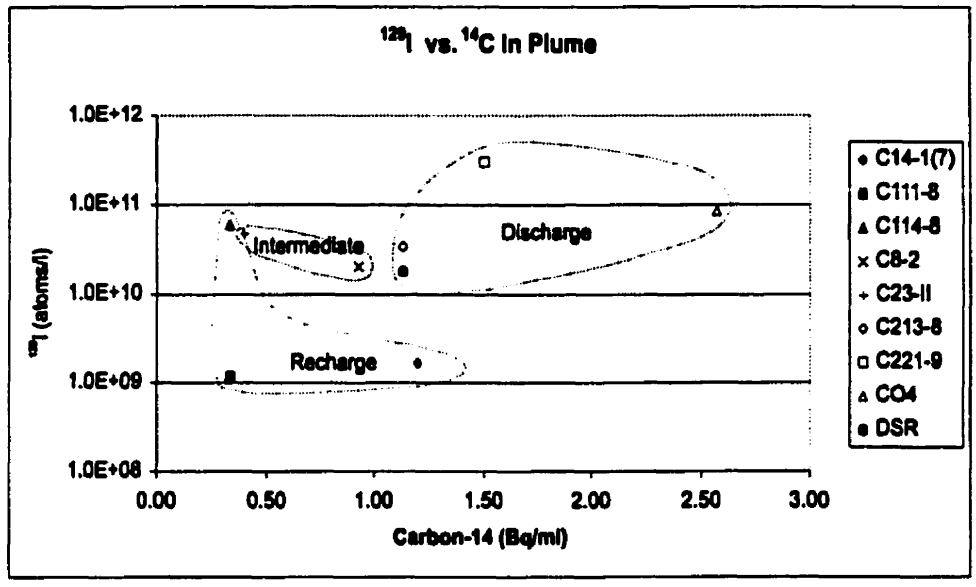

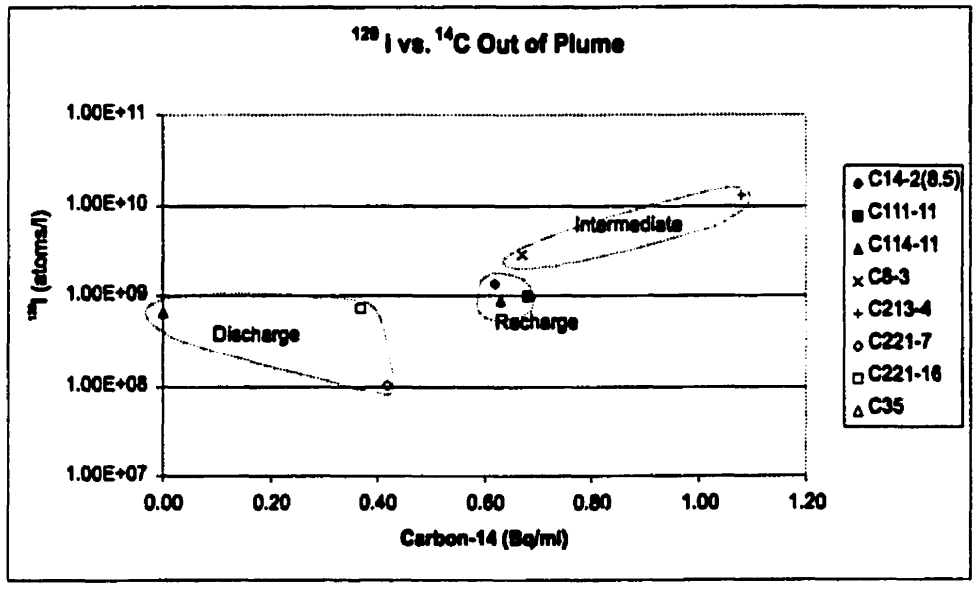

Figure 39 DOC and stable iodine in and out of plume.

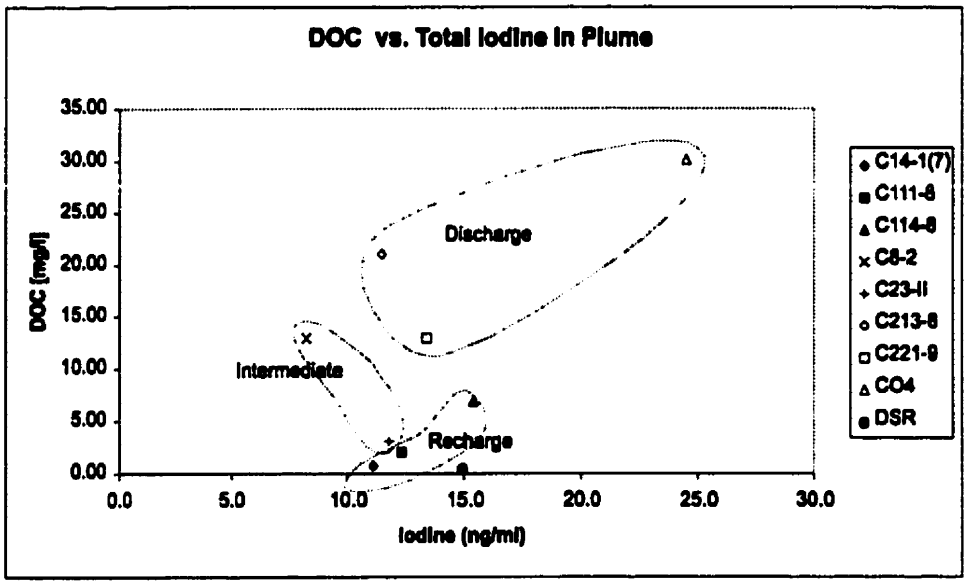

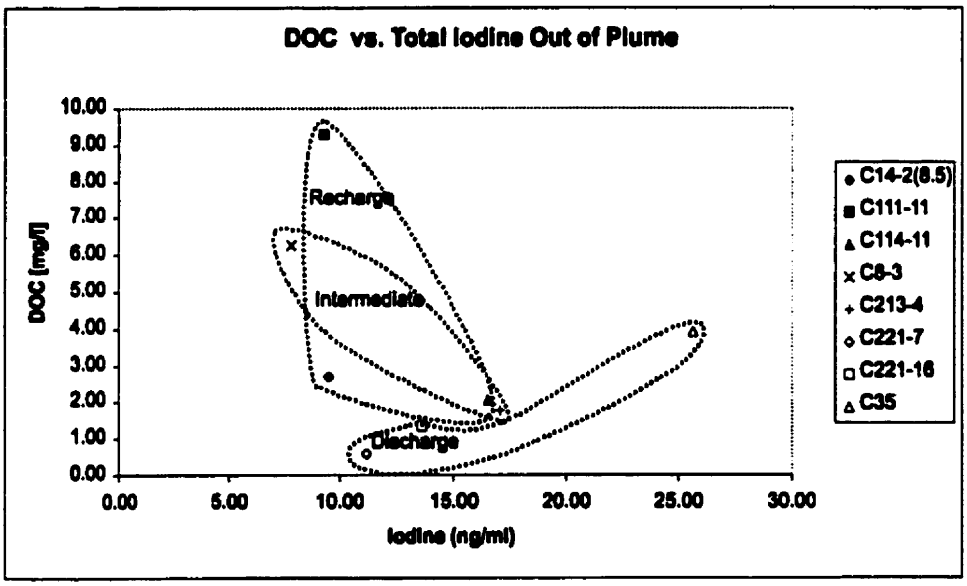

Figure 40 DOC and ^{129}I in and out of plume.

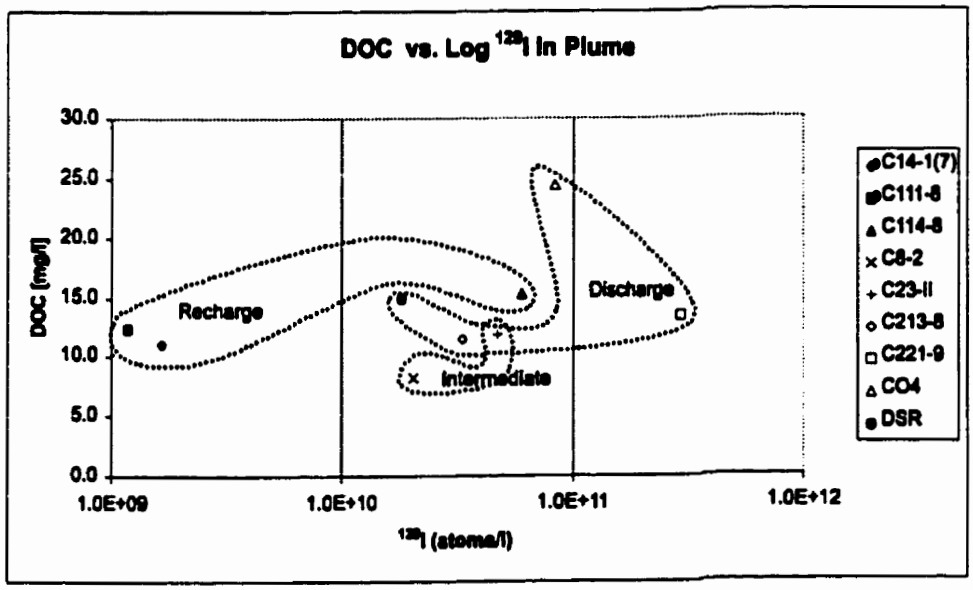

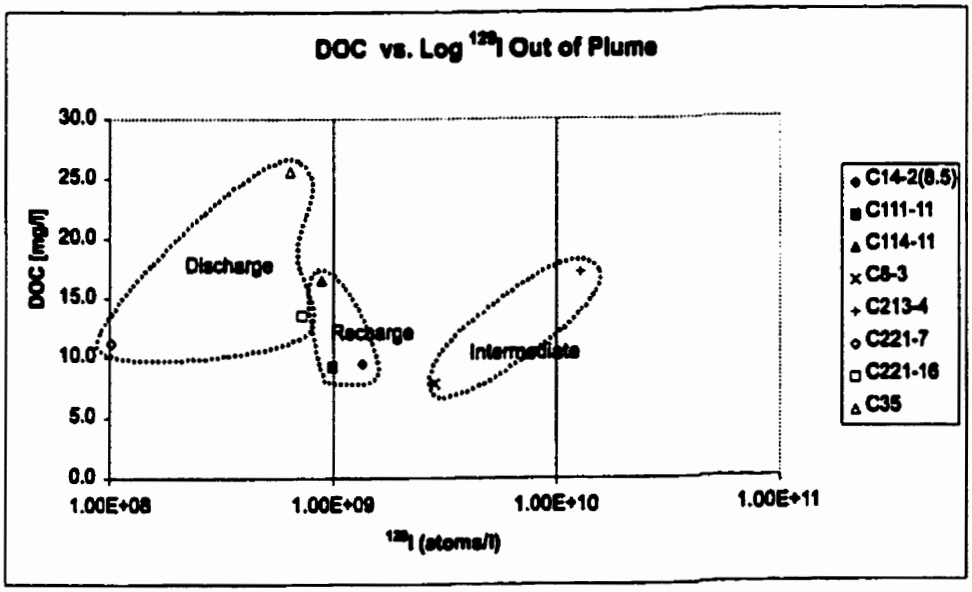

IV.3.2 Total Iodine & ^{129}I In Geologic Materials

Several sections of cored sediments and peats near C114 and CO4 were leached (Table 10) and combusted (Table 11) using the pyrohydrolysis and analytical techniques previously described (Sections III.2.1, III.2.4, III.3 and III.4). Stable I in leaches was measured by ICP-MS and the $^{129}I/^{127}I$ isotopic ratio and ^{129}I concentrations by AMS (Figure 41 and 42). A comparison of the data indicates that $^{129}I/^{127}I$ and ^{129}I is roughly two orders of magnitude higher in sediments within the plume than out of plume, considering the first and second leach treatments (Table 10). Consistently higher concentrations of stable I (and ^{129}I) is extracted in the second treatment (0.05-2.73%, 24.2-46.4% respectively) relative to the first extraction (0-1.1%, 2.3-14.3%, respectively) (Figure 43, Table 12). The stable iodide appears to be more tightly bound since not much of it is extracted by the magnesium chloride treatment (0-1.1%). The hydroxylamine hydrochloride treatment removed only slightly more iodide (0.05-2.7%), however; it is on the same order of magnitude as the magnesium chloride treatment. Treatment of the samples with KOH was done, however; the stable iodine (and ^{129}I) concentrations could not be obtained by ICP-MS. As a result, removal of the stable iodine and ^{129}I from the leaches was estimated by combining them and subtracting this from the total iodine determined from the combusted soil samples. This seems reasonable assuming that the recovery was 100% from the three chemical extractions including 1) exchangeable iodide, 2) iodide bound to iron and manganese oxides and 3) iodine bound to organic matter.

Table 10 Total iodine and ^{129}I from $MgCl_2$ and Hydroxylamine leach treatment.

	1M $MgCl_2$ @ pH 7 Leachate	Total I in sample (ng/g)	$^{129}I/^{127}I$ – background	^{129}I (atoms/g of soil)
Exchangeable	C114A (15-16.5')	0.40	2.40E-13	5.69E+5
	C114C (22.5-25')	0.40	2.55E-11	6.05E+7
	C210A	0.60	6.19E-11	1.47E+8
	C210B	0.40	8.58E-13	2.03E+6
	0.04M $NH_2OH{\cdot}HCl$ in 25% (v/v) HOAc	Total I in sample (ng/g)	$^{129}I/^{127}I$ – background	^{129}I (atoms/g of soil)
Fe-ox Mn-ox	C114A (15-16.5')	2.10	2.51E-12	5.63E+06
	C114C (22.5-25')	1.75	1.17E-10	2.76E+08
	C210A	7.70	1.10E-09	2.60E+09
	C210B	0.60	2.02E-12	4.47E+06
	1M KOH	Total I in sample (ng/g)	$^{129}I/^{127}I$ – background	^{129}I (atoms/g of soil)
Organics	C114A (15-16.5')	N/A*	1.60E-12	N/A*
	C114C (22.5-25')	N/A*	4.91E-11	N/A*
	C210A	N/A*	1.21E-10	N/A*
	C210B	N/A*	1.49E-12	N/A*

N/A* stable I measurements (ICP-MS) were not possible, as a result ^{129}I values were not possible.

Table 11 Total iodine and ^{129}I from pyrohydrolysis of sediments.

Combustion of Sediments	Total I in sample (ng/g)	$^{129}I/^{127}I$ – background	^{129}I (atoms/g of soil)
Core sample C114A (15'-16.5')=(4.5-5.0m)	190.07	4.90E-13	2.32E+07
Core sample C114C (22.5'-25')=(6.8-7.6m)	64.17	1.26E-11	5.95E+08
Core sample C210A (0-5')=(0-1.7m)	14095.85	1.34E-10	6.38E+09
Core sample C210B (15'-16.5')= (4.5-5.0m)	36.21	3.00E-13	1.42E+07
Core sample Twin Lake Dunes (0-5cm)	643.90	2.46E-13	1.16E+07
Core sample Twin Lake Dunes (-55cm)	159.18	7.97E-14	3.78E+06

Figure 41 Concentrations of stable iodine, $^{129}I/^{127}I$ ratio and ^{129}I for exchangeable iodide from $MgCl_2$ leach extraction solutions.

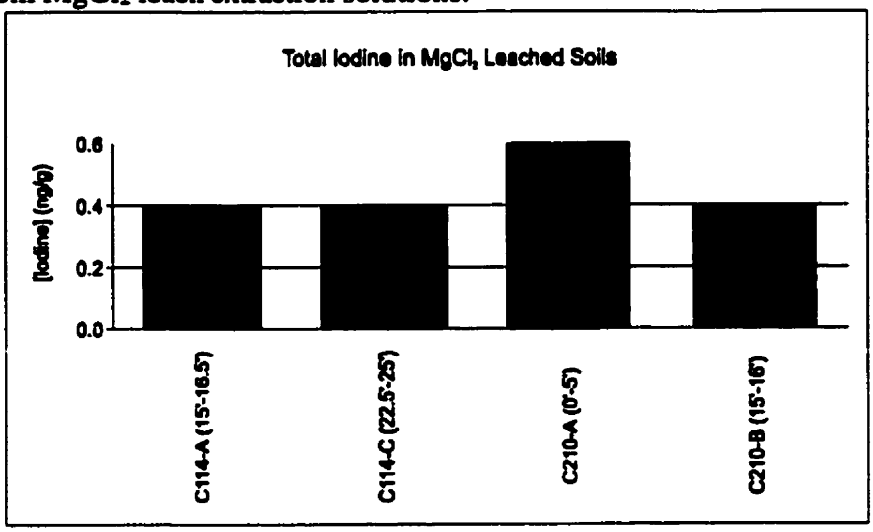

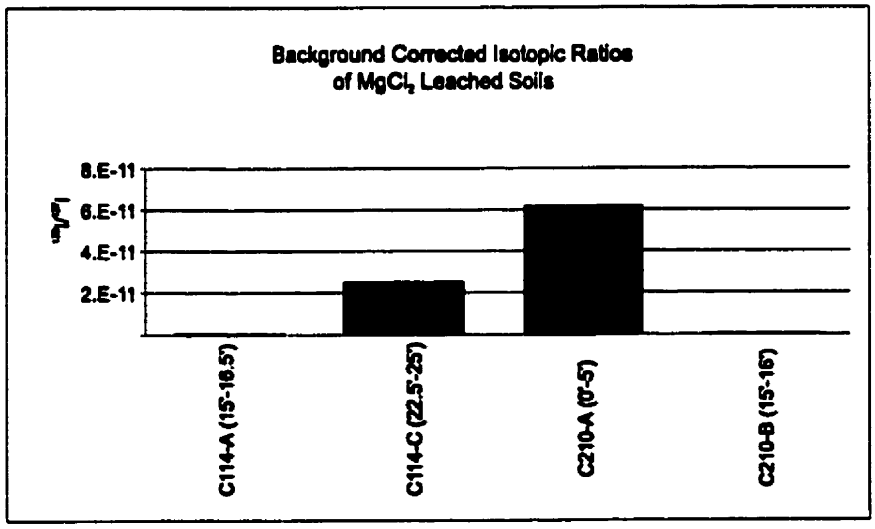

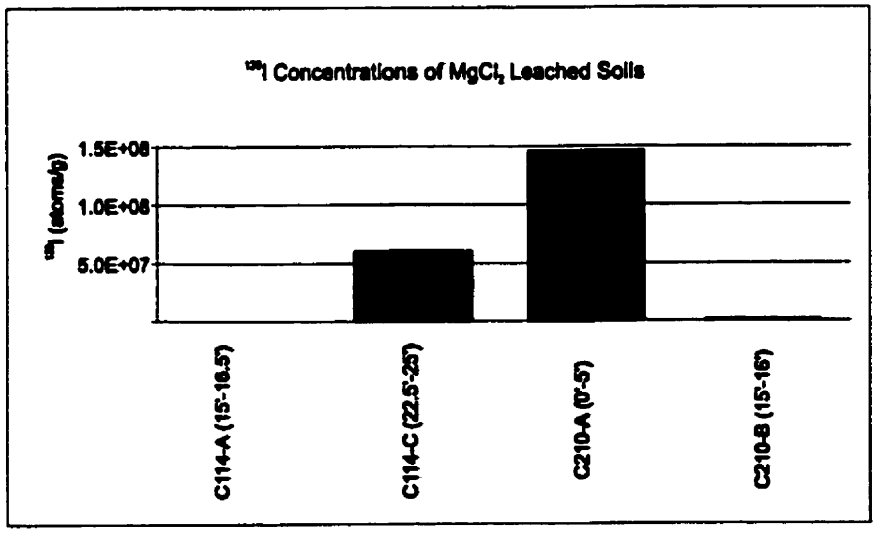

Figure 42 Concentrations of stable iodine, $^{129}I/^{127}I$ ratio and ^{129}I for Fe and Mn oxyhydroxide bound I from $NH_2OH \cdot HCl$ leach extraction solutions.

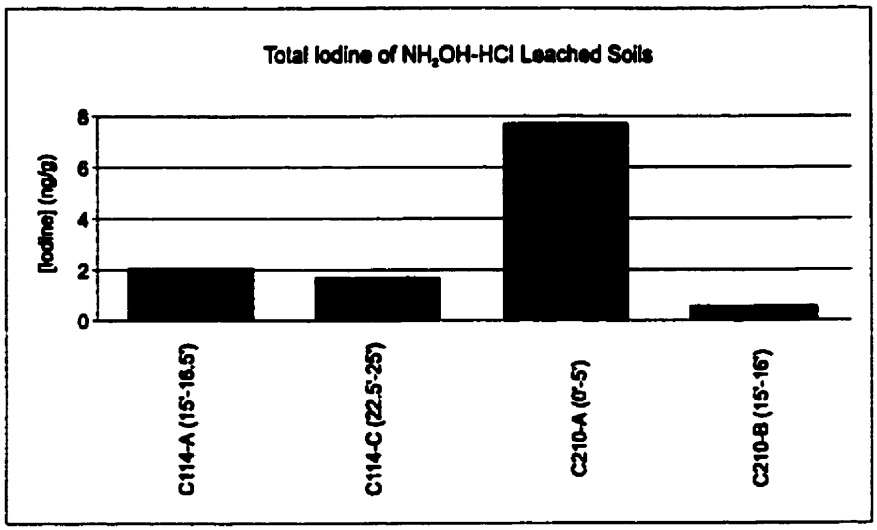

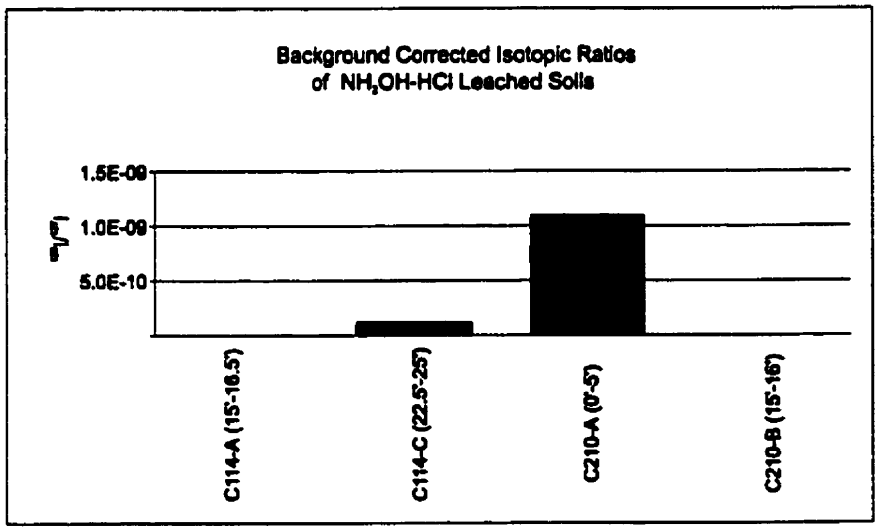

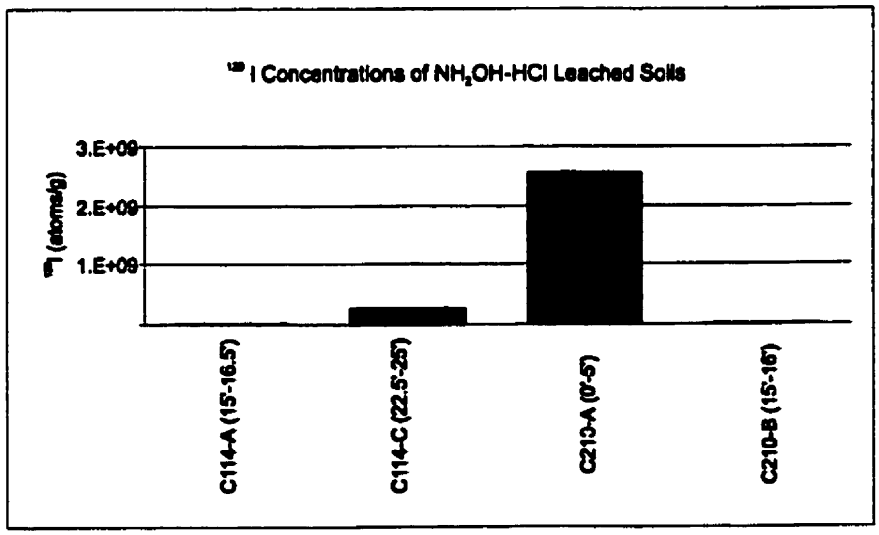

Figure 43 Total iodine and ^{129}I concentrations from combusted soil samples.

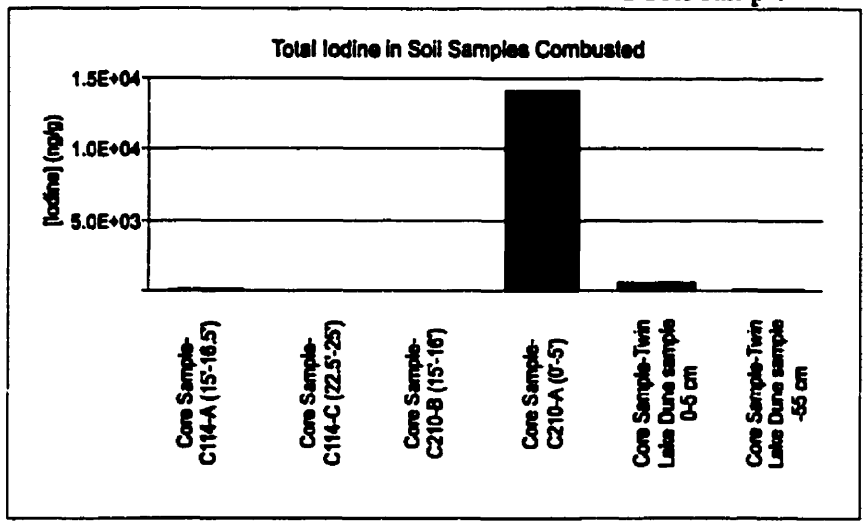

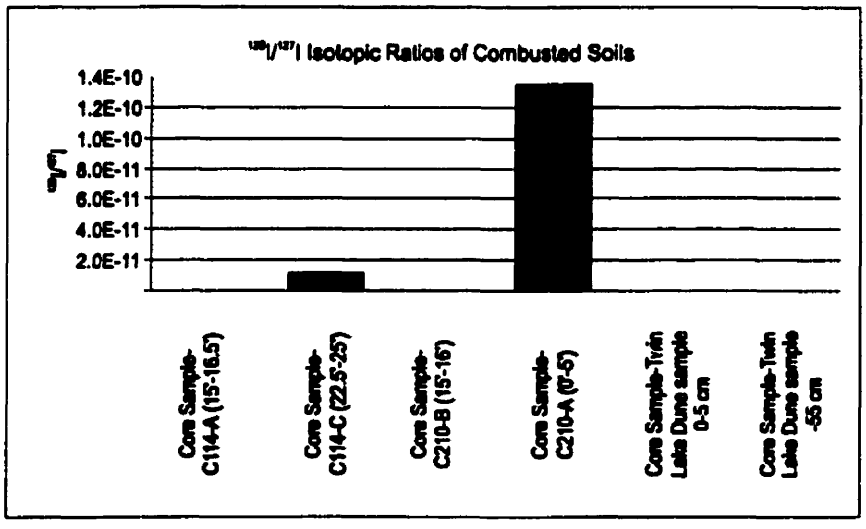

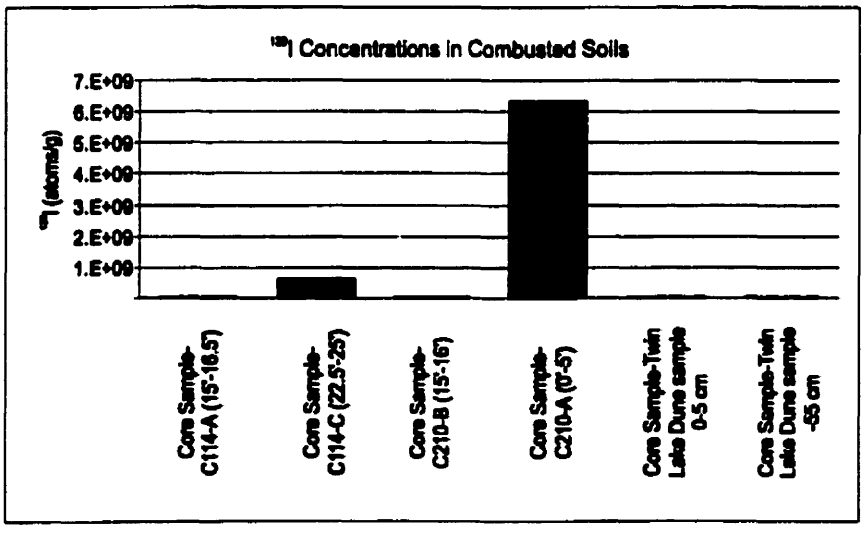

Table 12 Fractionation of total iodine and ^{129}I with various leachates and combustion.

	Leach Treatment			Combustion
Samples	**Exchangeable Iodide**	**Oxyhydroxide-bound Iodide**	**Iodine bound to Organic matter †**	**Total Iodine (ng/ml)**
C114A (15-16.5')	0.40 0.21%	2.10 1.10%	187.57 98.68%	190.07
C114C (22.5-25')	0.40 0.62%	1.75 2.73%	62.02 96.65%	64.17
C210A	0.60 0%	7.70 0.05	14087.55 99.94%	14095.85
C210B	0.40 1.10%	0.60 1.67%	35.21 97.23	36.21
Samples	**Exchangeable ^{129}I**	**Oxyhydroxide-bound ^{129}I**	**^{129}I bound to Organic matter †**	**Total ^{129}I (atoms/l)**
C114A (15-16.5')	5.69E+05* 2.45%	5.63E+06 24.24%	1.70E+07 73.31%	2.32E+07
C114C (22.5-25')	6.05E+07* 10.17%	2.76E+08 46.43%	2.58E+08 43.40%	5.95E+08
C210A	1.47E+08 2.30%	2.60E+09 40.69%	3.64E+09 57.01%	6.38E+09
C210B	2.03E+06* 14.32%	4.47E+06 31.43%	7.71E+06 54.25%	1.42E+07

† Values were calculated by adding Exchangeable and Oxyhydroxide bound and subtracting the obtained number
from the total Iodine from combustion reaction.
* Values at or below background.

IV.3.3 Soils & K_D

Figures 44 to 47 illustrate the partitioning of stable I (and ^{129}I) in soils in the various inorganic and organic fractions of I (and ^{129}I) extracted using chemical pre-treatments (Table 12). For stable I, the $MgCl_2$ treatment has little to no effect in the extraction of stable I for all four sediment samples (0-0.62%), whereas the hydroxylamine hydrochloride treatment extracted minute amounts of iodine (0.05-2.73%). The remainder of stable I is assumed to be organically bound iodine (96.6-99.9%). With ^{129}I, however; a different picture is observed. Relative to stable I, there is an increase in the amount of ^{129}I extracted using the magnesium chloride (2.3-14.3%) and hydroxylamine hydrochloride treatment (24.3-46.4%). The remaining iodine is assumed to be organically bound and residual iodine (43.4-73.3%). From these results, it is apparent that stable iodine is more tightly bound to organic matter than is ^{129}I, because of the inability for the chemical treatments to remove any significant amounts of stable iodine. This suggests that stable I and ^{129}I are being bound to different sites in the sediments over time.

To provide further scientific significance a comparison between the amounts of stable iodine and ^{129}I in the solid matrix samples and groundwaters was done to give an indication of its degree of retention, or distribution co-efficient (K_D). This quantitatively illustrates the distribution of ^{129}I and stable iodine within the hydrogeologic system. The results for the K_D's calculated from C14, C210 and Twin Lakes are given in Table 13. The calculated K_Ds for stable I outside the plume (C114-A, C210-B and Twin Lakes Dunes-55cm) are internally consistent within a factor of 5-10: (i.e. K_Ds of 147, 82.6, 10.6). However, the K_Ds for ^{129}I outside of the plume were (3.3, 5.8, 16.4) being internally consistent with a factor of 2-5. Interpretation of these data means that stable I appears to be more tightly bound to the

sediment. Some of it may be incorporated in the mineral or organic structure, whereas the ^{129}I is more loosely bound to surfaces and bound to iron and manganese oxyhydroxides, hence easier to remove with magnesium chloride and hydroxylamine hydrochloride chemical treatment.

Within the plume (samples C114C and C210A) a different picture emerges. There is little retention of either the stable or radioactive isotopes (for C114C, $K_{D\ stable} = 1.31$; $K_{D\ radioactive} = 1.09$) in high porosity zones in the silty sand. These values (at the lower edge of the range) suggest, as does the correlation between tritium and stable I, that stable iodine may be behaving conservatively in the groundwaters migrating through the sands from Area C to Duke Swamp. A possible explanation for the reduced stable I K_D values in the plume may be:

(1) not allowing enough time for equilibrium adsorption to take place due to the rapid movement of the contaminant plume in the subsurface or;

(2) large variation of hydraulic heads (up to 1m) between spring and fall resulting in large changes in iodine concentrations.

The K_D value for stable I and ^{129}I calculated for the contaminant plume in the discharge zone (C210-A) were 483 and 93, respectively. The much higher values in organic peats, relative to those for the sands, probably result from interaction with the very large microbial population to be expected in a zone of high organic content. A higher K_d for stable iodide (596) was measured for surficial sands (0-5 cm) sampled at Twin Lakes, which also contained a considerable quantity of organic matter. The retention (K_D) values for the peat samples from C210 lie in the range of K_D values for organic soils (range 1.4-368) listed in Sheppard and Thibeault (1990).

Table 13 K_D values for selected soils and groundwaters.

Sample	Depth (m)	^{127}I – soil µg/kg	^{129}I – soil atoms/kg	^{127}I – gw µg/l	^{129}I – gw atoms/l	K_D ^{127}I (l/kg)	K_D ^{129}I (l/kg)
Recharge							
114-A	4.6 - 5.1	190	$2.3x10^{10}$	2.3	$1.4x10^{9}$	82.6	16.4
114-C (plume)	6.9 - 7.7	64.2	$6.0x10^{11}$	49	$5.5x10^{11}$	1.31	1.09
Discharge							
210-A (plume)	0 - 1.5	14100	$6.4x10^{12}$	29	$6.9x10^{10}$	483	93
210-B	4.6 - 4.9	36.2	$1.4x10^{10}$	3.4	$4.2x10^{9}$	10.6	3.3
Surficial Sands							
Twin L. (fallout)	0 - .05	644	$1.2x10^{10}$	1.08 (C35)	$6.5x10^{8}$ (C35)	596	18.4
Twin L.	0.5- 0.55	159	$3.8x10^{9}$	1.08	$6.5x10^{8}$	147	5.8

Figure 44 Partitioning of total iodine and ^{129}I extracted from C114A (non-plume).

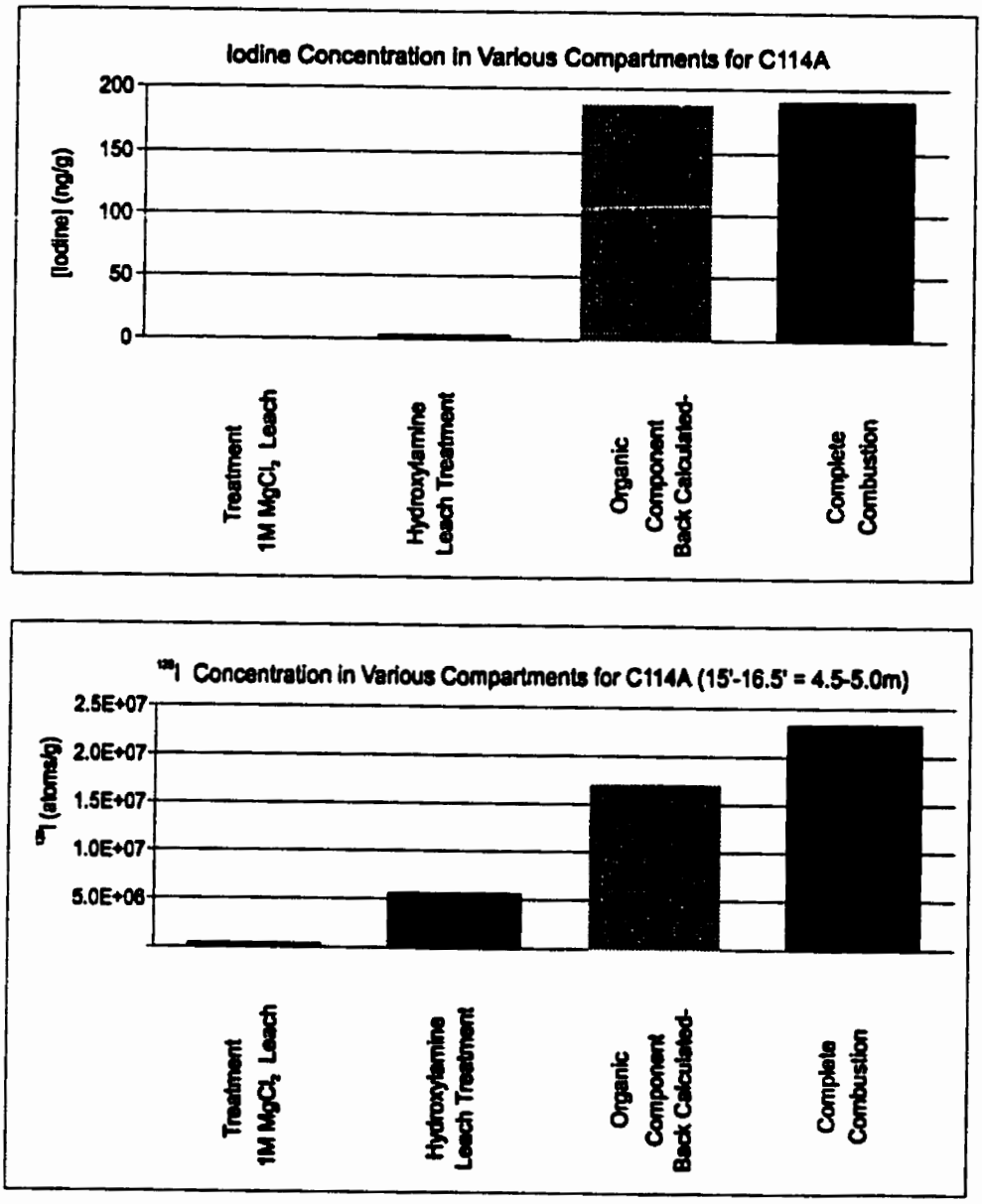

Figure 45 Partitioning of total iodine and ^{129}I extracted from C114C(plume).

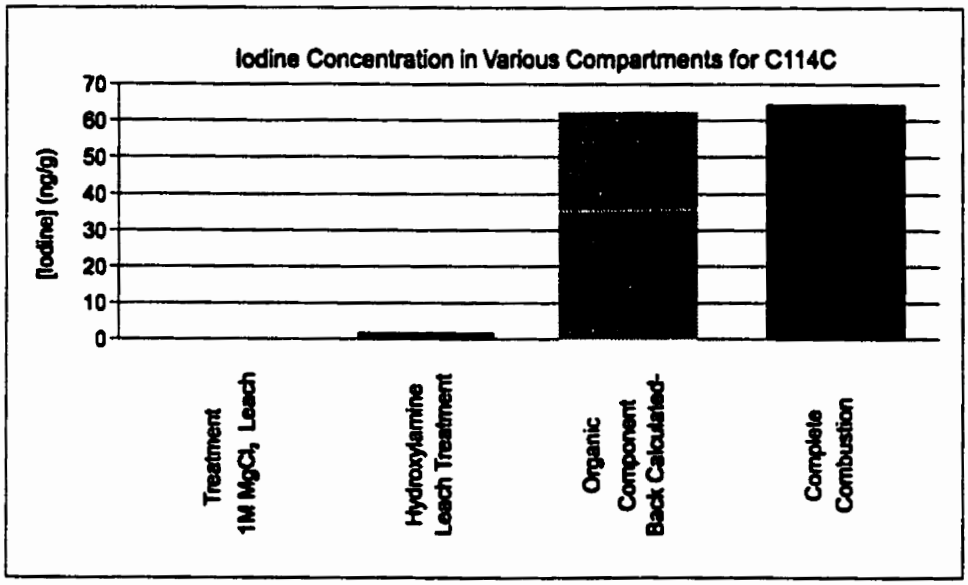

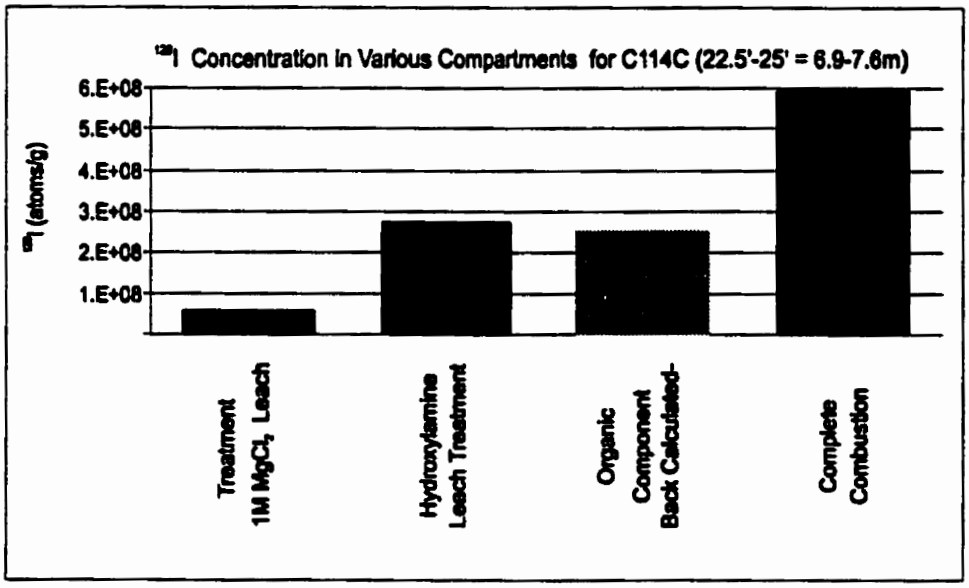

Figure 46 Partitioning of total iodine and ^{129}I extracted from C210A (plume).

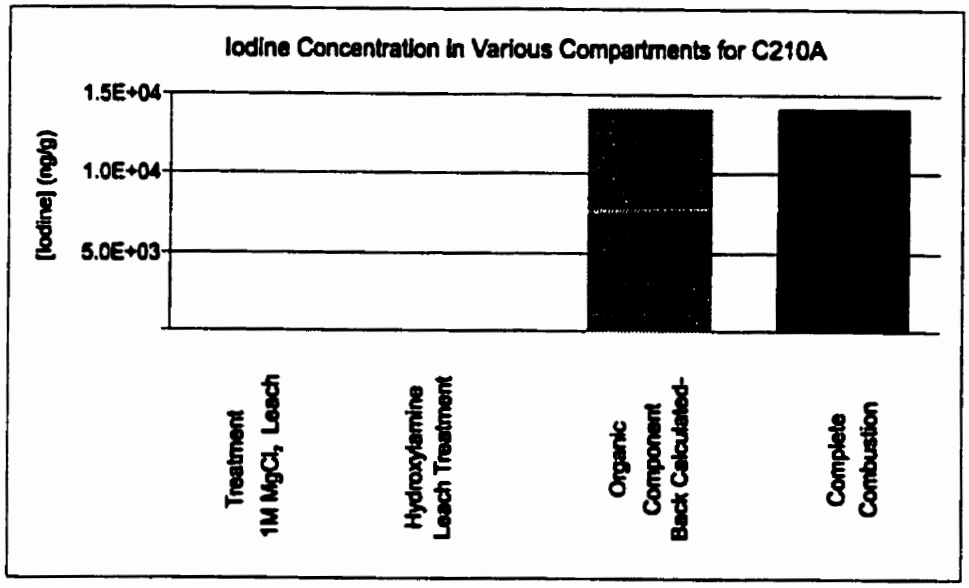

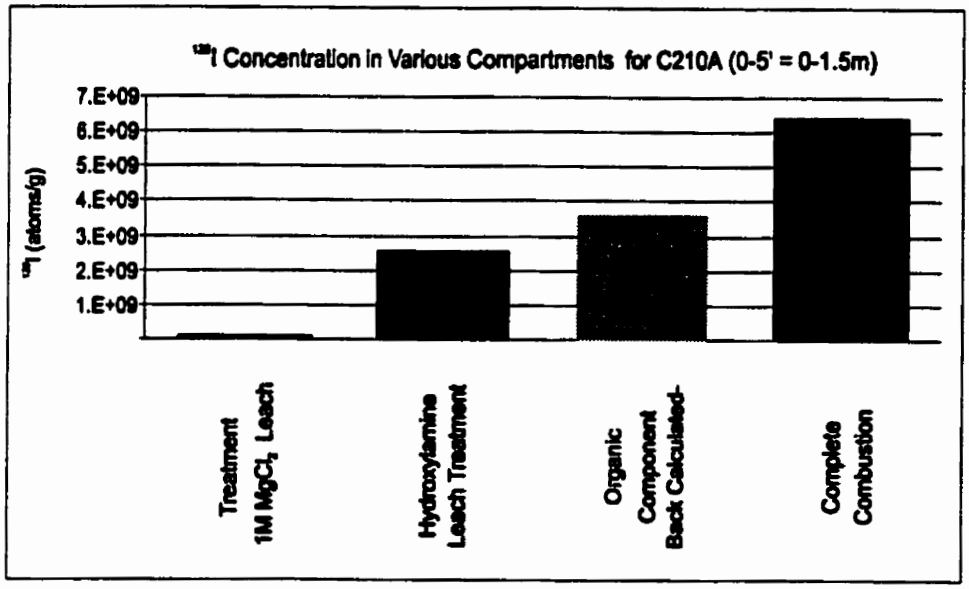

Figure 47 Partitioning of total iodine and ^{129}I extracted from C210B (non-plume).

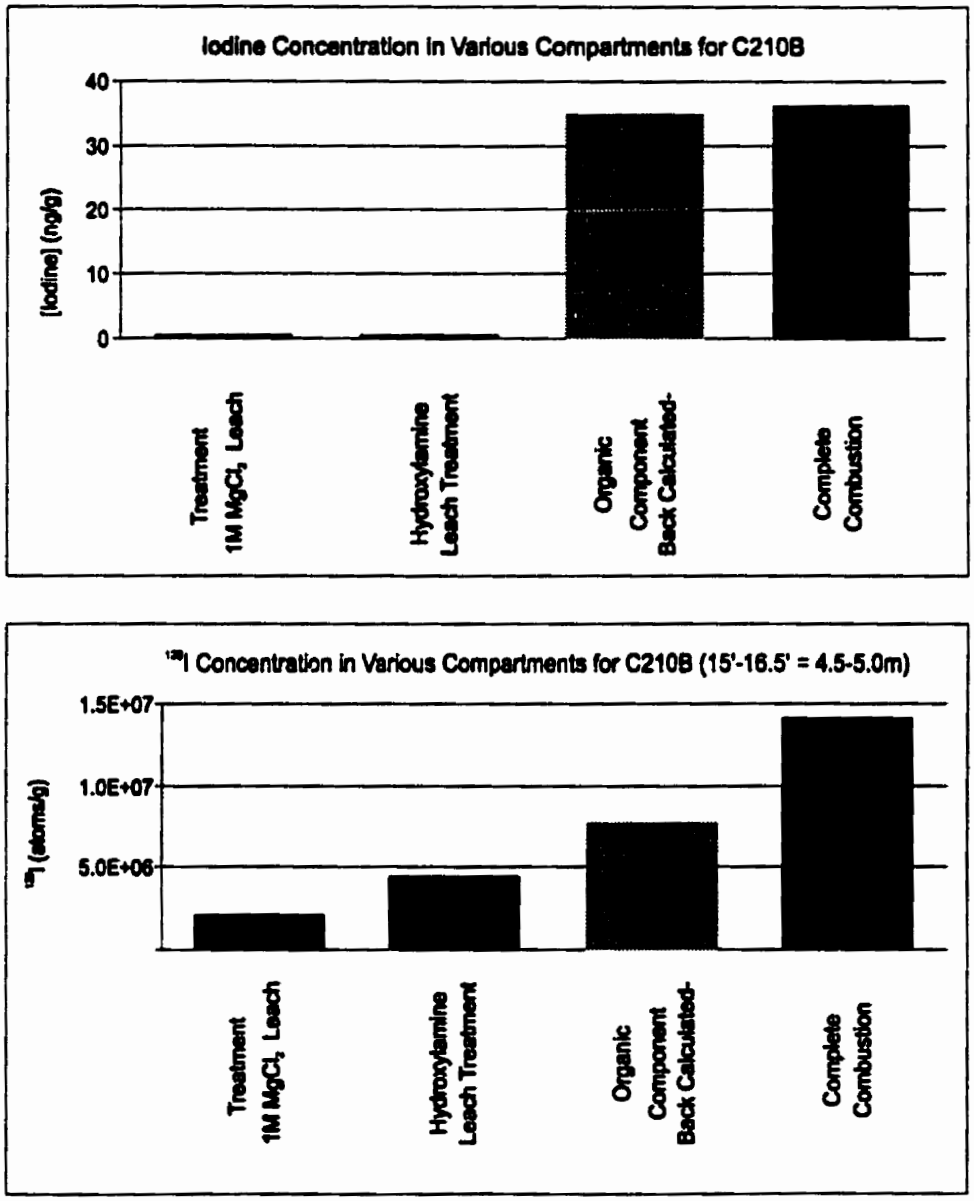

IV.3.4 Total Iodine & ^{129}I in Vegetation

Vegetation samples were combusted to release the bound iodine and to obtain a quantitative representation of partitioning of stable I and ^{129}I in the biosphere. Results are indicated in Table 14, illustrating that the original stable I, $^{129}I/^{127}I$ isotopic ratio and ^{129}I concentrations vary from sample to sample, indicating a positive correlation between time of exposure and iodine concentration (uptake) (Figure 48).

Figure 48 Total iodine and ^{129}I for combusted vegetation samples collected at Duke Swamp. Increasing concentrations of both I and ^{129}I in potted plants suggests uptake of volatilized I and ^{129}I.

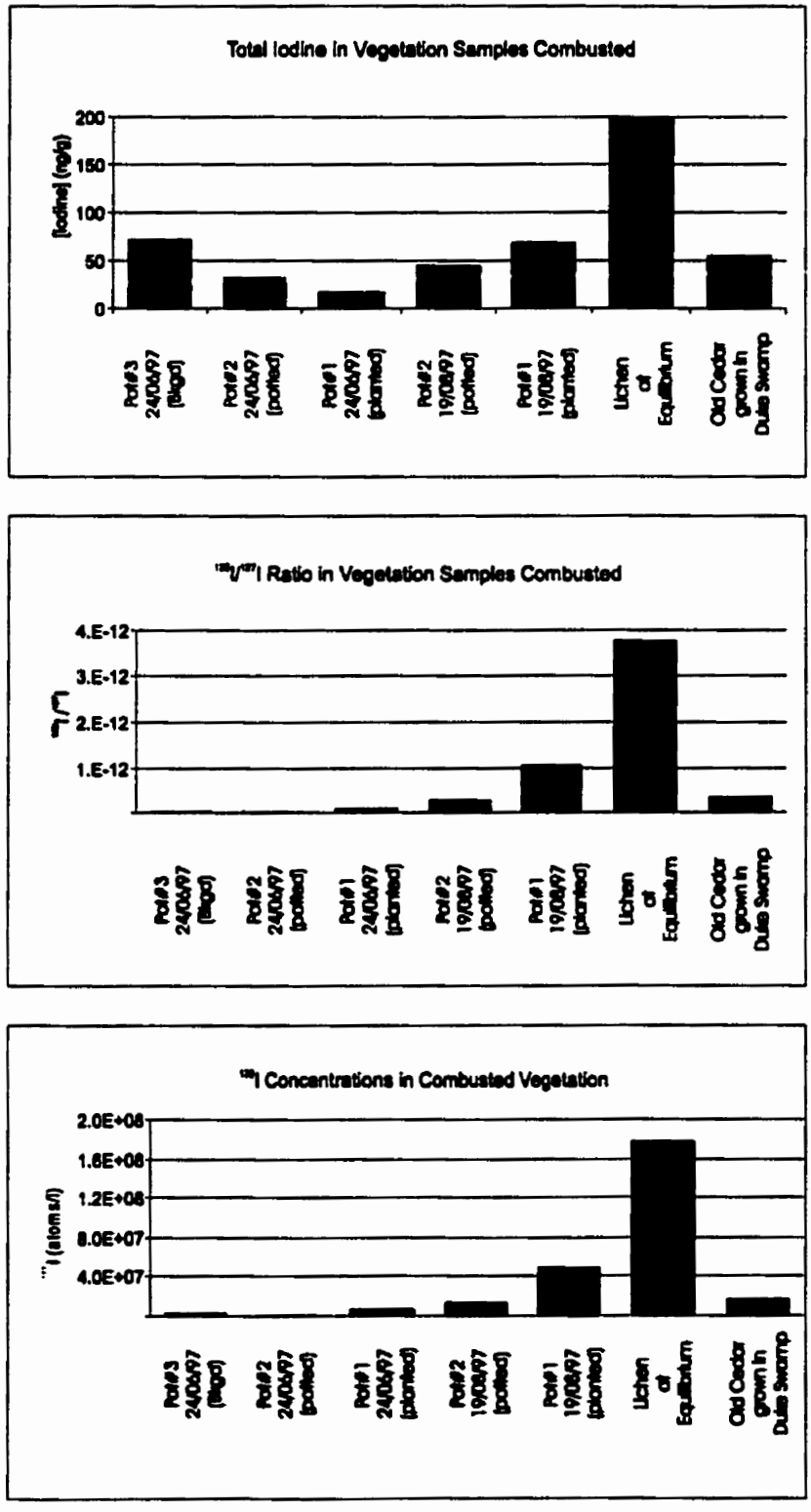

Table 14 Concentrations of total iodine and ^{129}I from pyrohydrolysis of vegetation

Combustion of Vegetation	Total I in sample (ng/g)	$^{129}I/^{127}I$ – background	^{129}I (atoms/g of vegetation)	Remarks
Potted 24.06.97 (Bkgd) Cedar Tree Pot#3	71.53	6.37E-14	3.02E+06	start of photosynthetic experiment
Potted 24.06.97 Cedar Tree Pot#2	31.86	5.37E-14	2.54E+06	
Planted 24.06.97 Cedar Tree Pot#1	15.76	1.41E-13	6.67E+06	
Potted 19.08.97 Cedar Tree Pot#2	44.82	2.88E-13	1.36E+07	end of photosynthetic experiment
Planted 19.08.97 Cedar Tree Pot#1	68.73	1.05E-12	4.96E+07	
Lichen sample at equilibrium with Swamp Environment	200.00	3.76E-12	1.79E+08	longterm, dynamic equilibrium
Cedar Tree grown in Duke Swamp	54.73	3.74E-13	1.77E+07	

Table 15 Summary of I and ^{129}I for selected vegetation and air samples taken at Duke Swamp

Sample	stable I ng/g	^{129}I atoms/g vegetation	^{129}I atoms/g I
cedar - 0 exposure.(av. of 3)	114	4.2×10^{7}	3.7×10^{14}
Potted cedar - 8 wks exp.	132	1.1×10^{8}	8.3×10^{14}
Planted cedar - 8 wks exp.	165	3.1×10^{8}	1.9×10^{15}
in-situ lichen	200 (est)	9.8×10^{8}	1.1×10^{16} (est)
air sample - 3 day	3 (est)	2.0×10^{7} atoms/m^3	6.9×10^{15} (est)

Taken from Milton *et al.*, 1998 Research Contract Report to AECB

IV.3.5 Vegetation & C_R

The data in Table 14 (and Figure 48) illustrate that ^{129}I was taken up rapidly by plants, from a mixed air and groundwater source (root and atmospheric uptake) and from atmospheric source only. This elucidates undisputedly that volatilization of iodine occurs and provides further evidence that evapotranspiration plays a role in this system.

As with the soils, it is necessary to provide further scientific significance for vegetation by calculating concentration ratios (C_R), similar to K_D in soils. This is a comparison between the amounts of stable iodine and ^{129}I in the vegetation samples and groundwaters to indicate the degree of adsorption by vegetation, or concentration ratios (C_R). C_R (water) is defined as atoms ^{129}I per kg vegetation (exposed in Duke Swam)/ atoms ^{129}I per litre of Duke Swamp water. The difference between the values for planted and potted plants was used to represent the atoms ^{129}I per kg vegetation (i.e. $(4.96 - 1.36) \times 10^{10}/8.4 \times 10^{10} = 0.428$). C_R (air) is defined as atoms ^{129}I per kg vegetation/atoms ^{129}I per m^3 air. In this case we have used the value for the potted plant to represent of the atoms per kg vegetation, (i.e. $(1.36 \times 10^{10}/2 \times 10^7 = 6.8 \times 10^2)$.

The data in Table 15 illustrate that the plants acquired ^{129}I, both from a mixed air and groundwater source, and from an atmospheric source only. This illustrates that volatilized iodine accompanies the water vapour and carbon dioxide known to be entering the atmosphere from the surface of the swamp.

The C_R (air) value is significantly higher than C_R (water). This implies the uptake of iodine via the stomata is a more significant process over time, than uptake via the roots. These results agree with the atmospheric uptake on the assimilation of ^{14}C and ^{3}H in plants (Milton *et al.*, 1998).

V. Conclusions

The primary objective was to investigate whether or not iodine traveled through the aquifer conservatively, if not, what effects organic matter in the sediments had. Results for stable I indicate the bulk of it was tightly bound to the aquifer sediments, possibly the organic phases. ^{129}I showed somewhat non-conservative behaviour by being loosely adsorbed to the soils along the way as was indicated from the results of the leach experiments (Table 10). As noted earlier in all areas sampled, the K_d for ^{129}I is significantly lower than that for stable I. This is possibly because the natural, stable I in the groundwater has come to equilibrium with these aquifer materials over many thousands of years in this environment. ^{129}I, on the other hand, has only had an opportunity to exchange with the more loosely bound I or surface I in the relatively short time it has been present in the waters. Data for the leach tests carried out on these sediments support this hypothesis (Table 12).

The secondary objective was to determine the mechanisms by which iodide was sequestered onto sediments as indicated by the amount of exchangeable iodide, oxy-hydroxide bound iodide and organically bound iodine. This was achieved and suggested the partitioning of stable I between environmental components (aqueous, organic and mineral phases). The results indicated that between 2-14% of ^{129}I was removed with 1M $MgCl_2$ at pH7, but less than 1% of stable I was removed. Between 24-46% of the ^{129}I was removed by an 8 hour exposure to hydroxylamine hydrochloride in HOAc at 96°C, whereas less than 2.73% of the stable iodide was removed by the same treatment. A KOH leach designed to degrade the organic molecules was used to determine fraction of the stable I and ^{129}I; unfortunately stable iodide analyses of the KOH leachates that were performed could not be analyzed for stable Iodide. Isotopic ratios for these fractions were determined but ^{129}I values

for the organic fraction were obtained from subtracting the total combusted stable I (and ^{129}I) from $MgCl_2$ (exchangeable iodide) and $NH_2OH{\cdot}HCl$ (Mn and Fe oxyhydroxide bound iodide) fractions.

The distribution of tritium in the contaminant plume is heterogeneous due to the variable nature of ^{3}H released from the multiple trenches and is transported by the aquifer system in waste management Area C. The flow and transport at Area C is better envisioned, as a collection of small, overlapping groundwater plumes, rather than a single homogeneous source-term. This is supported by the fact that the very large differences in the concentration of the nuclides over short vertical and horizontal distances, and also that there were variations in concentrations of the nuclides over time. This same philosophy on the nature of the tritium plume could pertain to that of iodine. Another component that is known to be of influence in the heterogeneity of the ^{3}H systematics is evapotranspiration along the flow path. Vegetation experiments proved that evapotranspiration does play a role in stable I and ^{129}I.

References

Ball, J.W. & Nordstrom, D.K. (1991). User's Manual for WATEQ4, with revised thermodynamic database and test cases for calculating speciation of major, trace and redox elements in natural waters. *U.S. Geological Survey Open File Report 91-183.* Menlo Park, CA.

Beaujean, H., Bohenstingl, J., Laser, M., Merz, E. & Schnez, H. (1973). Gaseous Radioactive Emissions from reprocessing plants and their possible reduction. *Environmental Behaviour of Radionuclides Released in the Nuclear Industry*, IAEA-SM-172/17, IAEA, Vienna.

Behrens, H. (1982). New insights into the chemical behaviour of radioiodine in aquatic environments. *Environmental Migration of Long-Lived Radionuclides.* IAEA-SM-257/36, IAEA, Vienna.

Behrens, H. (1984). Speciation of radioiodine in aquatic and terrestrial systems under the influence of biogeochemical processes. *Int. Conf. Nuclear and Radiochemistry.* pp.223-230.

Benes, P., Gjessing, E.T. & Steinnes, E. (1976). Interactions between humus and trace elements in fresh water. *Water Research.* 10, pp.771-716.

Bors, J., Erten, H. & Martens, R. (1991). Sorption studies of radioiodine on soils with special references to soil microbial biomass. *Radiochimica Acta.* 52/53, pp. 317-325.

Bors, J. & Martens, R. (1992). The contribution of microbial biomass to the adsorption of radioiodine in soils. *Journal of Environmental Radioactivity.* 15, pp.35-49.

Bors, J., Martens, R. & Kuhn, W. (1988). Studies on the role of natural and anthropogenic organic substances in the mobility of radioiodine in organic soils. *Radiochimica Acta.* 44/45, pp.201-206.

Brauer, F.P. & Ballou, N.E. (1975). Isotopic ratios and other radionuclides as nuclear power pollution indicators. *Isotope Ratios as Pollutant Source and Behaviour Indicators.* IAEA-SM-191/20, IAEA, Vienna.

Brauer, F.P. & Strebin Jr., R.S. (1982). Environmental concentration and migration of ^{129}I *Environmental Migration of Long-Lived Radionuclides.* IAEA-SM-257/43, IAEA, Vienna.

Bruner, H.D. (1963). Symposium on the Biology of Radioiodine: Statement of the Problem. *Health Physics.* **9**, pp.1083-1089.

Burns, K.I. & Ryan, M.R. (1995). Determination of ^{129}I low level radioactive waste by radiochemical instrumental neutron activation analysis. *Journal of Radioanalytical and Nuclear Chemistry.* 194 (1), pp.15-23.

Champ, D.R., Young, J.L., Robertson, D.E. & Abel, K.H. (1984). Chemical Speciation of long-lived radionuclides in a shallow groundwater flow system. *Water Poll.Res. J. Canada.* 19 (2). Environmental Research Branch, Chalk River Nuclear Laboratories, Chalk River, Ontario

Chant, L. A., Andrews, H.R., Cornett, R.J., Koslowsky, V., Milton, J.C.D., Van Der Berg, G.J., Verburg, T.G. & Wolterbeek, H.TH. (1996). ^{129}I and ^{36}Cl concentrations in lichens collected in 1990 from three regions around Chernobyl. *Appl. Radiat. Isot.* 47 (9/10), pp.933-937.

Clark, I.D. & Fritz, P. (1997). Environmental Isotopes in Hydrogeology. CRC Lewis Publishers, New York, 328 pp.

Cohen, B.L. (1985). The origin of I in soil and the ^{129}I problem. *Health Physics.* 49(2), pp.279-285.

Colard, J. F., Verly, W.G., Henry, J.A., & Boulenger, R.R. (1965). Fate of Iodine Radioisotopes in the Human and estimation of the Radiation Exposure. *Health Physics.* 11, pp. 23-35.

Dickin, A.P. (1997). Radiogenic Isotope Geology. Cambridge University Press. New York, USA. pp.369-388.

Dolinar, G.M., Rowat, J.H., Stephens, M.E., Lange, B.A., Killey, R.W.D., Rattan, D.S., Wilkinson, S.R., Walker, J.R., Jategaonkar, R.P., Stephenson, M., Lane, F.E., Wickware, S.L. & Philipose K.E. (1996). Preliminary Safety Analysis Report (PSAR) for the Intrusion Resistant Underground Structure (IRUS). *AECL-Misc-295* (Rev.4). Atomic Energy of Canada Limited, Chalk River, Ontario K0J 1J0, Canada.

Dunn, W. (1999). City of Ottawa, Public Works, personal communication.

Elmore, D., Gove, H.E., Ferraro, R., Kilius, L.R., Lee, H.W., Chang, K.H., Beukens, R.P., Litherland, A.E., Russo, C.J., Purser, K.H., Murrell, M.T. & Finkel, R.C. (1980). Determination of ^{129}I using tandem accelerator mass spectrometry. *Nature*, 286, pp.138-140.

Evans, G.J., Jervis, R.E. & Csillag, E.G. (1988). The air/water partitioning of radioiodine: An experimental assessment. *Journal of Radioanalytical and Nuclear Chemistry.* 124 (1), pp.145-155.

Evenden, W.G., Sheppard, S.C. & Killey, R.W.D. (1998). Carbon-14 and tritium in plants of a wetland containing contaminated groundwater. *Applied Geochemistry.* 13, pp.17-21.

Fabryka-Martin, J., Bentley, H., Elmore, D. & Airey, P. (1985). Natural Iodine-129 as an environmental tracer. *Geochimica et Cosmochimica Acta.*, 49, pp.337-347.

Fabryka-Martin, J., Davis, S., Elmore, D. & Kubik, P. (1989). *In-situ* production and migration of ^{129}I in the STRIPA Granite, Sweden. *Geochimica et Cosmochimica Acta.* 53, pp.1817-1823.

Fuge, R. & Johnson, C.C. (1986). The geochemistry of iodine- A review. *Environmental Geochem. Hlth.* 8, pp.31-54.

Goldschmidt, V.M. (1954). Geochemistry. (Ed. Muir, A.) Oxford University Press, London. pp.602-620.

Handl, J. (1996). Concentrations of ^{129}I in the biosphere. *Radiochimica Acta.* 72, pp.33-38.

Holland, J.Z. (1963). Physical origin and dispersion of radioiodine. *Health Physics.* 9, pp.1095-1103.

Killey, R.W.D., Rao, R.R. & Eyvindson, S. (1993). Radiocarbon speciation and distribution in an aquifer plume and groundwater discharge area, Chalk River Ontario. *AECL* 1135. Atomic Energy of Canada Limited, Chalk River, Ontario K0J 1J0, Canada.

Killey, R.W., Rao, R.R. & Eyvindson, S. (1998). Radiocarbon Speciation and Distribution in an Aquifer Plume and Groundwater Discharge Area, Chalk River, Ontario. *Applied Geochemistry.* 13, pp.3-16.

Kilius, L.R., Baba, N., Garwan, M.A., Litherland, A.E., Nadeau, M.-J., Rucklidge, J.C., Wilson, G.C. & Zhao, X.-L. (1990). AMS of heavy ions with small accelerators. *Nuclear Instruments and Methods in Physics Research* B52. pp.357-365.

Kuhn, W., Handl, J. & Schätzler, H.P. (1973). Transport of ^{131}I, ^{137}Cs, ^{106}Ru, ^{144}Ce and ^{54}Mn in an undisturbed soil under natural environment conditions. *Environmental Behaviour of Radionuclides Released in the Nuclear Industry.* IAEA-SM-172/19, IAEA, Vienna.

Lang, H. & Wolfrum, C. (1989). Nuclide sorption on heterogeneous natural surfaces. *Water-Rock Interaction.* pp.417-420.

Lederer, C.M., Hollander, J.M. & Perlman, I. (1967). Table of Isotopes. John Wiley & Sons, Inc. New York, USA. pp.272-274.

Leiser, K.H. & Steinkopff, TH. (1989). Chemistry of radioactive iodine in the Hydrosphere and in the Geosphere. *Radiochimica Acta.* 46, pp.49-55.

Miessler, G.L. & Tarr, D.A. (1991). Inorganic Chemistry. Prentice Hall, Inc. New Jersey, USA, pp.625.

Milton, G.M., Cornett, R.J., Kramer, S.J. & Vezina, A. (1992). Transfer of iodine and technetium from surface waters to sediments. *Radiochimica Acta.* 58/59, pp.291-296.

Milton, G.M., Kotzer, T.G., Alvarado Quiroz, N.G. & Clark, I.D. (1998). Partitioning of ^{129}I In The Environment: The Fate of Radioiodine in a Shallow Sand Aquifer System at Chalk River Laboratories, Ontario, Canada. Research Contract Report to AECB (Reference No. 87055-6-5043/001/SS). Atomic Energy of Canada Limited, Chalk River, Ontario K0J 1J0, Canada.

Milton, G.M., King, K.J., Sutton, J. & Enright S. (1998). Tracer studies of carbon source and utilization in a wetland on the canadian shield. *Applied Geochemistry* 13, pp.23-30.

Miyake, Y. & Tsunogai, S. (1963). Evaporation of iodine from the ocean. *Journal of Geophysical Research.* 68 (13), pp.3989-3993.

Muramatsu, Y. & Ohmomo, Y. (1986). Iodine-129 and iodine –127 in environmental samples collected from Tokaimura/Ibaraki, Japan. *The Science of Total Environment.* 48, pp.33-43.

Muramatsu, Y. & Ohmomo, Y. (1988). Tracer experiments for the determination of chemical forms of radioiodine in water samples. *Journal of Radioanalytical and Nuclear Chemistry.* 124 (1), pp.123-134.

Muramatsu, Y. & Yoshida, S. (1995). Determination of ^{129}I and ^{127}I in environmental samples by neutron activation analysis (NAA) and inductively coupled plasma mass spectrometry (ICP-MS). *Journal of Radioanalytical and Nuclear Chemistry.* 197 (1), pp.149-159.

Muramatsu, Y. & Yoshida, S. (1995). Volatilization of methyl iodide from soil-plant system. *Atmospheric Environment.* 29 (1), pp.21-25.

National Council on Radiation Protection and Measurements. (1983). *NCRP REPORT* No.75. Iodine-129: Evaluation of release from nuclear power generation. 7910 Woodmount Avenue, Bethesda, MD, 20814.

Noack, M.H. (1995). Estimating groundwater velocity for shallow unconfined aquifer using the $^{3}H/^{3}He^{*}$ dating technique: A comparison to other hydrogeologic methods. M. Sc. Thesis, Trent University: 138 pages.

Paquette, J., Wren, D.J., & Ford, B.L. (1986). Iodine Chemistry. *American Chemical Society Symposium Series The Three Mile Island Accident: Diagnosis and Prognosis.* 293, pp.193-210.

Raja, M.E. & Babcock, K.L. (1961). Soil Chemistry of radio-iodine. *Soil Science.* 91 (1), University of California, Berkeley. pp.1-5.

Robertson, D.E. & Perkins, R.W. (1975). Radioisotope ratios in characterizing the movement of different physical and chemical species through natural soils. *Isotope Ratios as Pollutant Source and Behaviour Indicators.* IAEA-SM-191/24, IAEA, Vienna.

Ross, J. & Gascoyne, M. (1995). Methods for sampling and analysis of groundwaters in Canadian Nuclear Fuel Waste Management Program. *AECL Tech. Report* TR-588, COG-93-36.

Saas, A. & Grauby, A. (1973). Mecanismes de transfer dans les sols cultives des radionucleides rejetes par les centrales electro-nucleaires dans le system flueve-sol irrigue-nappe. *Environmental Behaviour of Radionuclides Released in the Nuclear Industry.* IAEA-SM-172/57, IAEA, Vienna.

Schüttelkopff, H. & Pimpl, M. (1982). Radioecological studies on Plutonium and Iodine-129 in the surroundings of the Karlsruhe reprocessing plant. Environmental Migration of Long-Lived Radionuclides. IAEA-SM-257/100, IAEA, Vienna.

Sheppard, M.I. & Thibeault, D. H. (1990). Default soil solid/liquid partition coefficients, K_ds for four major soil types; a compendium. *Health Physics* Vol. 59, No 4, pp. 471-482.

Sheppard, M.I. & Thibault, D.H. (1992). Chemical behaviour of Iodine in organic and mineral soils. *Applied Geochemistry.* 4, pp.265-273.

Sheppard, S.C. (1996). Importance of chemical speciation of Iodine in relation to dose estimates from ^{129}I. *AECL* 11669. Atomic Energy of Canada Limited, Pinawa, Manitoba R0E 1L0, Canada.

Soldat, J.K. (1963). The relationship between ^{131}I concentrations in various environmental samples. *Health Physics.* 9, pp.1167-1171.

Stewart, A.G. (1990). For debate: Drifting continents and endemic goitre in Northern Pakistan. *British Medical Journal*, 9thJune, **300**, pp.1507-1512.

Tessier, A., Campbell, P.G.C. & Bisson, M. (1979). Sequential extraction procedure for the speciation of particulate trace metals. *Analytical Chemistry.* 51 (7), June. pp.844-850.

Uchida, S., Sumiya, M., Muramatsu, Y., Ohmomo, Y., Yamaguchi, S., Obata, H. & Umebayashi, M. (1988). Deposition velocity of gaseous I to Rice grains. *Health Physics.* 55 (5), pp.779-782.

Uchida, S., Muramatsu, Y., Sumiya, M. & Ohmomo, Y. (1991). Biological half-life of gaseous elemental iodine deposited onto rice grains. *Health Physics.* 60 (5), pp.678-679.

Whitehead, D.C. (1974). The sorption of iodine by soil components. *J.Sci.Fd Agric.* 25, pp.73-79.

Whitehead, D.C. (1978). Iodine in soil profiles in relation to iron and aluminum oxides and organic matter. *The journal of Soil Science.* 29, pp.88-94.

Whitehead, D.C. (1984). The distribution and transformations of Iodine in the environment. *Environment International.* 10, pp.321-339.

Wood, D.H., Elefson, E.E., Horstman, V.G. & Bustad, L.K. (1963). Thyroid Uptake of Radioiodine Following Various Routes of Administration. *Health Physics.* 9, pp.1217-1220.

Yoshida, S. & Muramatsu, Y. (1995). Determination of organic, inorganic and particulate iodine in the coastal atmosphere of Japan. *Journal of Radioanalytical and Nuclear Chemistry.* 196 (2), pp.295-302.